CalVal Envisat

Envisat RA2/MWR ocean data validation and cross-calibration activities. Yearly report 2008.

Contract No 60453/00 - lot2.C

Reference : CLS.DOS/NT/09.040

Nomenclature : SALP-RP-MA-EA-21633-CLS

Issue : 1rev 1

Date : January 22, 2009

SALP Service Altimetrie & Localisation Precise

CLS Collecte Localisation Satellites

cnes Centre National d'Études Spatiales

CLS - 8-10 Rue Hermès - Parc Technologique du Canal - 31520 Ramonville St-Agne - FRANCE
Téléphone 33 5 61 39 47 00 / Télécopie 33 5 61 75 10 14

Chronology Issues :		
Issue :	Date :	Reason for change :
1.0	22/01/2009	Created
1.1	03/07/2009	Revision after comments from N. Picot

	AUTHORS	COMPANY	DATE	INITIALS
WRITTEN BY	A. Ollivier Y. Faugere	CLS CLS		
APPROVED BY	JP. Dumont	CLS		
QUALITY VISA	DT/AQM	CLS		
APPLICATION AUTHORISED BY				

Index sheet :	
Context	
Keywords	Envisat, Jason-1, Jason-2, Calval, , MSL, orbits, reprocessing
hyperlink	

Distribution :		
Company	Means of distribution	Names
CLS/DOS	J. DORANDEU	1 electonic copy
	V. ROSMORDUC	1 electonic copy
	P. ESCUDIER	1 electonic copy
DOC/CLS	DOCUMENTATION	1 electonic copy
CNES	T. GUINLE	1 CD
CNES	P. BOUBE	1 CD
CNES	D. CHERMAIN	1 CD
CNES	N. PICOT	1 electonic copy
CNES	E. BRONNER	1 electonic copy
CNES	J. LAMBIN	1 electonic copy
CNES	A. LOMBARD	1 electonic copy

List of tables and figures :

List of Tables

List of Figures

List of items to be defined or to be confirmed :

Applicable documents / reference documents :

Contents

LIST OF ACRONYMS

ECMWF	European Center for Medium range Weather Forecasts
GDR-A	Geophysical Data Record version A (before cycle 41 for Envisat mission)
GDR-B	Geophysical Data Record version B (after cycle 41 for Envisat mission)
MSL	Mean Sea Level
MWR	MicroWave Radiometer
POE	Precise Orbit Estimation
SLA	Sea Level Anomalies
SSB	Sea State Bias
USO	Ultra Stable Oscillator

1. Introduction

This report is an overview of Envisat validation and cross calibration studies carried out at CLS during year 2008. It is basically concerned with long-term monitoring of the Envisat altimeter system over ocean.

Envisat GDR data are routinely ingested in the Calval 1-Hz altimeter database maintained by the CLS Spatial Oceanography Division in the frame of the CNES Altietry Ground Segment (SSALTO) and funded by ESA through F-PAC activities (SALP contract N° 60453/00 - lot2.C). In this frame, besides continuous analysis in terms of altimeter data quality, Envisat GDR Quality Assessment Reports (e.g. Faugere et al. 2003 [27]) are routinely produced in conjunction with data dissemination.

Data from GDR cycles 9 through 72 spanning six years have been used for this analysis. All relevant altimeter parameters deduced from Ocean 1 retracking, radiometer parameters and geophysical corrections are evaluated and tested.

Some of the results described here were presented at the OSTST meeting (Nice, November 2008) and at the Quality Working Group (QWG) meetings (Dorking, May 2008 and Rome, November 2008).

The work performed in terms of data quality assessment also includes cross-calibration with Jason-1, ERS-2 and Jason-2. This kind of comparisons between coincident altimeter missions provides a large number of estimations and consequently efficient long-term monitoring of instrument measurements. This enables the detection of instrument drifts and inter-mission biases essential to obtain a consistent multi-satellite data set. The full reprocessing of Jason-1 products in GDR C version began mid-2008 and is expected to be available by mid 2009. Concerning Envisat, a full reprocessing in GDR C version will also start in 2009. Therefore, a new homogeneous Envisat/Jason-1 data set will be available next year.

Since July 2008, the new available Jason-2 data were also used for the cross-calibration with Envisat, mostly concerning IGDR data, as far as GDR were not available yet in 2008. The study showed a very good consistency between both missions with a standard deviation of cross-over differences of 4.5 cm for IGDR and 3.4 cm for (IGDR + POE orbit). The geographically correlated biases between Envisat and Jason 2 were shown to be lower than with Jason 1 on IGDR, evidencing a better quality of Jason-2 and Envisat's MOE than Jason-1's ([7], [60] and part). These results are encouraging for insuring a good continuity on the long term monitoring already initiated with Jason-1 since 2002.

After a preliminary section describing the data used, the report is split into 5 main sections: first, data coverage and measurement validity issues are presented. Second, a monitoring of the main altimeter and radiometer parameters is performed, describing the major impact in terms of data accuracy. Then, performances are assessed and discussed with respect to the major sources of errors. Then, Envisat Sea Surface height (SSH) bias is analyzed. Finally, an additional part presents the particular investigations that have been performed during this year:
- an extensive study about MSL issues,
- a comparison of 5 types of orbits,
- cross-calibration between Jason-2 and Envisat results,

- a detailled analyze of geographically correlated biases betwen Jason-1 and Envisat...

2. Quality overview

Ra-2 instrumental status:
On January 17th 2008, **a drop of the RA2 S-band transmission power occurred**. Consequently, all the S-band parameters, including the dual ionospheric correction are not relevant and MUST NOT be used from the following date: 17 January 2008, 23:23:40 (Cycle 65 pass 289). Investigations have been conducted and the failure of the S-Band power stage is considered to be permanent.
Users are advised to use the ionospheric correction from GIM model, which is available in GDR data products.

The **USO anomaly** which was affecting intermittently (see Figure 2) Ra-2 data since cycle 46 **disappeared** since cycle 65 pass 451 (2008/01/23). This anomaly, which remains unexplained, did not reappear since then. Since August 2006, a temporary procedure has been implemented by ESA to correct the effect of the USO anomaly. Using the proposed auxiliary files, Envisat Ra-2 data remain at the same high level of accuracy.
Users are strongly advised not to use the range parameter in Ku and S Band without this correction, even for the non-anomalous periods, in order to correct the range from the long term drift of the USO device. More information is available on http://earth.esa.int/pcs/envisat/ra2/auxdata/

Note that since Mars 2008, a new procedure for the IF mask calibration mode was changed. It had actually been recognized that an IF Mask anomaly was caused by a wrong setting of the AGC used for the IF Calibration Mode from time to time. The NEW procedure consists in setting all the AGC?s to 3dB before entering the IF Calibration Mode and resetting all the parameters to the original values before entering in the Measurement mode. It is operationally used since cycle 66 for all IF Calibrations and this ensures 100% of valid IF Masks to be acquired.

Missing measurements:
The unavailability of data over ocean for year 2008 is about 1.3% in average. This ratio, much smaller than the two previous years (6% in average) had never been so small during the whole mission period. This drop is explained by an improvement of the data dissemination since May 2008.
The MWR unavailability is very stable and very low around 0.4%.

Long term monitoring of RA-2 and MWR parameters:
The ocean-1 altimeter and radiometer parameters are consistent with expected values. They have a very good stability and high performances, comparable to Jason-1. A very good availability on every surface and very low editing ratios over ocean are observed since the beginning of the mission. The high frequency content of Ku-band Ra-2 parameters is very stable.

The MWR performances are very good. Note that since the beginning of the mission, the instrumental parameters at 36.5 GHz were known to be slighly drifting. Moreover from cycle 46 onwards, the comparison to ECMWF model is hardened by the numerous improvements of this operational model inducing (around 1.5mm) jumps in the time series.

The loss of the S Band at the beginning of the year occurred in a low solar activity period, therefore thanks to the GIM model correction used instead of the dual-frequency correction in the SSH equation, data were weakly impacted in terms of variance.

Mean Sea Level:
The Envisat Mean Sea Level trend estimated at CLS is different from Jason-1 before September 2005. On the contrary both Mean Sea Level are very similar afterward, which is positive and encouraging for the quality of both data sets. Comparisons between both mission now getting closer enabled to show that the wet tropospheric correction is becoming a large source of error in the trend computation. Actually, jumps occurred on the ECMWF side signing as trends on the long term MSL monitoring. On the other hand, the radiometric correction is getting more and more accurate (drift corrections, side lobe effects correction...) on the long term and shall be taken into account in the MSL studies. Furthermore, ascending and descending passes still show worrying discrepancies depending on the orbit used and in a stronger way than for Jason-1. Finally, full reprocessing of the mission planned for 2009 is getting prepared and should hopefully improve our understanding of the long term MSL analysis.

3. Data used and processing

3.1. Data used

Envisat Geophysical Data Records (GDRs) from cycle 10 to cycle 72 have been used to derive the results presented in this report. This corresponds to nearly six-years spanning from September 30th 2002 to November 17th 2008. The routine production started on September 2003 with cycle 15. In parallel, a backward reprocessing of cycles 14 to 9 was implemented. With only 7 days of available data, cycle 9 has not been used in this report. 12 GDR cycles have been produced this year: cycles 62 to 72 as part of the current processing.

The Envisat GDR data are generated using two softwares: the IPF, from Level0 to Level1B, and the CMA, from Level1B to Level2. As shown in Table 1 several IPF processing chain and CMA Reference Software have been used to produce all the GDR cycles. Tables 2 and 3 describe the main evolutions respectively associated with the IPF and CMA versions.

Cycles	IPF version	CMA version
9 to 10	4.58	6.3
11 to 12	4.57	6.3
13 to 14	4.56	6.3
15 to 21	4.54	6.1
22 to 24	4.56	6.2
25 to 26	4.56	6.3
27 to 28	4.57	6.3
29 to 40	4.58	6.3
38 to 40	5.02	7.1
41 to 47 pass 790	5.02	7.1
47 to 48 pass 849	5.06	9.0
48 to 51 pass 7	5.02	7.1
51 to 58 pass 843	5.03	8.0
58 to 64	5.06	9.0
65 to 67	5.06	9.1
68 to 72	5.06	9.2

Table 1: *I*PF/CMA Processing versions

Note that for cycle 47-48, the instrument sub-system Radio Frequency Module was switched to

B-side during 37 days, from the 15/05/2006 14:21:50 to the 21/06/2006 11:37:32 (cycle 47 pass 794 to cycle 48 pass 847). First of all, an error in the configuration Side-B file made cycles 47 and 48 uncorrect. In 2008, passes 1 to 790 of cycle 47 and passes 1 to 849 of cycle 48 were reprocessed and delivered, RA2 RFSS properly configured to side B redundancy. Those two cycles are now used into the following report.

Version	Changes
IPF 4.56	-Extrapolation of AGC value to the Waveform center (49.5) for both Ku- and S-Band -Correction for an error found in the evaluation of S band AGC
IPF 4.57	No impact on data
IPF 4.58	-Addition of a Pass Number Field in Fast Delivery Level 2 products
IPF 5.02	-MWR Side Lobe correction upgrade -USO clock period units correction -Rain Flag tuning to compensate for the increase of the S band Sigma0 -Monthly IF mask taken into account -DORIS Navigator CFI upgrade (RA-2 and MWR) -S-band anomaly flag
IPF 5.03	-Correction for an error found in the Channel 2 brightness temperature -Correction for an error in the window delay (for the 80 and 20 MHz bandwidths) -S-band anomaly flag upgrade, now properly implemented -Correction of Rx-Fine parameter -MWR second channel corrected (Side Lobes correction)
IPF 5.06	None

Table 2: *I*PF changes impacting the Envisat GDR or Level2 data

The change from IPF 4.58/CMA6.3 to IPF 5.02/CMA7.1 strongly impacted the data. The Sea-State bias table has been recomputed ([42]) accounting for the impact of the new orbit and the new geophysical corrections (MOG2D, GOT00 ocean tide correction with the S2 component corrected once only, new wind speed algorithm from Abdalla, 2006 [1]). The new SSB correction is shifted in average by +2.0 cm in comparison with the previous one. New standards are used for the computation of the Envisat Precise Orbit Estimation. One of the main evolutions is the use

of the GRACE gravity model EIGEN GC03C. This new model implies a strong reduction of the geographically correlated radial orbit errors. In order to take into account the dynamical effects and wind forcing, a new correction is computed from the MOG2D (Carrere and Lyard, 2003 [9]) barotropic model forced by pressure (without S1 and S2 constituents) and wind. The use of such a correction in the SSH strongly improves the performances. All the corresponding evolutions are detailed in [22].

The change from IPF 5.06/CMA9.1 to IPF 5.06/CMA9.2 has a weak impact on the data regarding the short period of time available:
- Change of orbit: New standards are used for the computation of the Envisat Precise Orbit Estimation (POD GDR-C configuration including notably a time varying gravity field, ...). The impact should be weak but studies performed on Jason-1 for the GDR C reprocessing show an unexpected trend on long term monitoring. Updates of the orbit standard solved this problem in the so called GDR C' version and will be improved once more (by reviewing the time variable gravity terms) in a GDR C" (LPOD 2005 solution) version that will be used for ENVISAT reprocessing.
- Change of DAC correction: A new High Resolution Dynamic Atmospheric Correction MOG2D correction was computed and added to the products. Internal studies show that this new correction improves the variance by a gain of 1 to 2cm^2 for Jason-1 and Envisat with a greater impact near coasts and on open ocean, in the South pacific area (Bellingshausen basin), [12].

Version	Changes
CMA 6.1	-MSS CLS01 -Rain flag -MWR neural algorithm -Sea Ice tuning -Sea State Bias Table file -GOT00.2 Ocean Tide Sol 1 Map file -FES 2002 Ocean Tide Sol 2 Map file -FES 2002 Tidal Loading Coeff Map
CMA 6.2	No impacts on Envisat products
CMA 6.3	-Updated OCOG retracking thresholds Ice1 Conf file -Increased GDR data coverage by the use of both consolidated and non-consolidated data prods in inputs.
CMA 7.1	-Improving the mispointing estimation

.../...

Version	Changes
	-Addition of square of the SWH in Ku and S band -Addition of GOT2000.2 loading tide -FES2004 tide and loading tide -New DEM AUX file (MACESS) merge of ACE land elevation data and Smith and Sandwell ocean bathymetry -New orbit standards -New SSB solution -new wind table -Mog2D upgraded -New S1S2 wave model in dry troposphere -GOT00.2 includes two extra waves, S1 and S2 -GIM model ionospheric correction added in the products
CMA 8	No impacts
CMA 9	Correction of an anomaly in the relative orbit field inside the product header. No scientific impact.
CMA 9.1	Separating the processing of Jason-1 and Envisat No scientific impact.
CMA 9.2	-New POD orbit configuration. -New Dynamic Atmospheric Correction (DAC/MOG2D High Resolution)

Table 3: *C*MA changes impacting the Envisat GDR

3.2. Processing

3.2.1. GDR products and quality assesment method

To perform this quality assessment work, conventional validation tools are used including editing procedures, crossover analysis, collinear differences, and a large number of statistical monitoring and visualization tools. All these tools are integrated and maintained as part of the CNES SALP altimetry ground segment and F-PAC (French Processing and Archiving Centre) tools operated at CLS premises. Each cycle is carefully routinely analyzed before data release to end users. The main data quality features are reported in a cyclic quality assessment report available on http://www.aviso.oceanobs.com/html/donnees/calval/validation_report/en/welcome_uk.html. The purpose of this document is to report the major features of the data quality from the Envisat mission.

As for all other existing altimeters, the Envisat GDR data are ingested in the Calval 1-Hz altimeter database maintained by the CLS Spatial Oceanography Division. This allows us to cross-calibrate and cross-compare Envisat data to other missions. In this study data from Jason-1 (GDRs cycles 27 to 252), ERS-2 (OPRs Cycle 78 to 108) are used. Jason-1 is the most suitable for Envisat cross calibration as it is available throughout the Envisat mission and has been extensively calibrated to T/P (Dorandeu et al., 2004b [19]). In 2007, a full reprocessing of Jason-1 data GDR-B version was completed in order to have an homogeneous data set [4]. Since May 2008 however, the new GDR-C version came out. The full reprocessing of Jason-1 products in GDR C version began mid-2008 and is expected to be available by mid 2009. Concerning Envisat, a full reprocessing will also begin in 2009. Therefore, a new homogeneous Envisat/Jason-1 data set will be available next year. The cross-calibration between Envisat and Jason-1 takes into account Jason-1 reprocessing. The periods concerned by each version is summed up on Figure 1.

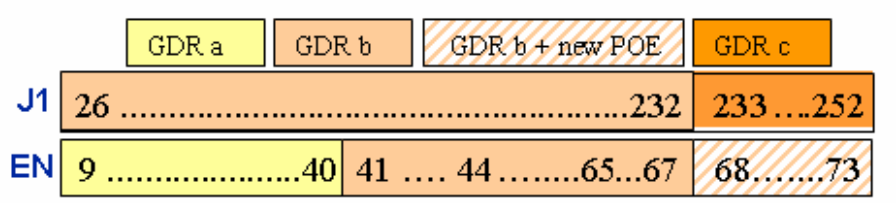

Figure 1: *Status on the GDR reprocessing for Jason-1 and Envisat.*

Comparisons between Jason-1 and Envisat altimeter and radiometer parameters have been carried out using 10-day dual crossovers for SSH comparison and 3-hour dual crossovers for altimeter and radiometer comparisons. The geographical distribution of the dual crossovers with short time lags strongly changes from one Envisat cycle to another. Indeed, contrary to Envisat which is sun-synchronous, Jason-1 observes the same place at the same local time every 12 cycles (120-day). Following the method detailed in Stum et al. (1998) [71], estimates of the differences are computed using a 120 day running window to keep a constant geographical coverage. ERS-2, flying on same ground track as Envisat only 30 minutes apart, has had a coverage limited to the North Atlantic since the failure of the on-board register in June 2003 (EOHelp message of 4 July 2003). To improve the significance of the Envisat/ERS-2 comparison, long term monitoring of altimeter parameters difference is performed on this restricted area all over the Envisat period using a

repeat-track method.

3.2.2. Particular updates added to the GDR products

Most of this work has been carried out using parameters available in the GDR products. However, a few updates have been necessary to complete the analysis (those are listed in the product disclaimer document available at http://earth.esa.int/dataproducts/availability/ [61]):

- **S-Band anomaly**: A method has been developed to detect data corrupted by S-Band anomaly. It has been applied until cycle 53. From cycle 54 onwards the product flag, available since cycle 51, has been used (see 4.3.1.). Since cycle 60, the cause of the anomaly was found and the anomaly solved. No anomaly occurs anymore since then.
- **Sea ice flag**: A method has been developed to detect data corrupted by sea ice (see 4.3.2.)
- **Filtered dual-frequency ionosphere correction**: A 300-km low pass filter is applied along track on the dual frequency ionosphere correction to reduce the noise of the correction. This correction is applied up to the cycle 64, after that, it cannot be computed anymore, due to the S-Band Power drop (17th January 2008) the GIM ionospheric correction is then used.
- **Filtered dual-frequency ionosphere correction (bis)**: For cycles 9-40 from the sea state bias (SSB) used to correct the S-Band Range was updated in its right S-Band version. The dual-frequency ionosphere correction was therefore recomputed accounting for the S-Band SSB solution on S-Band range. Before that, both S and Ku-Band ranges used for that correction were corrected from the Ku-Band SSB (Labroue (2004 [41])).
- **Geophysical corrections**: The new geophysical correction associated with version CMA7 have been updated on the whole data-set in order to have the most homogeneous time series: wind table and SSB, new S1S2 wave model in dry troposphere, GOT00.2 with two extra waves, FES2004, S1 and S2
- **MOG2D HR**: The new High resolution DAC implemented into the CMA 9.2 from cycle 69 on Envisat (see Table 3 and Part) was also updated on the whole data-set.
- **Inverse barometer and dry troposphere corrections**: Pressure values used to compute the inverse barometer and the dry troposphere corrections have been derived from the ECMWF gaussian grids. Indeed, errors due to the topography, up to several centimeters near the coasts, significantly impact the accuracy the so-called Gaussian grids used as input of the Envisat (and Jason-1) ground processing (e.g. Dorandeu et al., 2004b [19]).
- **GIM/IRI ionosphere corrections**: Jason-1 doesn't fly at the same altitude as Envisat which means that ionosphere corrections are not comparable. Moreover, ERS-2 has a mono-frequency altimeter on-board. Therefore it is not possible to use these satellites to assess the Envisat ionosphere path delay. Thus the JPL GPS-based global Ionospheric Maps (GIM) containing the vertical ionospheric total electron content are used here. Note that GIM maps contain the vertical ionospheric total electron content in the 0-1400km altitude range. As Envisat flies around 800km, the International Reference Ionosphere (IRI) model is uses to estimate the GIM correction at the altitude of Envisat:

$GIM_{[0-800]} = GIM_{[0-1400]} \times \frac{IRI_{[800]}}{IRI_{[1400]}}$. Since the S-Band loss (17th January 2008) this correction is used for the SSH computation. Also note that since cycle 41 onwards, this GIM ionosphere correction is available in the GDR products.

- **USO correction**: The range needs to be corrected for the Ultra-Stable Oscillator (USO) clock period variations. From the beginning of the mission it underwent several behaviors and the way it is corrected depends on the cycle. It is detailled hereafter in part 3.2.3..

3.2.3. USO correction's specificities

The USO clock period is used to performs the computation of the Ra-2 window time delay and the range needs to be corrected :
- on the whole period, from a drift due to the aging of the device
- during some periods (detailed in Figure 2), from a strong anomaly detailed hereafter.

Description of the USO anomaly:
On the 1st of February 2006 (12:05:36), at the end of cycle 44, for an unknown reason a change of behavior of the USO device occurred. This anomaly, already observed for a short period during cycle 30, created a 5.5m jump on the range parameter and oscillations of about 20-30cm of amplitude at the orbital period. The anomaly became permanent on cycle 46 to 56. On the 1st of March 2007, the USO recovered in a non-anomalous mode. Between cycles 56 and 61, Ra2 data was not affected by the anomaly. On the 27th of September 2007 (cycle 62), a new change of behavior of the Ultra Stable Oscillator (USO) clock frequency occurred. A short break in the anomaly occurred between cycles 63 and 64, followed by another one on the 23th of January which was permanent over the whole year 2008. The anomaly and associated correction is detailed in [51]. The quality assessment of these data has been performed using the USO temporary correction provided by ESA. Users are strongly advised not to use the range parameter in Ku and S Band without this correction during the anomaly periods.

The correction of the Ultra-Stable Oscillator (USO) clock period variation applied to the range depends on the cycle considered. This is detailed hereafter:
For cycle 9 to 40, (outside of the anomaly periods): The method to correct the USO clock period is described in Celani (2002 [14]). The correction is regularly updated in the IPF ground processing via an Auxiliary data file. However, due to an anomaly in the ADF format, the correction was not taken into account (Martini, 2003 [51]) in the products for cycles lower or equal to 40. ESA supplies auxiliary files to allow users correcting their own database (Martini, 2003 [51]) (http://earth.esa.int/pcs/envisat/ra2/auxdata/). The distributed auxiliary corrections containing the drift + bias have to be used. The supplied correction has to be subtracted from the original altimetric range (EOP-GOQ and PCF team, 2005) and consequently added to SSH.
Note that for our database, the distributed auxiliary correction was smoothed over a 1-month period to filter peaks and short period variations.

For cycle 41 to 45, (outside of the anomaly periods): The USO drift + bias is already taken into account in the products. No additional auxiliary correction has to be used.

After cycle 45, (and for all the previous anomaly periods): ESA supplies auxiliary files to allow users correcting their own database (Martini, 2003 [51])

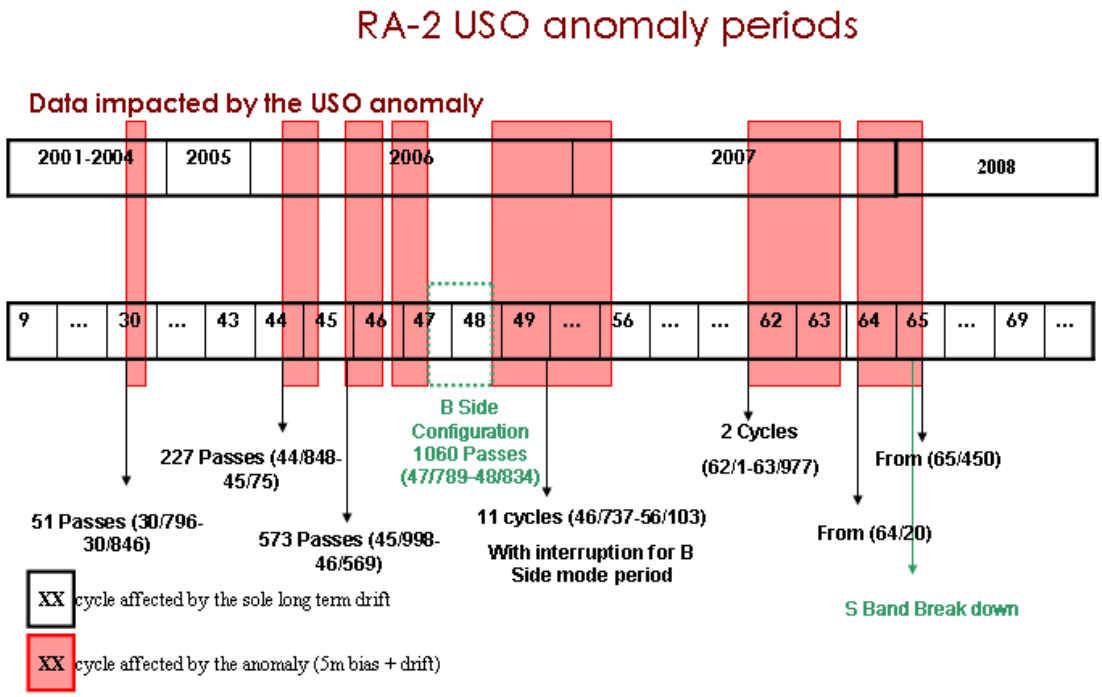

Figure 2: *Chronology of USO Correction anomaly.*

(http://earth.esa.int/pcs/envisat/ra2/auxdata/). The distributed auxiliary corrections containing the drift + anomaly correction have to be used.

4. Missing and edited measurements

This section mainly intends to analyze the ability of the Envisat altimeter system to correctly sample ocean surfaces. This obviously includes the tracking capabilities, but also the frequency of unavailable data and the ratio of valid measurements likely to be used by applications after the editing process.

4.1. Missing measurements

From a theoretical ground track, a dedicated collocation tool allows determination of missing measurements relative to what is nominally expected. The cycle by cycle percentage of missing measurements over ocean has been plotted in Figure 3. The measurement unavailability over the whole mission is about 6% in average. Eleven cycles have more than 10% of unavailability, notably from cycle 13 to cycle 17. Passes 1 to 452 of cycle 15 have not been delivered because of a wrong setting of RA-2. Several long RA-2 events occurred during cycles 13, 14, 16, 17, 22, 34, 51, 53, 55, 56, 59, 62 which resulted in a significant number of missing passes.
In 2008, the average ratio of missing RA2 measurements over ocean is 1.3%. This ratio, much smaller than the two previous years, had never been so small during the whole mission period. This drop is explained by an improvement of the data dissemination since May 2008.

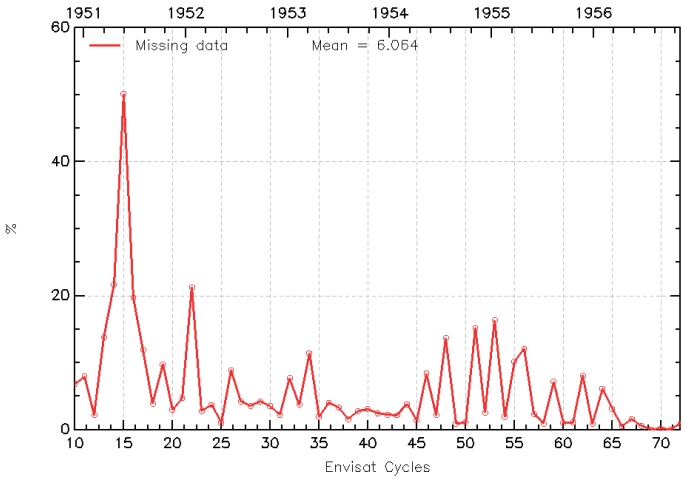

Figure 3: *Monitoring of the percentage of missing measurements relative to what is theoretically expected over ocean*

Figure 4 shows an example of missing measurements for cycle 72 . The measurements which are missing over the Himalaya are due to the IF Calibration Mode occurring on ascending passes only. This procedure was not always the same: for cycles prior to 55, it was performed over the Himalaya on both ascending and descending passes and for cycles 56 to 66 it was performed on ascending passes only but on the Rocky Mountains as well as on the Himalaya). Afterward, it is performed on ascending passes above the Himalaya only.

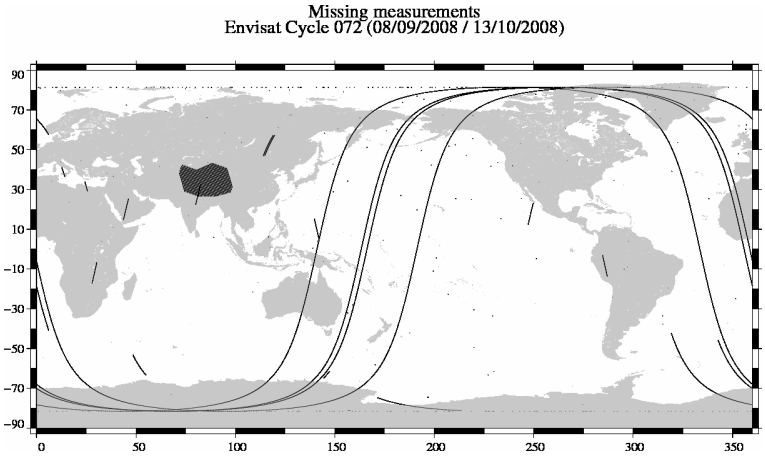

Figure 4: *Envisat missing measurements for cycle 72*

Finally, it has been found that some pass segments were quasi-systematically missing. Figure 5 shows the pass segments missing more than 5 times over the 11 last cycles. Some of them are explained (PLO permanent acquisition sites (ESA/Rome, GAVDOS/ Creta), others are not. Apart from that, the data retention rate is very good on every surface observed. This might be due to the tracker used by Envisat Ra-2, the Model Free Tracker (MFT).

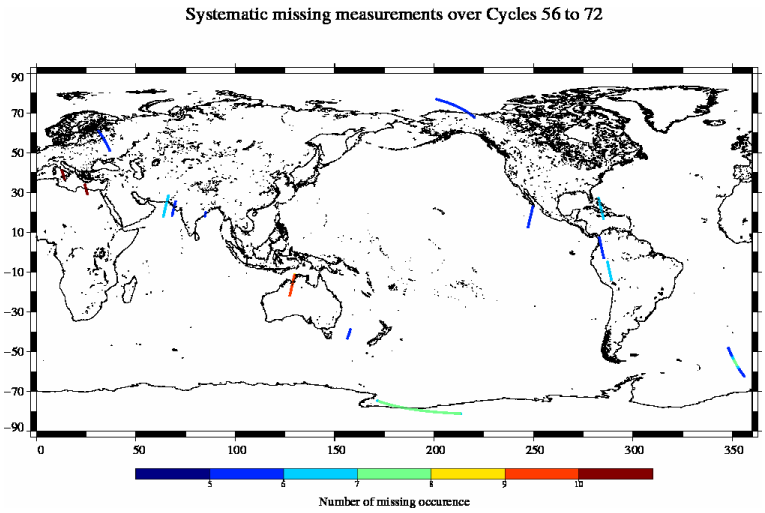

Figure 5: *Pass segments unavailable more than 5 times between cycles 56 and 72 . The color indicates the occurrence of unavailability*

Finally, the list of instrument and platform events is available in Part . Apart from instrumental and platform events, up to 3% of measurements can be missing because of data generation problems at ground segment level: LRAC or PDHS level1 data generation problems or ingestion problems on F-PAC side.

4.2. Missing MWR data

The Envisat MWR exhibits nearly 100% (Dedieu et al., 2005) of availability since the beginning of the mission. However, MWR corrections can be missing in the GDRs due to data generation problems at ground segment level. When the Land/sea radiometer flag is set to land over ocean, it means that the radiometer data is missing. The percentage of missing MWR corrections over ocean has been plotted in Figure 6. The radiometer unavailability is not constant: it is greater than 4% for cycles 14 to 19 and for cycles 58 and 60, and lower than 2% elsewhere. In 2008, the MWR unavailability is very stable and very low around 0.4%.

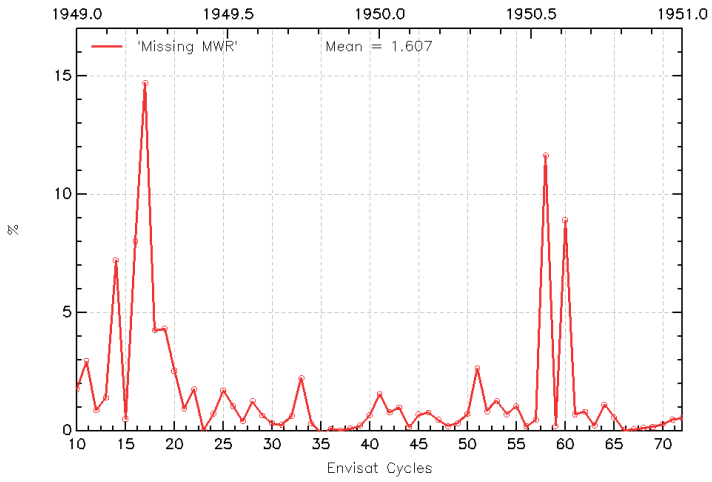

Figure 6: *Cycle per cycle percentages of missing MWR measurements*

4.3. Edited measurements

Data editing is necessary to remove altimeter measurements having lower accuracy. There are 4 steps in the editing procedure. The first step of the editing procedure consisted in removing data impacted by the S-Band anomaly. Note that this step is not necessary anymore from cycle 60 onwards, when the source of the anomaly was solved. Therefore, the first step is now the removal of data corrupted by sea ice. Then, measurements are edited using thresholds on several parameters. The third step uses cubic splines adjustments to the ENVISAT Sea Surface Height (SSH) to detect remaining spurious measurements. The last step consists in removing entire pass where SSH-MSS mean and standard deviation have unexpected value.

4.3.1. Measurements impacted by S-Band anomaly

During the Commissioning Phase, it has been discovered that the RA-2 data are affected by the so-called S-Band anomaly. The anomaly results in the accumulation of the S-Band echo

waveforms (Laxon and Roca, 2002 [44]). It happens randomly after an acquisition sequence and is only stopped by switching the Ra-2 in a Stand-By mode. When this anomaly occurs, the S-Band waveforms are not meaningful. Consequently, all the S-Band parameters and the Dual Frequency ionosphere correction are not reliable. Notably, the S-Band Sigma0 is unrealistically high during these events. Thus applying a threshold of 5 dB on the (Ku-S) Sigma0 differences is very efficient for detecting the impacted data over ocean. The ratio of flagged measurements over ocean is plotted in Figure 7. A method has been developed to flag the impacted data over all surfaces (Martini et al., 2005 [52]). This flag is available in the GDR product since cycle 51 and has been applied in our internal data base from cycle 54 onwards.

Except from cycle 10 where 33% of the data are impacted (before any solution as found), between 0 and 8% of the data are affected by the S-Band anomaly. From cycle 31 onwards, some modifications have been performed by ESA to decrease the duration of these events: instrument switch-offs (Heater 2 mode) were performed twice a day over the Himalayan and Rocky mountain region. This prevents the S-Band anomaly from lasting more than half a day. Thanks to this procedure the ratio of impacted data decreased from 4.2% (cycles 11 to 30) to 2.2% (cycles 31 to 38). On the 27th of June 2007 (cycle 60) an on-board patch solving the problem has been successfully uploaded. Since then and until the S-Band loss, no occurrences of the anomaly have been detected.

Finally, an algorithm for the S-Band waveform reconstruction has been developed which will enable recovery of data affected by the anomaly. The correction will be achieved with the full mission reprocessing campaign scheduled for 2009.

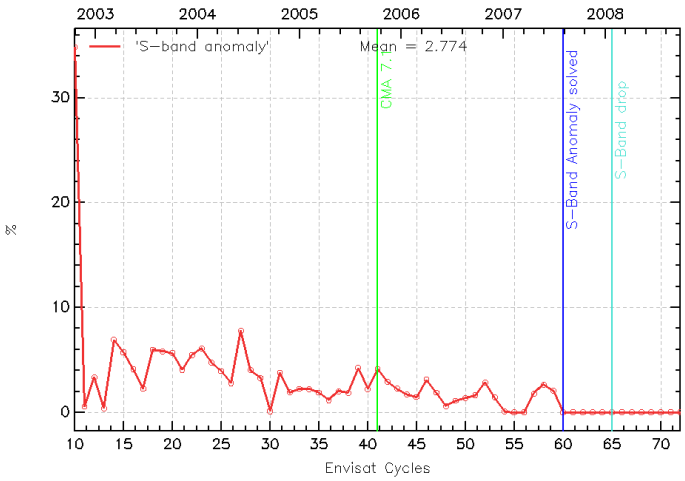

Figure 7: *Cycle per cycle percentages of data impacted by the S-Band anomaly and major events concerning the band.*

4.3.2. Measurements impacted by Sea Ice

Since Envisat operates between 82N and 82S of latitude, sea ice detection is an important issue for oceanic applications. No ice flag is currently available in the Envisat products, therefore alternate

sea ice detection techniques are used in order to retain only open ocean data. A study performed during the validation phase showed that the combination of altimetric and radiometric criteria was particularly efficient to flag most of the data over ice. The method is described in detail in (Faugere et al, 2003 [28]). We employ the Peakiness parameter (Lillibridge et al, 2005 [48]) in conjunction with the MWR- ECMWF wet troposphere difference which appears to be a good means to complement the Peakiness parameter in all ice conditions.

The ratio of flagged measurements over ocean is plotted on Figure 8

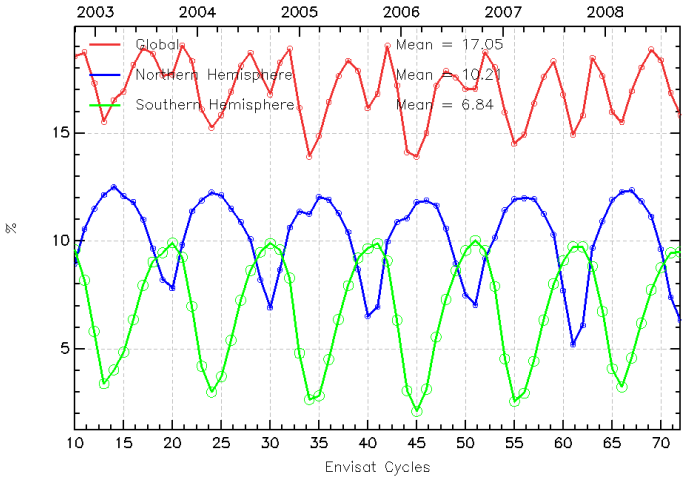

Figure 8: *% of edited points by sea ice flag over ocean*

In September 2007, a record-breaking minimum of flagged data for the Northern Hemisphere zone around cycles 61-63 see Figure 33, due to a low ice extend record. This was observed by different Envisat instruments including its altimeter RA2. For the first time, a altimeter satellite could observe open ocean surfaces up to 82°N above Siberia in September. See further details on http://www.aviso.oceanobs.com/en/applications/glace/glaces-de-mer/l-etendue-des-glaces-de-l-arctique-vue-par-l-altimetre-d-envisat/index.html.

Note that between cycle 61 and 63, an increase of the global cyclic standard deviation of sea level anomaly was noticed. This is due to 2007's low ice extent record. For the first time, an altimetric satellite measured open water sea surface height North East Siberia until 82° during September-October 2007 (see Figure 9). Inaccurate Mean Sea Surface or tide models in this area might explain these low SLA performances.

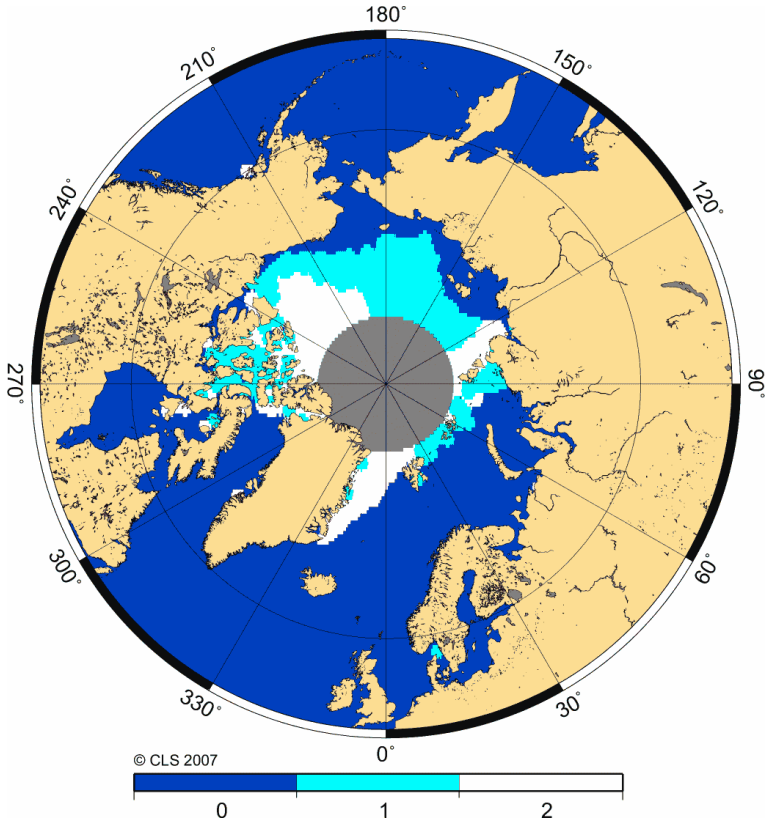

Figure 9: *Sea ice coverage seen by Envisat RA-2, averaged 1° by 1° over September 2007 and compared to an average over the previous years (2003-2006). Dark blue = open ocean, White = usual ice coverage, Light blue = open ocean seen in 2007 where sea ice was observed previously.*

4.3.3. Editing by thresholds

The second step of the editing procedure consists in using thresholds on several parameters. The minimum and maximum thresholds used in the routine quality assessment are given in table 4.

Parameter	Min thresholds	Max thresholds
Sea surface height (m)	−130	100
Variability relative to MSS (m)	−2	2
Number of 18Hz valid points	10	–
Std deviation of 18Hz range (m)	0	0.25
Off nadir angle from waveform (deg2)	−0.200	0.160
		.../...

Parameter	Min thresholds	Max thresholds
Dry troposphere correction (m)	−2.500	−1.900
Inverted barometer correction (m)	−2.000	2.000
MWR wet troposphere correction (m)	−0.500	0.001
Dual Ionosphere correction (m)	−0.200	−0.001
Significant waveheight (m)	0.0	11.0
Sea State Bias (m)	−0.5	0
Backscatter coefficient (dB)	7	30
Ocean tide height (m)	−5	5
Long period tide height (m)	−0.500	0.500
Earth tide (m)	−1.000	1.000
Pole tide (m)	−5.000	5.000
RA2 wind speed (m/s)	0.000	30.000

Table 4: *E*diting criteria

The thresholds are expected to remain constant throughout the ENVISAT mission, so that monitoring the number of edited measurements allows a survey of data quality. The percentage of edited measurements over ocean for the main altimeter and radiometer parameters has been plotted in Figure 10. These ratios are very stable and surprisingly low over the period if compared to other altimeters. The RMS of elementary measurements has the strongest ratio among the altimeter parameters, more than 1% in average. On cycle 47, a special operation was executed to limit RA-2 Chirp Bandwidth to 80MHz. It has impacted this parameter as well as the dual frequency ratio. A slight seasonal signal is visible on the curve, mostly due to sea state seasonal variations. The number of elementary measurements has a surprisingly low ratio, except for cycles 14 and 20 when wrong configuration files were uploaded on-board after a RA-2 event. A slight increase is noticed from cycle 54 onwards due to the use of the product S-Band anomaly flag instead of the criteria based on KU/S Sigma0 difference. The square of the off-nadir angle derived from waveforms leads to very stable editing ratio but with a drop on cycle 41, due to a change of the algorithm in CMA7.1. Variations of this parameter can reveal actual platform mispointing, if any, but can also reveal waveform contamination by rain or by sea-ice. It is indeed computed from the slope of trailing edge when fitting a typical ocean model to the waveforms. No seasonal signal is visible which may prove that the sea-ice detection method is efficient. The dual frequency ratio shows a slight increasing trend between cycles 15 and 28 which cannot be considered as significant, given the scatter of the curve. The Ku-band SWH, sigma0 also present a slight increase, mainly since cycle 41. Concerning MWR ratios it is very stable and low before cycle 41 and still low but more cahotic afterwards. The variations cohincidate with the ECMWF model changes presented further.

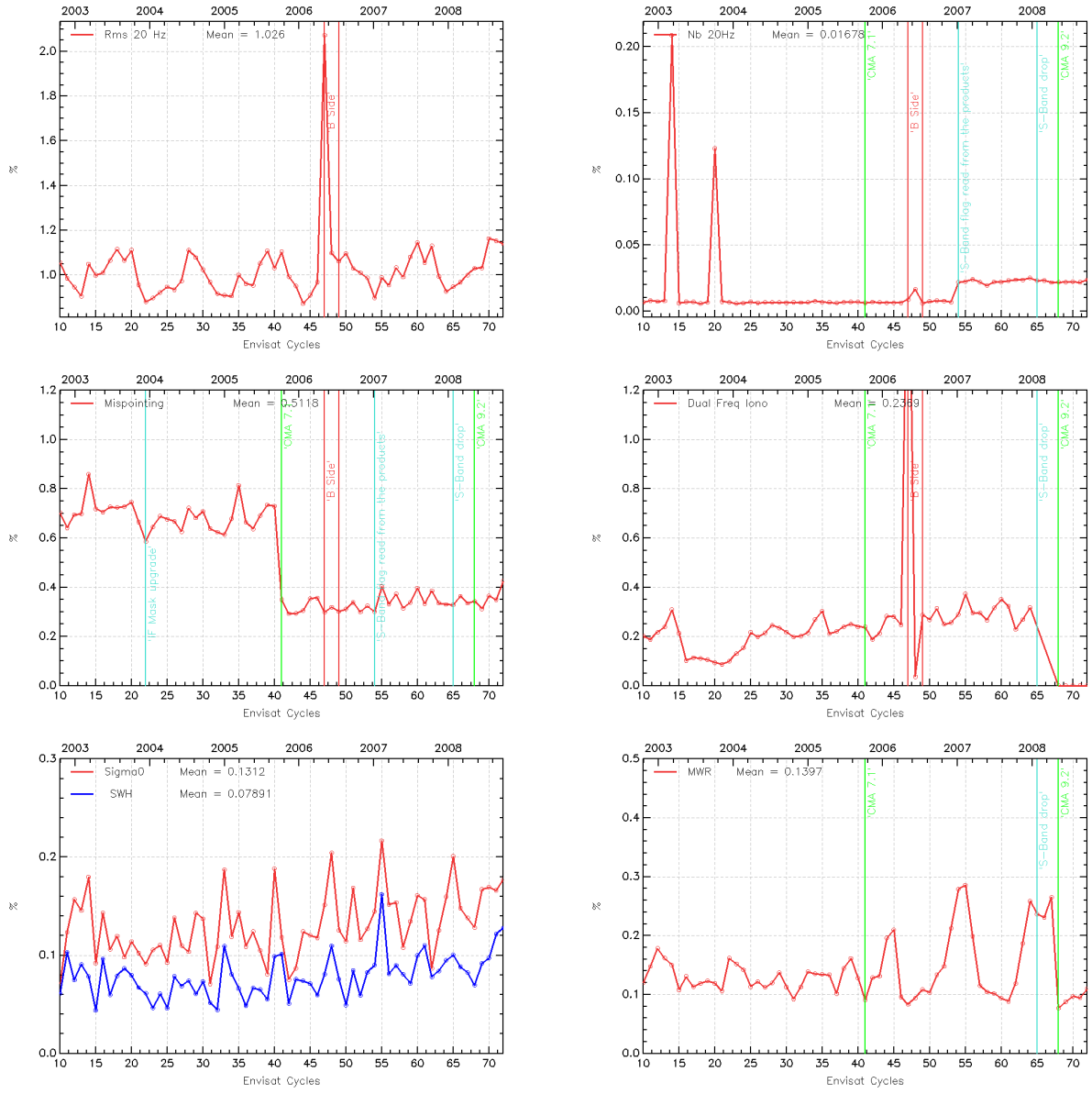

Figure 10: *Cycle per cycle percentages of edited measurements by the main Envisat altimeter and radiometer parameters:* ***Top-Left****) Rms of 20 Hz range measurements > 25 cm,* ***Top-Right****) Number of 20-Hz range measurements < 10,* ***Middle-Left****) Dual frequency ionosphere correction out of [-40 , 4 cm],* ***Middle-Right****) Square of off-nadir angle (from waveforms) out of the [-0.2 deg2, 0.16 deg2] range,* ***Bot-Left****) MWR wet troposphere correction out of the [-50 cm, -0.1 cm] range,* ***Bot-Right****)Ku-band Significant wave height outside > 11 m, Ku band backscatter coefficient out of the [7 dB, 30 dB] range.*

4.3.4. Editing on SLA

It has been necessary to apply additional editing criteria on SSH-MSS differences in order to remove remaining spurious data. The first criterion consists in removing measurements with SSH-MSS greater than 2m. The strong value on cycle 30 is due to the first occurrence of the USO anomaly. The second criterion was necessary to detect measurements impacted by maneuvers. Maneuvers are necessary to compensate the effect of gravitational forces but can have a strong impact on the orbit quality. Two types of maneuvers are operated to maintain the satellite ground track within the +/-1km deadband around the reference ground track: in-plane maneuvers, every 30-50 days, which only impact the altitude of the satellite and out-of-plane maneuvers, three times a year, to control the inclination of the satellite (Rudolph et al., 2005). The out-of-plane maneuvers are the most problematic for the orbit computation. The second criterion consists in testing the mean and standard deviation of the SSH-MSS over each entire pass. If one of the two values, computed on a selected dataset, is abnormally high, then the entire pass is edited.

A specific study has been performed to determine how to compute the statistics, and what threshold should be applied. The statistics have to be computed on very stable area. The criteria for selecting the area and the thresholds are detailed is:

- The latitude: the range value can be degraded near the ice, despite the use of the ice flag. Moreover, the MSS is less accurate over 66 $^\circ$, as it has been computed without Topex data.
- The oceanic variability: the standard deviation of SLA can be very high because of the mesoscale variability. Areas with high oceanic variability have to be removed to detect the abnormally high standard deviation.
- The bathymetry and distance from the coast: A lot of corrections (tides for example) are less accurate in low bathymetry areas and near the coast (Japan sea).
- The sample: The statistic have to be computed on a significant number of points

All those criteria have been tested and combined as part as a specific study in a previous yearly report. The conclusion is that two criteria are needed:
1st **criteria**:
for small portion of pass (less than 200 points) the sample is not big enough to compute reliable statistic. The selection must not be severe: Selected areas: —latitude—<66 $^\circ$, variability<30cm, bathymetry>1000m, distance to coast>100km Threshold: 30 cm on mean and standard deviation
2nd **criteria**:
for other passes Selected areas: —latitude—<66 $^\circ$, variability<10cm, bathymetry>1000m, distance>100km Threshold: 15 cm on mean and standard deviation

The percentage of edited measurements over ocean for the main altimeter and radiometer parameters has been plotted in Figure 11. On cycles 11, 12, 21 and 26, several full passes have been edited because of bad orbit quality related to out-of-plane maneuver or lack of Doris data (cycle 11).The special operation on RA-2 Chirp Bandwidth mentioned previously impacted the SSH editing ratio on cycle 47. On cycle 56 an USO anomaly recovery, occurred at the beginning of cycle and impacted the SSH statistic editing per pass.The behavior of the Ultra Stable Oscillator (USO) clock frequency on this cycle is chaotic. The transitions between anomaly and normal mode

has been very straight and the USO correction does not allow us to well correct some passes.

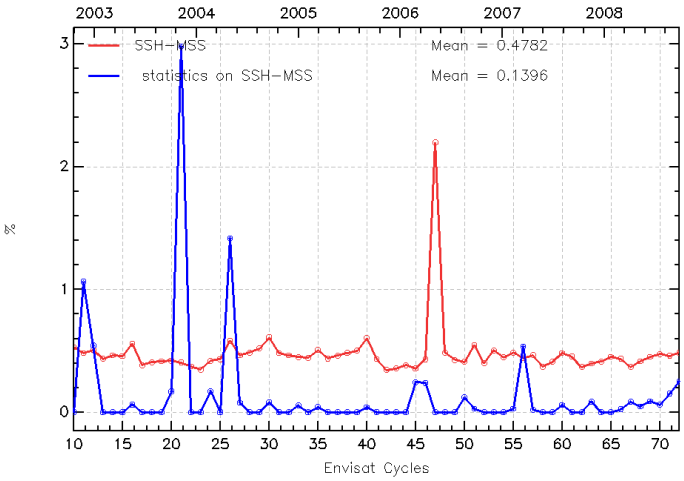

Figure 11: *SSH-MSS out of the [-2, 2m] and edited using thresholds on the mean and standard deviation of SSH-MSS on each pass*

Note that for cycles 71 and 72, some entire tracks were edited on the SLA statistic criteria because their standard deviations were above the thresholds due to a geophysical reason: a strong eddy near South Africa (see Figures 12). Although the thresholds were chosen on a robust 15 years multimissions statistics basis, this eddy causes an over-editing on the three current altimetric missions (Jason-1, Jason-2 and Envisat). Consequently, the concerned criteria needs to be refined to avoid such irrelevant editing.

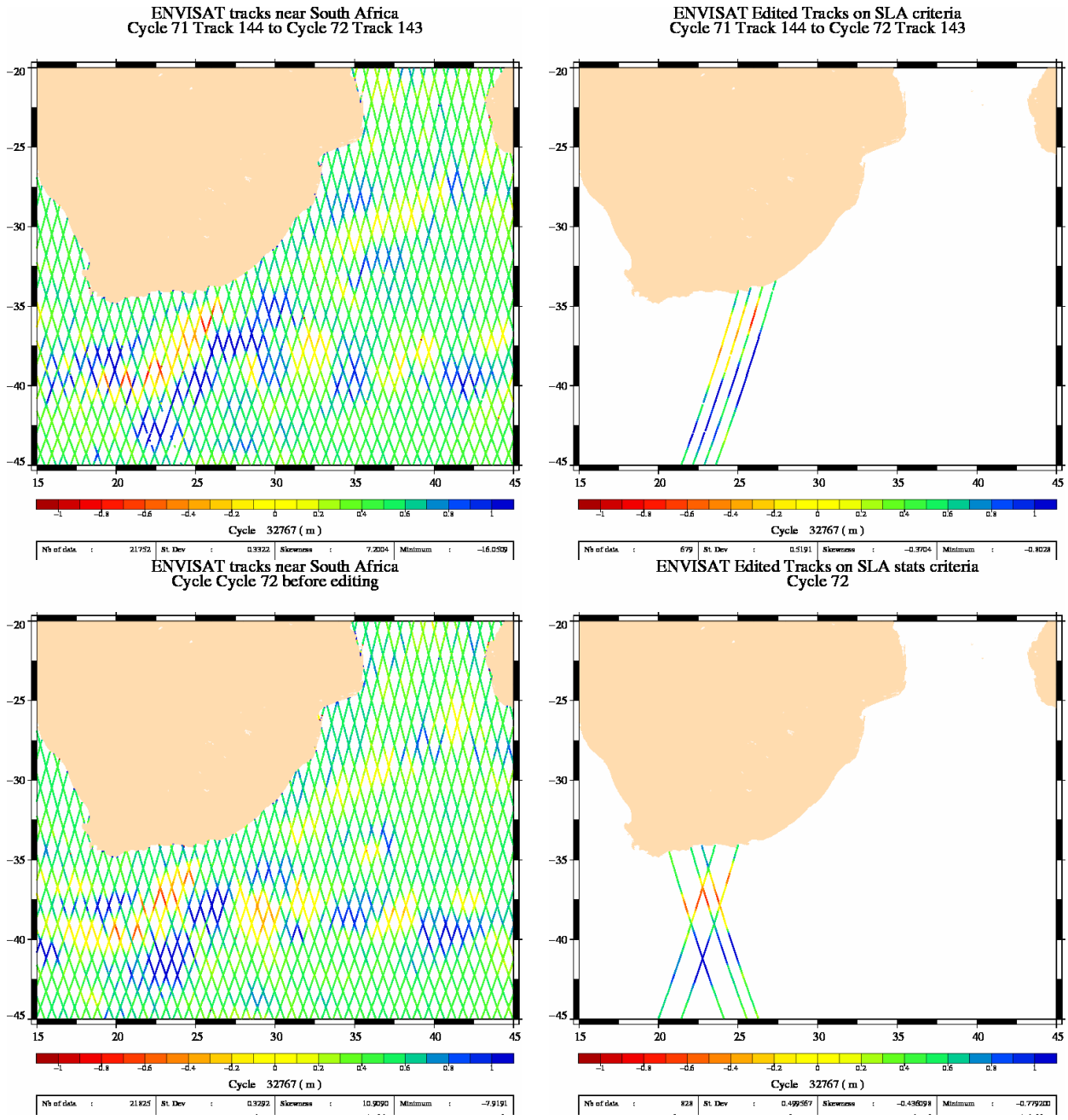

Figure 12: ***Top-Left*** *Strong variability eddy, Cycle 71.* ***Top-Right*** *Over edited data, Cycle 71.****Bot-Left*** *Strong variability eddy, Cycle 72.* ***Bot-Right*** *Over edited data, Cycle 72.*

5. Long term monitoring of altimeter and radiometer parameters

All GDR fields are systematically checked and carefully monitored as part of the Envisat routine calibration and validation tasks. However, only the main Ku-band parameters are presented here, as they are the most significant in terms of data quality and instrumental stability. Furthermore, all statistics are computed on valid ocean datasets after the editing procedure.

5.1. Number and standard deviation of 20Hz elementary Ku-Band data

As part of the ground segment processing, a regression is performed to derive the 1 Hz range from 20 Hz data. Through an iterative regression process, elementary ranges too far from the regression line are discarded until convergence is reached. The mean number and RMS of Ku 20Hz elementary data used to compute the 1Hz average are plotted in figure 13. These two parameters are nearly constant, which provides an indication of the RA-2 altimeter stability. The mean number of Ku 20Hz values over one cycle is about 19.97. This value is very high compared to other altimeters. It is almost not disturbed in wet areas or near the coast. The two drops on the Ku-band on cycles 14 and 20 are due to wrong setting of the RA-2 just after recovery. A slight seasonal signal is visible on the mean RMS of Ku 20Hz. Higher values correspond to higher waves occurring during the austral winter. The mean value is about 9.0 cm. This value represents a rough estimation of the 20 Hz altimeter noise (Zanifé et al. 2003 [78], Vincent et al. 2003a [76]). Assuming that the 20Hz measurements have uncorrelated noise, it corresponds to a noise of about 2 cm at 1Hz. It is consistent with the expected noise values.

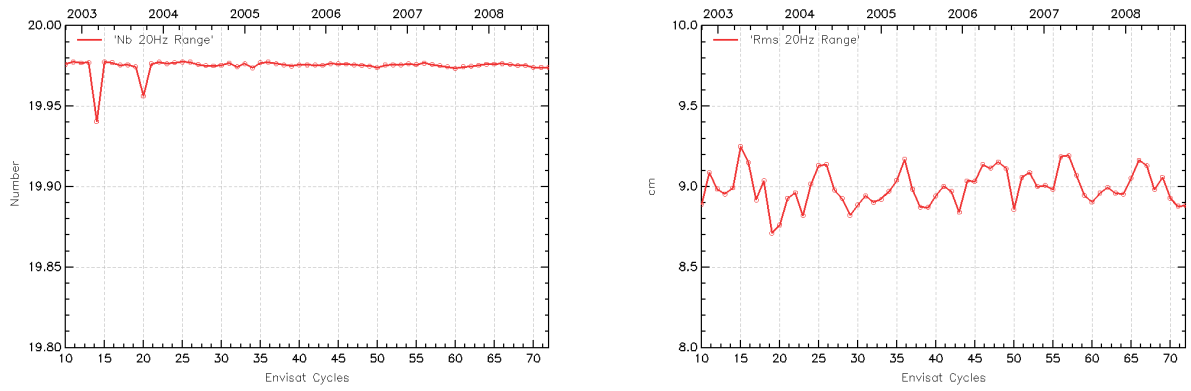

Figure 13: ***left)*** *Mean per cycle of the number of 20 Hz elementary range measurements used to compute 1 Hz range.* ***right)*** *Mean per cycle of the standard deviation of 20 Hz measurements.*

The corresponding S-Band parameters have a less stable behaviour (see figure 14). The S-Band mean number and RMS of 20Hz measurements have respectively an increasing and decreasing trend. Moreover jumps are noticed on the two plots on cycle 41 due to a change in the IPF Level 1 processing chain (Rx dist Fine). Moreover, from this cycle, the ascending and descending values are slightly different on the S-Band mean RMS of 20Hz measurements.

Histograms of RMS of Ku Range on cycle 72 is plotted in figure 15.

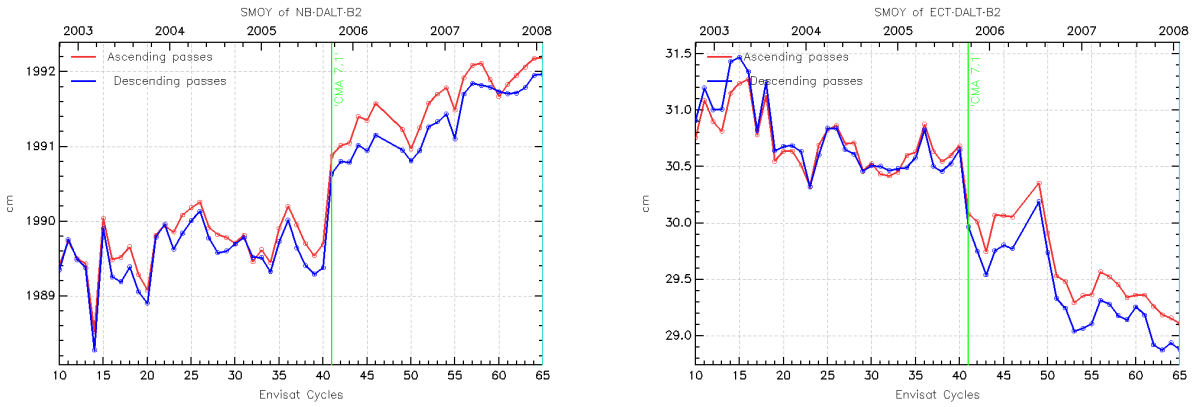

Figure 14: *Mean per cycle of the S-Band standard deviation of 20 Hz measurements separating ascending and descending passes (cm)*

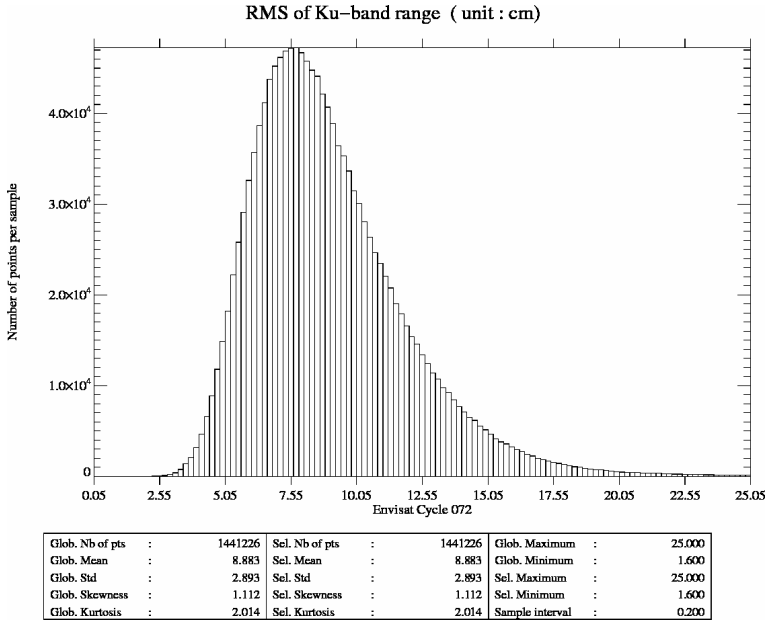

Figure 15: *Histogram of RMS of Ku range (cm). Cycle 72 .*

5.2. Off-nadir angle from waveforms

The off-nadir angle is estimated from the waveform shape during the altimeter processing. The square of the off-nadir angle is plotted in Figure 16. The mean value is between 0.02 deg2 and 0.03deg2 before cycle 41. There is a slight rising trend over this period and a 0.005 deg2 jump between cycles 21 and 22 which is due to the upgrade of the IF mask filter auxiliary data file. The mean value observed during this period is not significant in terms of actual platform mispointing. This is due to the way the slope of the waveform trailing edge is computed. On cycle 41, a 0.02 deg2 drop occurs, due to an improvement of the mispointing estimation in IPF 5.02. The mispointing was estimated through the waveform trailing edge slope using an adaptative window that defines the beginning and the end of the slope. To avoid the filter bump effect that leads to high value of the mispointing, an optimum and fixed gate was estimated and implemented. Note

that the rising trend observed previously desappeared. This is probably an effect of the regular update of the IF filter since cycle 41. Finally, a smaller value is noticed for the cycle 48, for which altimeter was turned to its B-Side for a short period (cf. details in part **??**).

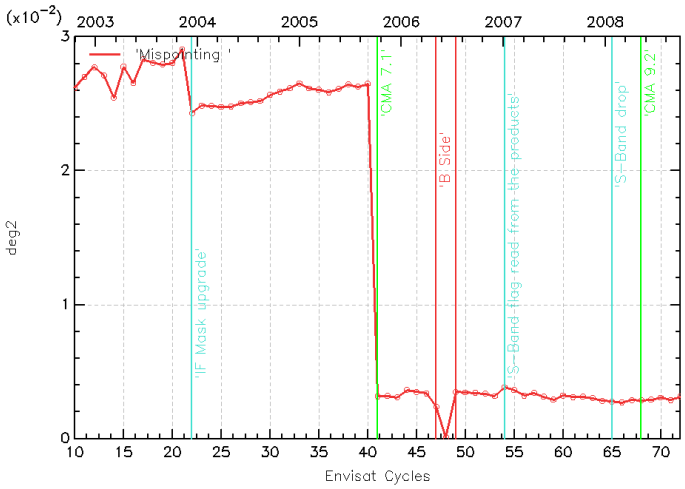

Figure 16: *Mean per cycle of the square of the off-nadir angle deduced from waveforms (deg2).*

The histogram of the squared mispointing is plotted in figure 17.

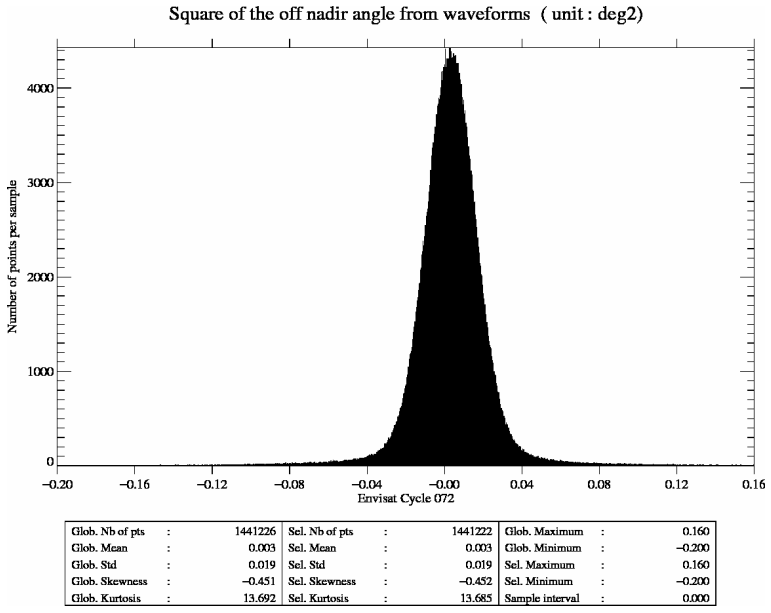

Figure 17: *Histogram of off-nadir angle from waveforms (deg2). Cycle 72 .*

5.3. Significant Wave Height

The cycle by cycle mean and standard deviation of Ku and S-Band SWH are also plotted in figure 18. The curve reflects sea state variations. The mean value of Ku SWH is 2.66 m. The S-Band mean SWH is very close, less than 10 cm apart. The cycle by cycle mean of

Envisat-Jason-1 differences and ERS-2-Envisat differences are plotted in Figure 18. Note that for ERS, data concern the sole North Atlantic ocean (since july 2003, see **??**). For contractual reasons, they are not monitored anymore after cycle 42. These differences are quite stable. Envisat SWH is respectively 14 cm and 22 cm higher than Jason-1 and ERS-2 SWH. As for range parameters, some strange behaviours on S-Band SWH are also noticed (see Figure 19): jumps occurred during the S-Band time series (cycle 41 and 51) due to a change in the IPF Level 1 processing chain (Rx dist fine), and inconsistencies between ascending and descending passes.

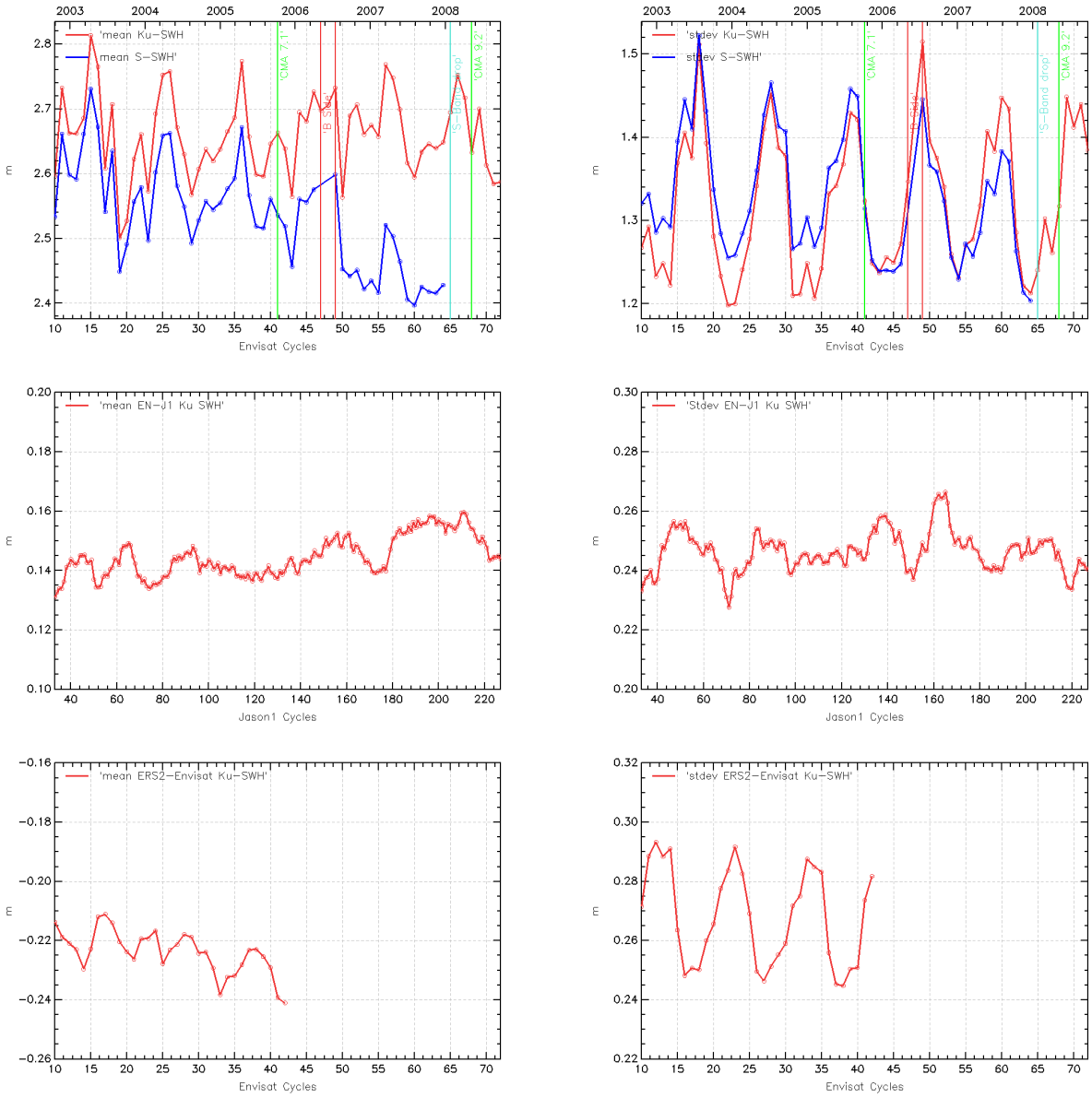

Figure 18: *Global statistics (m) of Envisat Ku and S SWH* ***top****) Mean and Standard deviation.* ***middle****) Mean Envisat-Jason-1 Ku SWH differences at 3h EN/J1 crossovers computed with 120 days running means.* ***bottom****) Mean and Standard deviation of ERS-2-Envisat Ku SWH collinear differences over the Atlantic Ocean.*

Histograms of Ku SWH is plotted in figure 20. The Ku SWH histogram has a good shape.

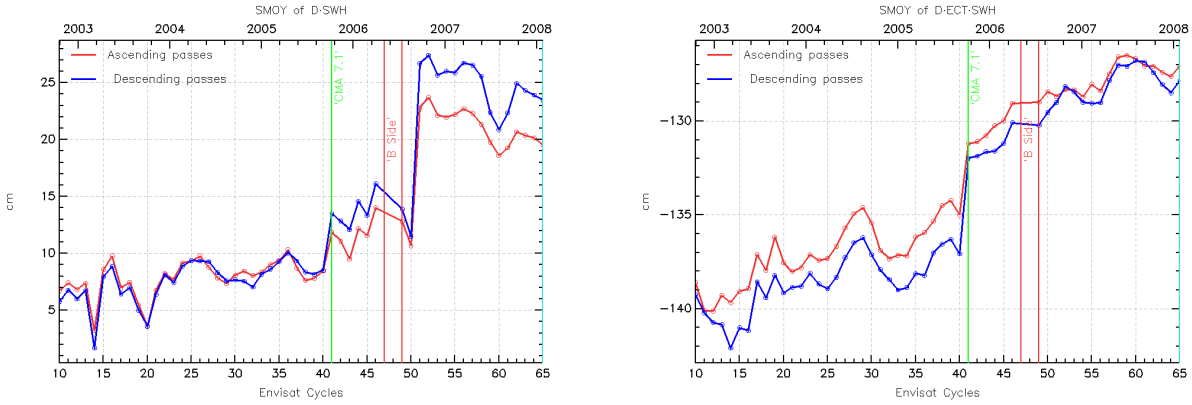

Figure 19: ***left)*** *Mean per cycle of SWH(Ku)-SWH(S).* ***right)*** *Mean per cycle of RMS20Hz[SWH(Ku)]-RMS20Hz[SWH(S)].*

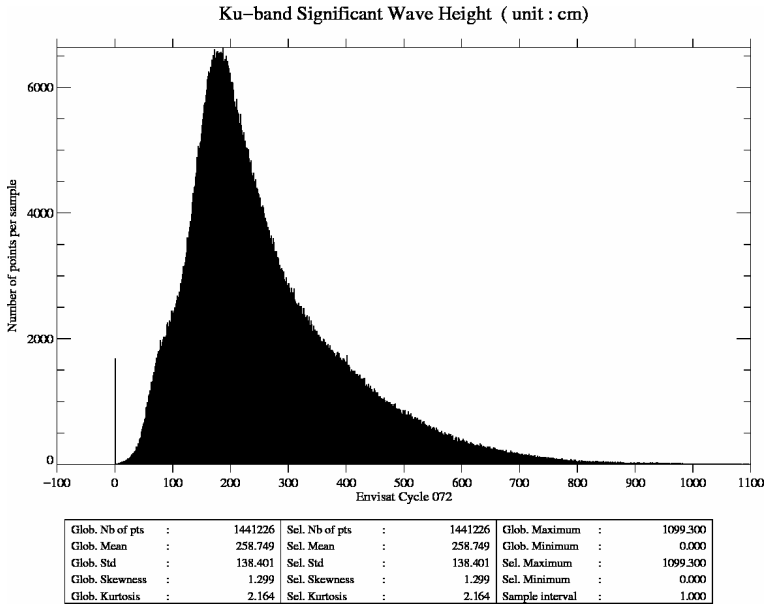

Figure 20: *Histogram of Ku SWH (m). Cycle 72 .*

5.4. Backscatter coefficient

The cycle by cycle mean and standard deviation Ku and S-Band Sigma0 are plotted in Figure 22. Note that a -3.5 dB bias has been applied (Roca et al., 2003 [63]) on the Ku-band Sigma0 in order to be compliant with the wind speed model (Witter and Chelton, 1991 [77]). The mean values in Ku band are stable, around 11.1 dB. Two 0.66 dB jumps are visible on the S-Band on cycles 14 and 22. They are due to a correction of the AGC evaluation. This modification has been included in IPF version 4.56, used from cycle 22 onwards for the current processing and for all the reprocessed cycles. The cycle by cycle mean of Envisat-Jason-1 differences and ERS-2-Envisat differences are plotted in figure 22. The mean difference between Envisat and Jason-1 Ku-band Sigma0 is -2.9 dB. This high value is explained by the fact that, Envisat Sigma0 value has been biased and not Jason-1. This mean difference has increased by 4.10-2dB/year between cycles 38 and 140 Jason-1 (corresponding to cycle 13 to 41 of Envisat) and remains constant afterwards. This drift was checked to be unchanged after correcting it from the atmospheric attenuation computed with a homogenous reprocessed set of brightness temperature. These sigma0 differences obviously impact the wind consistency between the two satellites. Note that the wind from the ECMWF model, which does not assimilate Jason-1 data, shows a very good agreement with the Jason-1 wind with a slope close to 6 cm/s/yr whereas Envisat wind trend is much lower, 1.3cm/s/year (see [4]. This trend difference could mean that the Envisat wind slightly drifts. This potential trend, though slight, has to be closely monitored.

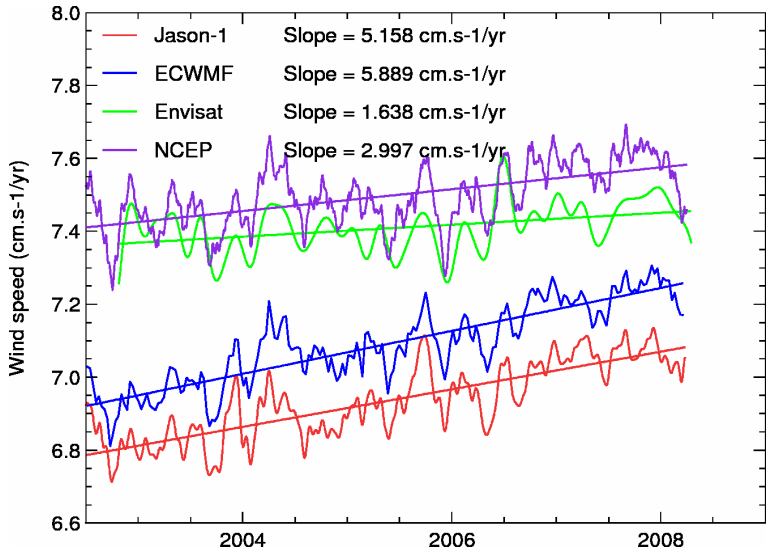

Figure 21: *Wind speed from different sources (EN, J1, ECMWF, NCEP).*

The mean ERS-2-Envisat Ku-band Sigma0 difference is 0.05 dB. However, this mean value accounts for the calibration correction applied in the ground processing to be compliant with the wind speed algorithm (Witter and Chelton, 1991 [77]). The monitoring of (ERS-2 - Envisat) Sigma0 differences exhibits a 0.1 dB jump between cycles 38 and 39. This jump occurs at the end of cycle 38, on the 4th July 2005 11:29 UTC. Since no jump is observed on the Envisat/Jason-1 differences, it may be attributed to ERS-2.

Histograms of Ku Sigma0 is plotted in figure 23. The Ku Sigma0 histogram has a good shape.

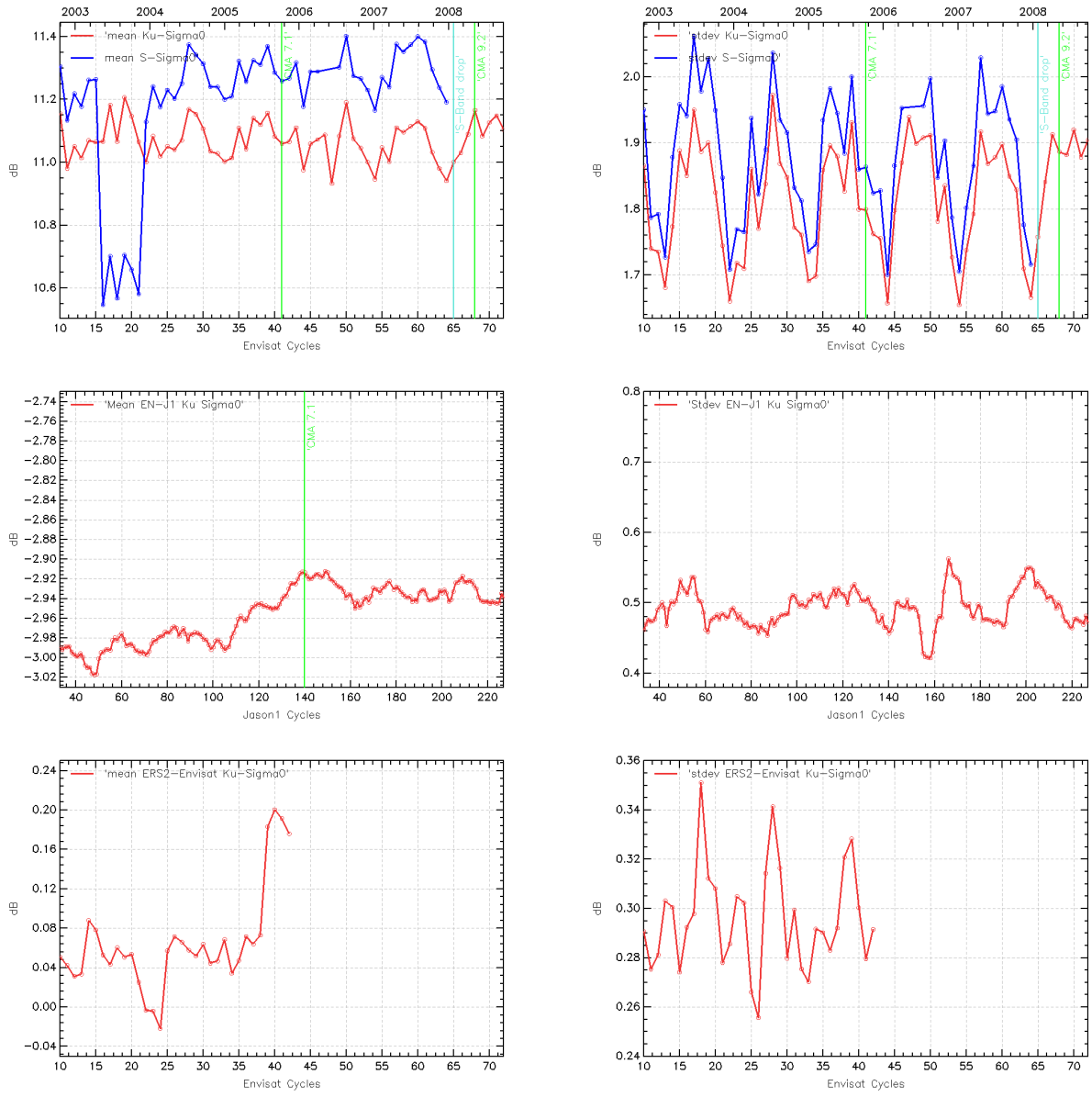

Figure 22: *Global statistics (dB) of* ***top****) Envisat Ku and S Sigma0 Mean and Standard deviation.* ***middle****) Mean Envisat-Jason-1 Ku Sigma0 differences at 3h EN/J1 crossovers computed with 120 days running means.* ***bottom****) Mean and Standard deviation of ERS-2-Envisat Ku Sigma0 collinear differences over the Atlantic Ocean.*

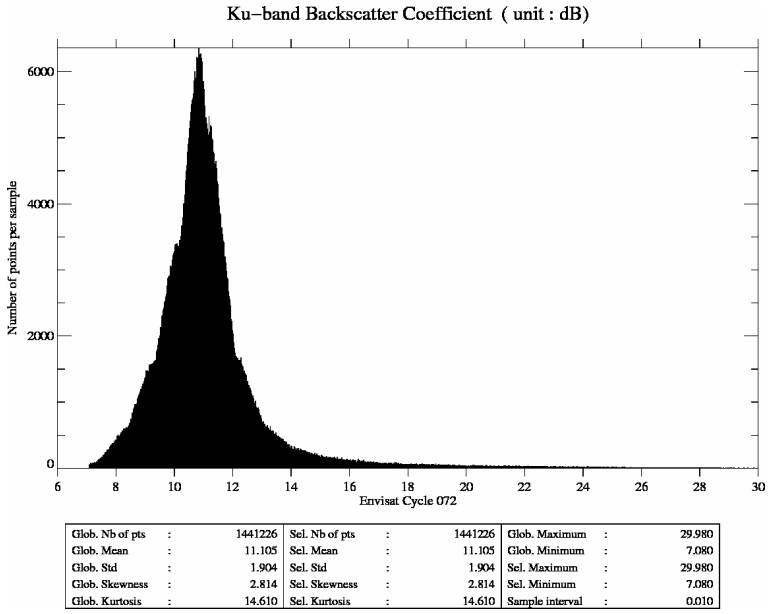

Figure 23: *Histogram of Ku Sigma0 (dB). Cycle 72 .*

5.5. Dual frequency ionosphere correction

As performed on TOPEX (Le Traon et al. 1994 [45]) and Jason-1 (Chambers et al. 2002 [15]) it is recommended to filter dual frequency ionosphere correction on each altimeter dataset to reduce noise. A 300-km low pass filter is thus applied along track on the dual frequency ionosphere correction. As previously mentioned, the JPL GIM ionosphere corrections are computed to assess the dual frequency altimeter based ionosphere correction. The cycle by cycle mean of dual frequency and JPL GIM ionosphere correction are plotted in figure 24. The mean value of the two corrections is clearly decreasing since the beginning of Envisat mission due to inter-annual reduction of the solar activity. The mean differences (GIM-Dual frequency), plotted in figure 24, is stable around -0.8 cm. It is stronger in absolute value for high ionosphere corrections, for descending passes (in the daytime). The standard deviation of the difference is plotted in figure 24. Low values, less than 2 cm, indicate a good correlation between dual-frequency and GIM corrections. Notice that, in the GDR products, the same sea state bias (SSB) has been used to correct the Ku and S-Band Ranges for cycles 9-40. Since cycle 41, a suitable Ku and S-Band SSB correction is used on the two bands before computing the dual frequency ionosphere correction from Ku and S-Band ranges (Labroue 2004 [41]). In this analysis, the sea state bias (SSB) used to correct the S-Band Ranges for cycles 9-40 is updated in its right S-Band version. The differences with the GDR correction are very small with no impact on the global statistics and only small geographic variations between -1 mm and +1.5 mm (Labroue 2004 [41]). However, the update was done because the impact was shown to be significant in the Mean Sea Level Trend estimation of around 0.4 mm/year (Particular investigation MSL).

Since the S-Band loss, this correction is not available anymore. As written before, the GIM Ionospheric correction is used instead. The same GIM model is used to compute the GIM corrections on Envisat and Jason-1. The quality of Envisat's ionosphere correction can thus be assessed by monitoring the dual-frequency -GIM based ionosphere correction on Jason-1. The cycle by cycle mean of dual frequency and JPL GIM ionosphere correction are also plotted in figure 42. Different trends are observed on the two curves.
Concerning the discrepencies between both missions, note that, in terms of noise, the higher noise for Jason-1 is due to a higher noise in the C band (used for Jason-1 bifrequency ionosphere) than in S-Band (used for Envisat one). The filtering step applied on both ionospheres from the products anable to have comparable noise level for both missions. In terms of bias, differences are likely due to the difference of altitude for both missions, but the stability of Envisat ionosphere difference (Bifrequency-GIM) can also be seen as an anomaly at the beginning of Envisat mission (before cycle 22), reducing the dependancy between the absolute value and the bias on this correction (observed on Jason-1). This would deserve more investigation.

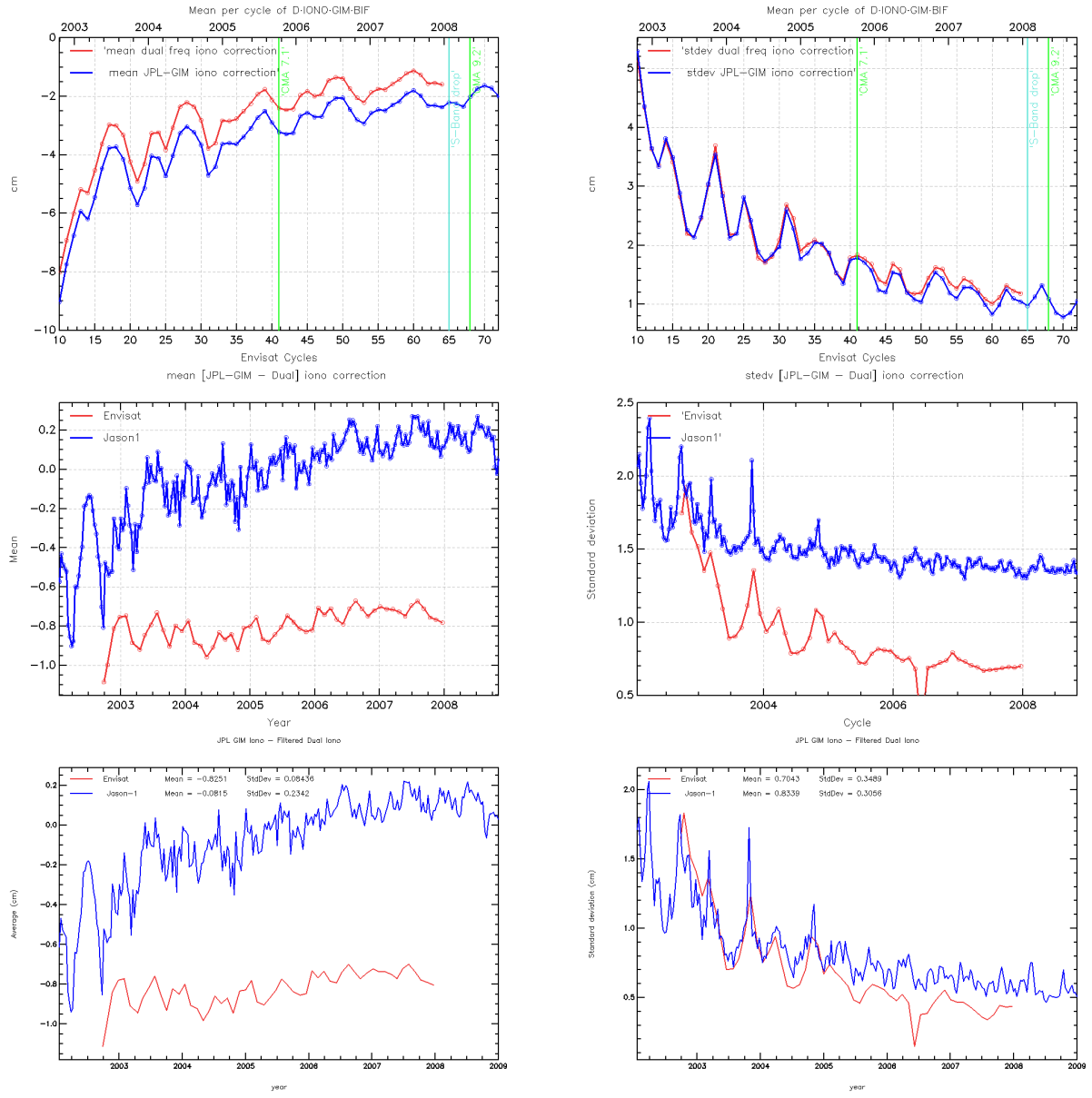

Figure 24: *Comparison of global statistics of Envisat dual-frequency and JPL-GIM ionosphere corrections (cm).* ***top****) Mean and standard deviation per cycle of Dual Frequency and GIM correction.* ***middle****) Mean and standard deviation per cycle of the difference Dual Frequency - GIM correction for Envisat and Jason-1.***bot****) Mean and standard deviation of the difference Filtered Dual ionosphere (used at CLS) - GIM for Envisat and Jason-1*

5.6. MWR wet troposphere correction

A neural network formulation is used in the inversion algorithm retrieving the wet troposphere correction from the measured brightness temperatures (Obligis et al., 2005 [58]). As an example, the scatter plot of MWR correction according to ECMWF model for cycle 72 is given in figure 25.

Since the beginning of the mission, the instrumental parameters at 36.5 GHz have been drifting

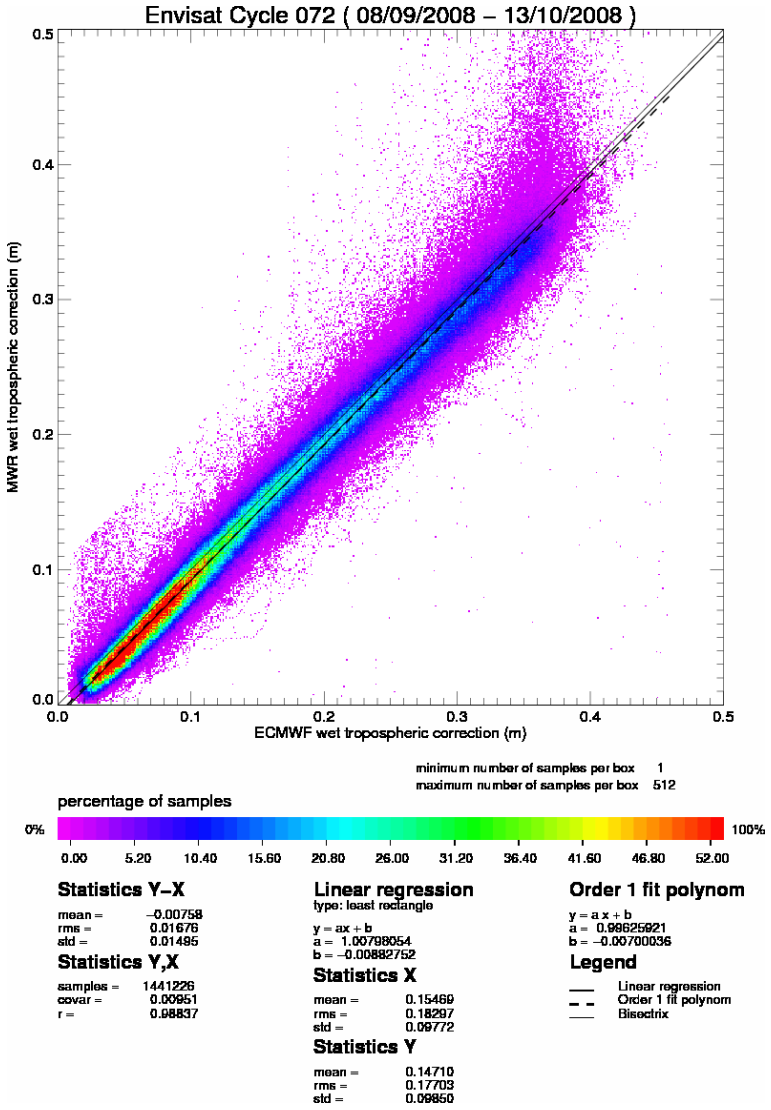

Figure 25: *Scatter plot of MWR correction according to ECMWF model (m)*

and investigations are in progress to identify the source for these drifts. In particular, different behavior is observed depending on the brightness temperature values. Mean and standard deviation of (MWR-ECMWF model) differences are plotted in figure 26. The difference is not really stable, though the global mean remains small. It rises by 3mm between cycles 11 and 27, which corresponds to 1.8 mm/year. Then, it decreases by 2mm between cycle 27 and 46. Finally, an annual signal of about 1.5mm of amplitude seems to appear on cycle 47, followed by a steep increase up to cycle 70, and another decrease afterwards. Moreover this annual signal has not the same amplitude on ascending (night) and descending (day) passes (figure 28). As explained into S. Abdalla's presentation (QWG 2008), this annual signal would more likely be due to successive jumps in the model because similar paterns can be seen when comparing the difference of correction radiometric - model on Jason-1(see 40). On the plot, the main model changes are marked out by vertical lines on the plots (see ECMWF web site [21]).
The standard deviation is also very variable throughout the mission. It drops down by 2 mm from cycle 13, decreases afterwards linearly from cycles 14 to 41 and adopts a cahotic behavior until cycle 65 where it stabilizes around 1.5 cm. This decrease cohincidates with another change

of model but because MWR seems to undergo a biger jump than ECMWF series, it could also be due to a larger amount of data taken into acount at the end of the mission (see part 4.3.4..)
A complete monitoring of all the radiometer parameters is available in the cyclic Envisat Microwave Radiometer Assessment available at http://earth.esa.int/pcs/envisat/mwr/reports/ ([16]).

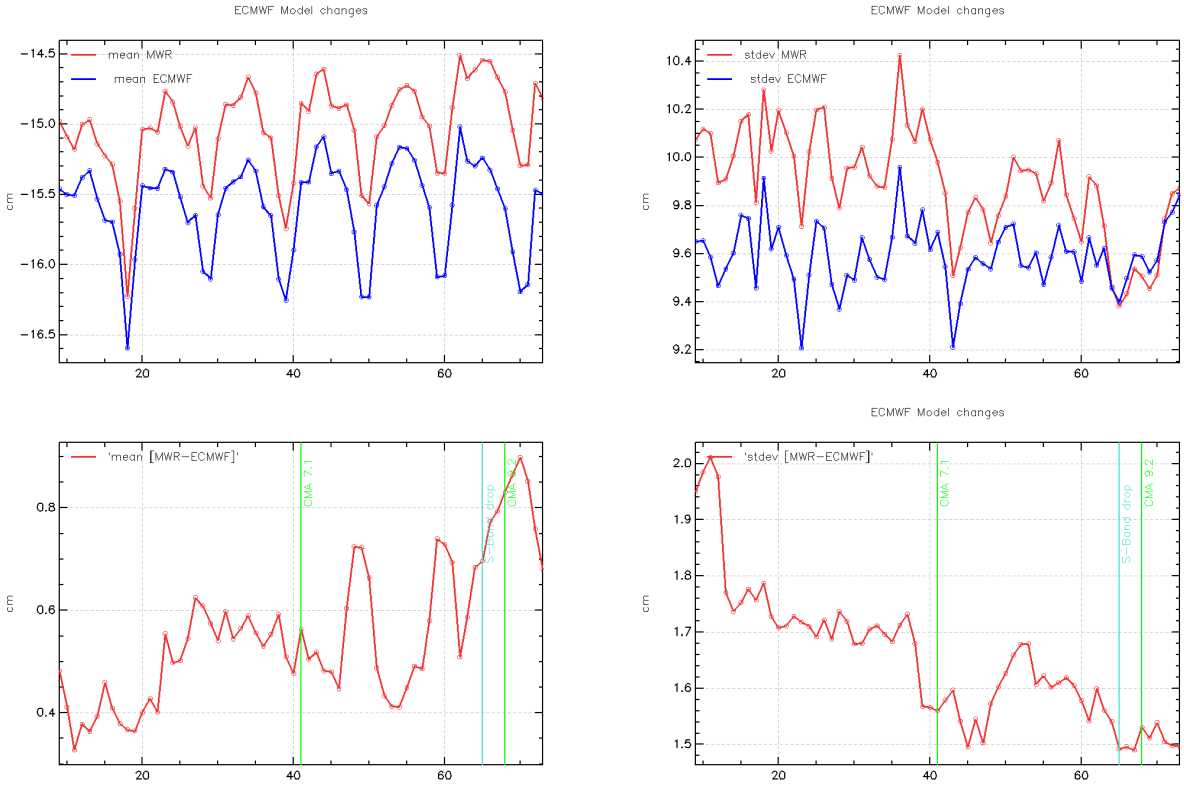

Figure 26: *Comparison of global statistics of Envisat MWR and ECMWF wet troposphere corrections (cm).* ***top****) Mean and standard deviation per cycle of MWR and ECMWF corrections* ***bot****) Mean and standard deviation of the differences. Vertical lines represent the major events.*

The (ERS-2 -Envisat) cyclic 23.8 GHz brightess temperatures differences over the Atlantic area are plotted on figure 29. The ERS-2 drift proposed by Eymard et al., 2003 [24] is applied. The correction of the drift proposed by Scharroo et al., 2004 [69], should decrease the mean difference by 0.8K as described in Mertz et al., 2004 [55]. Nevertheless, the mean difference variations are more steady for the period after cycle 21. The (ERS-2 -Envisat) TB36.5 GHz values are also reported in figure 29. The differences before and after cycle 18 have a different behaviour: one observes a great decrease from -2 to -4 K between cycles 13 and 17 whereas the curve seems to be steadier after cycle 18. This is not an impact of the coverage of the data since in the restricted area, the statistics reveals the same features. They also show an unusual behaviour of the TB values during that period. Note that this behaviour is not visible on hottest or coldest values but mainly on the mean values. The impact of the drift of the TB36.5 on (ERS-2 -Envisat) wet troposphere correction differences is visible in figure 30.

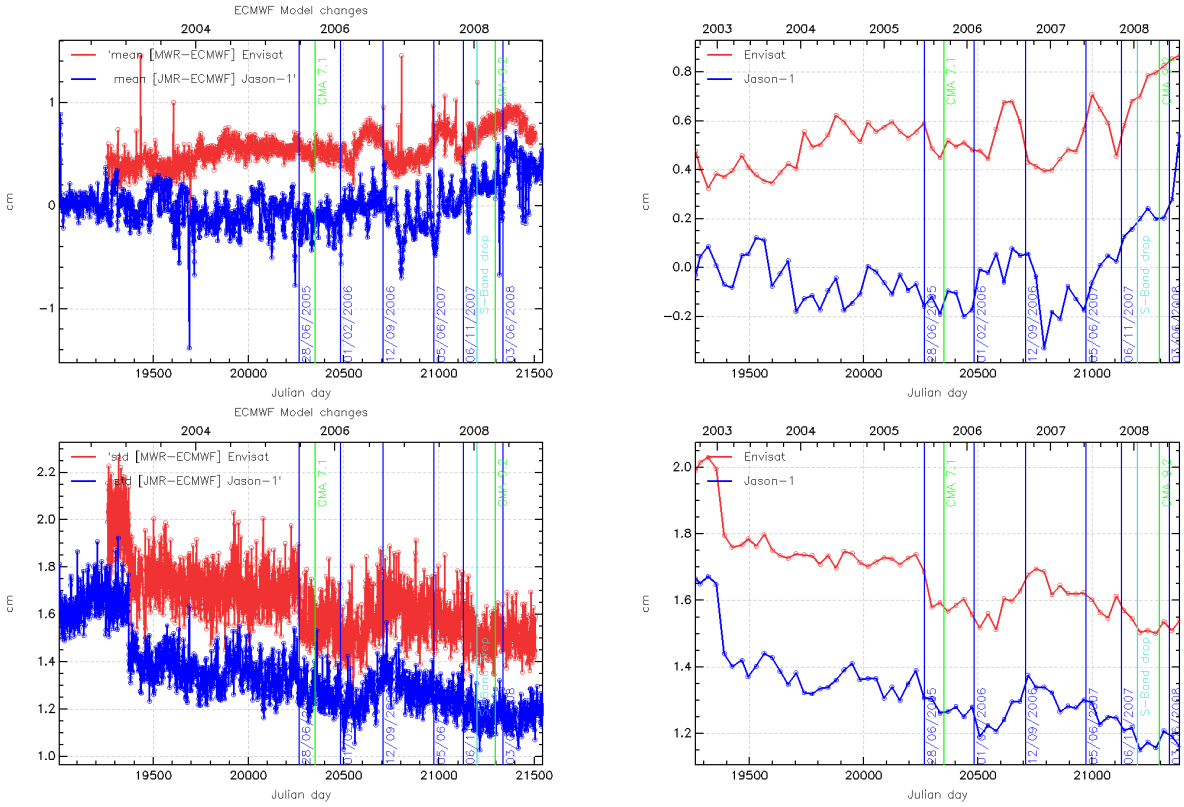

Figure 27: *Comparison of global statistics of Envisat MWR/Jason-1 JMR and ECMWF wet troposphere corrections. Mean per day (**left**) and mean per cycle (**right**) of the differences of correction. Blue vertical ones represent the major changes of ECMWF model.*

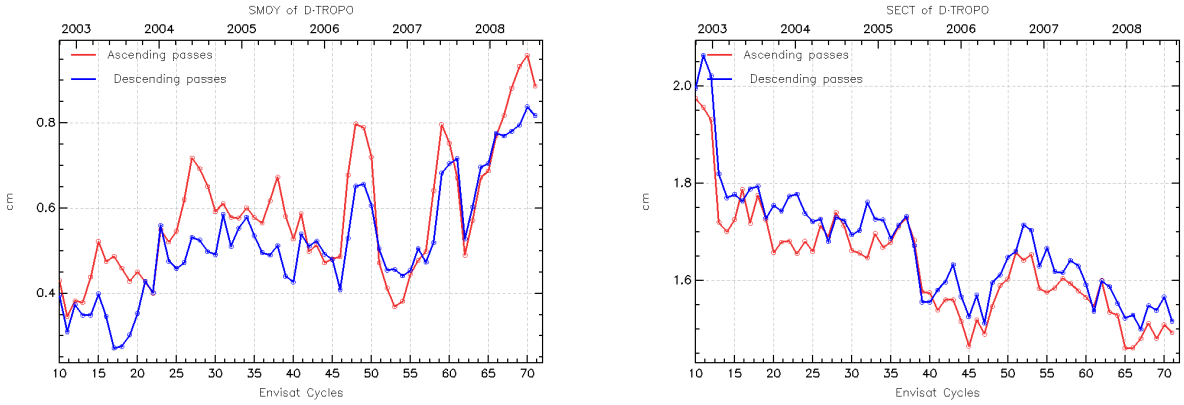

Figure 28: *Comparison of global statistics of Envisat MWR and ECMWF wet troposphere corrections separating ascending and descending passes (cm). Mean (**left**) and standard deviation (**right**) per cycle of MWR and ECMWF corrections.*

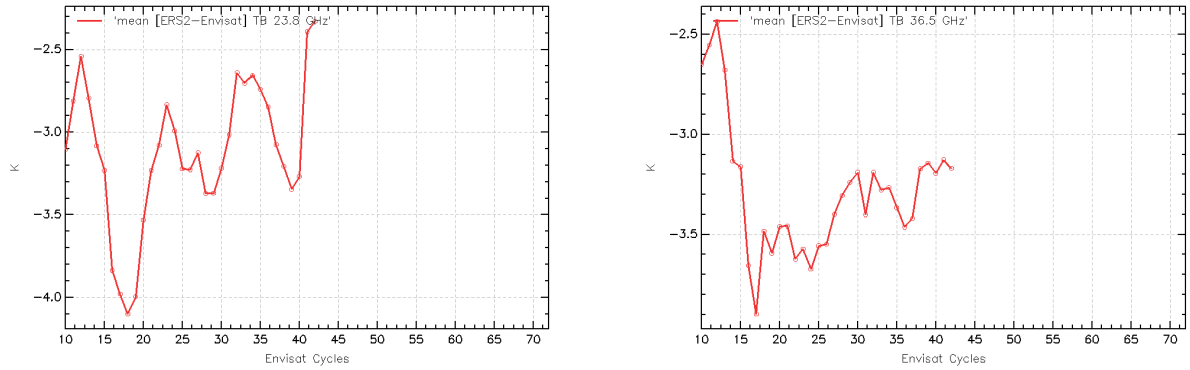

Figure 29: *Monitoring of the (ERS-2 - Envisat) brightness temperatures*

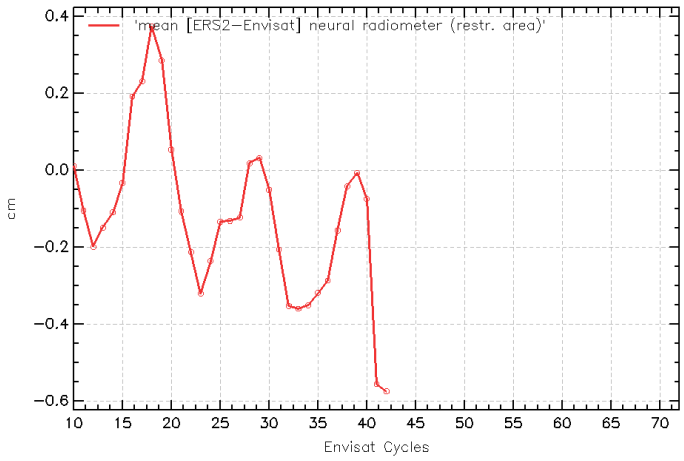

Figure 30: *Monitoring of the (ERS-2 - Envisat) wet troposphere correction*

6. Sea Surface Height performance assessment

One of the main objectives of the Calibration and Validation activities is to assess the performance of the whole altimeter system. This means that the quality of each parameter of the product is evaluated, in particular if it is likely to be used in the Sea Surface Height (SSH) computations. Conventional tools like crossover differences and repeat-track analyses are systematically used in order to monitor the quality of the system.

6.1. SSH definition

The standard SSH calculation for Envisat is defined below.

$$SSH = Orbit - Altimeter\ Range - \sum_{i=1}^{n} Correction_i$$

$$\begin{aligned}\sum_{i=1}^{n} Correction_i &= Dry\ troposphere\ correction : new\ S1\ and S2\ atmospheric\ tides\ applied \\ &+ Combined\ atmospheric\ correction :\ MOG2D\ and\ inverse\ barometer \\ &+ Radiometer\ wet\ troposphere\ correction \\ &+ Filtered\ dual\ frequency\ ionospheric\ correction\ /GIM\ model\ after\ cycle\ 64 \\ &+ Non\ parametric\ sea\ state\ bias\ correction \\ &+ Geocentric\ ocean\ tide\ height,\ GOT\ 2000 :\ S1\ atmospheric\ tide\ is\ applied \\ &+ Solid\ earth\ tide\ height \\ &+ Geocentric\ pole\ tide\ height\end{aligned}$$

As said in 3.2.1., the new geophysical correction associated with version CMA7 have been updated on the whole data-set in order to have the most homogeneous time series. For Envisat, the only discontinuities existing in our dataset are :

- Between cycle 40 and 41 and between 68 and 69 due to the orbit, computed using:
  - GRIM5 gravity model for cycles 9 to 40
  - EIGEN-CG03C from cycle 41 to 68
  - a time variable gravity field after 69.
- Between cycle 40 and 41 due to :
  - IF monthly estimations from cycle 41 onwards
  - Retracking using Rx Dist Fine
  - MWR side Lobe correction

The USO auxiliary correction distributed by ESA are used in Envisat SSH computation.

6.2. Single crossover mean

To analyse the time invariant errors, we have computed local averages of crossover differences over cycles 10 to 40 and 41 to 72 . The maps of the mean differences at crossovers are shown in

Figure 31. On the 10-40 map, systematic differences between ascending and descending passes are observed in some areas. Mean ascending/descending differences are locally higher than 4 cm (Southern Pacific and Southern Atlantic). These patterns, called geographically correlated radial orbit errors, are induced by errors in the gravity models currently used in the orbit computation. Notice that the signal visible around the equator on ERS-2 (Scharroo, 2002 [67]), related to poor quality of the ionosphere correction, is not present for Envisat thanks to a good correction of the dual frequency correction. On the 41-72 map the geographically correlated orbit errors are almost fully removed thanks to the use of EIGEN-CG03C gravity model. Small signals remain in Indian and Pacific Oceans.

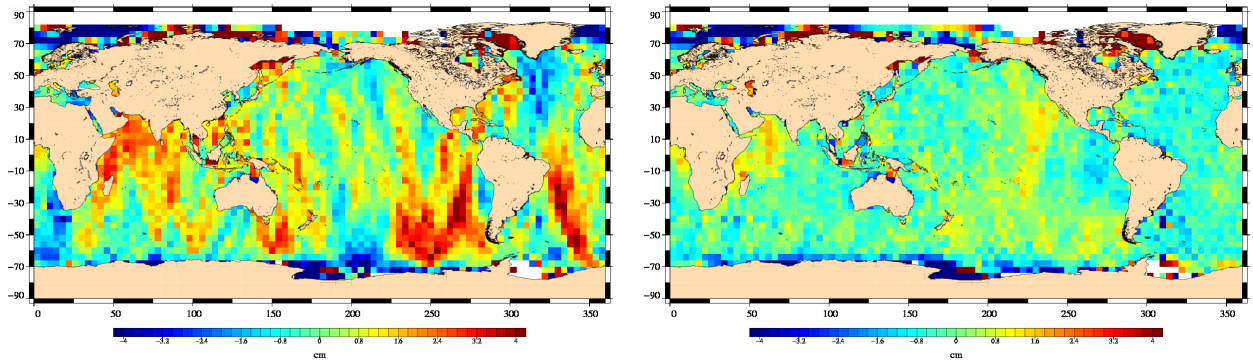

Figure 31: *Maps of the time invariant crossover (over 35-days with a selection at 10 days) mean differences (cm) for Envisat averaged in (3 ° x 3 °) geographical bins over cycles 10 to 40 (**left**), over cycles 41 to 72 using the GDR C POE orbit (**right**).*

Besides the systematic ascending-descending errors, a time varying error can also be observed at crossovers. The cyclic mean ascending-descending SSH differences at crossovers shows this error in Figure 32. The cyclic mean crossover differences have been plotted in three different configurations: full data set, deep ocean data, and deep ocean data with low variability, and excluding high latitudes. A strong annual signal is evidenced on the 3 curves. Its amplitude is approximately 1 cm.
A specific study has been carried out in order to analyse deeply this signal. The results of this study are available in the dedicated part of this document. The main results of this study is first that the amplitude is geographically dependent, and then that the geographical patterns depend on the oceanic tide model used in the SSH.

Figure 33 is another way to show that both altimeters have very similar performances. It shows that Envisat and Jason-1 have similar Standard deviation of along track SLA before cycle 41 and that Envisat's curve stands around 1mm under Jason's afterwards. Note that looking both at the along track performance enables to enlight the seasonnal Grace gravity model, wich cannot be seen with the cross over analysis only.

Figure 34 shows a good consistency after mid 2005. Note that the 2 last points are slightly higher (5mm) than the others. More data are needed though to be able to drow any conclusion.

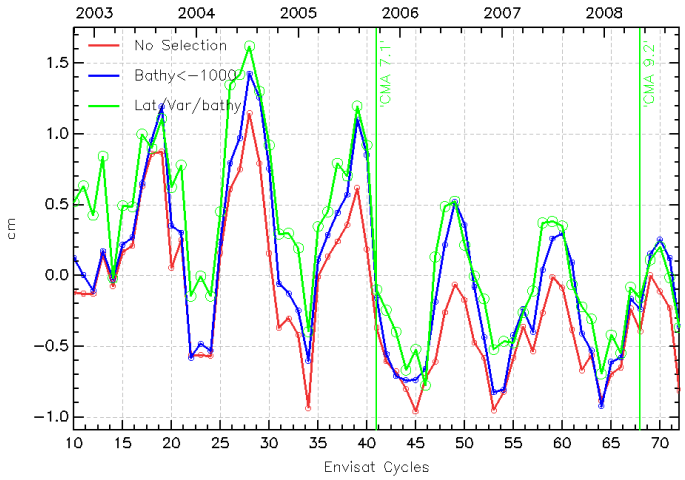

Figure 32: *Time varying crossover (over 35-days with a selection at 10 days) mean differences (cm). Cycle per cycle Envisat crossover mean differences. An annual cycle is clearly visible. Blue: shallow waters (1000 m) are excluded. Green: shallow waters excluded, latitude within [-50S, +50N], high ocean variability areas excluded*

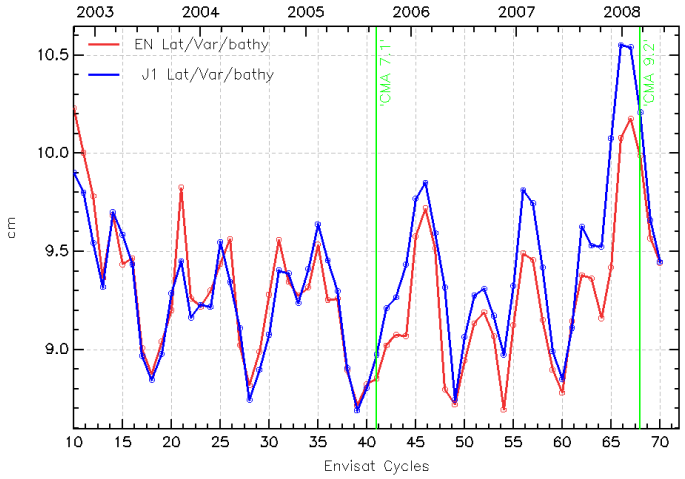

Figure 33: *Standard deviation of along track SLA (m), shallow waters excluded, latitude within [-50S, +50N], high ocean variability areas excluded*

6.3. Variance at crossovers

The variance of crossover differences conventionally gives an estimate of the overall altimeter system performance. Indeed, it gathers error sources coming from orbit, geophysical corrections, instrumental noise, and part of the ocean variability. The standard deviation of the Envisat SSH crossover differences has been plotted in Figure 35, depending on three data selection criteria. Without any selection, a seasonal signal is observed because variations in sea ice coverage induce changes in ocean sampling by altimeter measurements. When only retaining deep ocean areas, excluding high latitudes (higher than 50 deg.) and high ocean variability areas, the standard

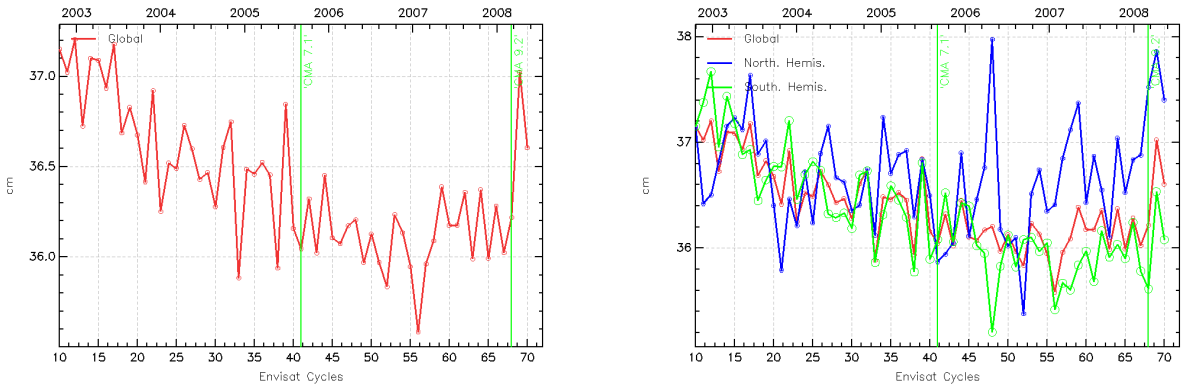

Figure 34: *Mean EN-J1 SSH differences at dual crossovers (cm) for Envisat on global ocean (**left**), and separating Northern and Southern hemispheres (**right**).*

deviation then gives reliable estimate of the altimeter system performances. In that case most of the cycles have a standard deviation between 7.5 and 7.7 cm. But there are some exceptions that can be explained. Cycles 15 and 48 are strongly different because of the low number of crossover points. There are less than 10000 crossovers whereas other cycles lead to more than 20000. Cycles 21 and 26 have higher values because of bad orbit quality over a few passes related to out-of-plane maneuvers. Cycle 21 has a strong value (8.5 cm) because of the combined effect of 2 maneuvers, intense solar activity between these 2 maneuvers, and lack of laser measurements between these two maneuvers. Cycle 11 has a relative high value because of missing Doris data. No degradation of the performances have been noticed since the beginning of the USO anomaly on cycle 46. This shows that the correction provided by ESA allows Envisat Ra2 data to maintain the same level of quality.

Similarly, no degradation of the performances have been noticed since the S Band power drop, thanks to the efficiant use of the GIM ionospheric correction instead of the missing bifrequency correction. To avoid any jump, the GIM correction is applied with a 8mm bias computed on the last 40 days of SLA difference with GIM and bifrequency corrections (see Figure 42). Therefore, the GIM ionospheric correction can be considered to have a good quality for this period of low solar activity. Further studies should be made to evaluate its impact on a higher solar activity period.

In order to compare Envisat and Jason-1 performances at crossovers, Envisat and Jason-1 crossovers have been computed on the same area excluding latitude higher than 50 degree, shallow waters and using exactly the same interpolation scheme to compute SSH values at crossover locations. Performances at crossovers are compared, for the two satellites on Figure 36. The standard deviation of Envisat/Envisat and Jason-1/Jason-1 SSH crossover differences are respectively 6 cm and 5.7 cm. The use of MLE4 retracking on Jason-1 leads to slightly lower than Envisat standard deviation at crossovers. A slight decrease is visible on Envisat plot at cycle 41, thanks to the new standards used for the POE orbit. From cycle 41 onwards, the performances of the two missions are very close.

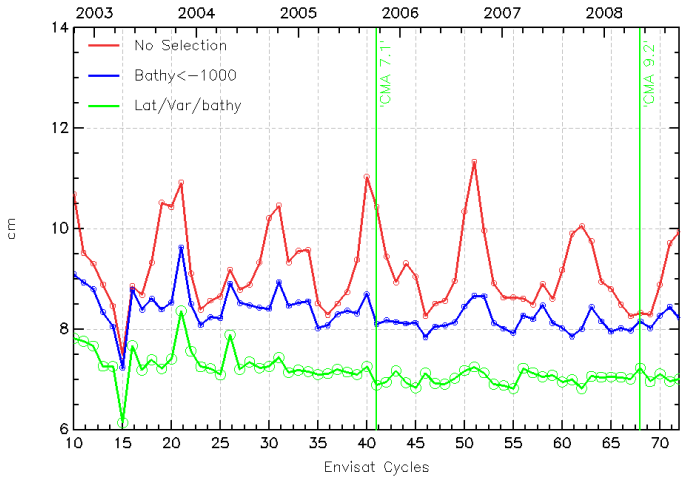

Figure 35: *Standard deviation (cm) of Envisat 35-day SSH crossover differences depending on data selection. Red: without any selection. Blue: shallow waters (1000 m) are excluded. Green: shallow waters excluded, latitude within [-50S, +50N], high ocean variability areas excluded.*

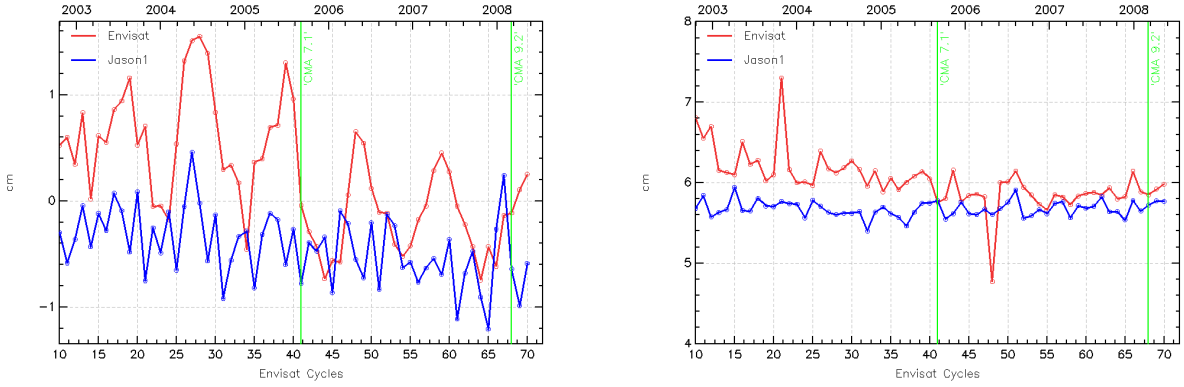

Figure 36: *Comparison of average (left) and standard deviation (right) (cm) of Envisat (red) and Jason-1 (blue) 10-day SSH crossover differences*

7. Particular investigations

This year many investigations were carried on. This part is dedicated to them.

7.1. Study on ENVISAT Mean Sea Level Trend

7.1.1. Introduction

Since Envisat launch, some discrepancies between its Mean Sea Level trend and other mission's were investigated.
However after many improvements and updates over the whole time series, its similarity to Jason-1's MSL (used for climate studies) and to tide gauges after cycle 22 and even more significantly after cycle 41 is very encouraging.

Yet, efforts were made to:
- understand the beginning of the mission (up to cycle 22) non physical descending trend
- consolidate our knowledge in order to make it useful by the climate orientated studies

This study is a summary of the past 2 years studies on the MSL subject. It intends to settle the basis of the MSL monitoring before the full mission reprocessing planned for 2009.

It is organized in 3 parts:
- A status on the current MSL seen by Jason-1 and Envisat missions
- The impact of recent updates and sensitivity studies will then be detailed in a part including the joint work performed with Remko Scharoo from Altimetrics.
- Finally, a list of all the possible causes of errors in the MSL Envisat computation will be performed: Geophysical, instrumental and orbital potential sources will be listed.

7.1.2. Multimission Mean Sea Level trends

7.1.2.1. MSL recipe

In order to have comparable time resolution between Envisat and Jason-1, each point of the MSL monitoring are computed with quarter of Envisat cycle (35/4 = 8.75 days) periodicity: the closest fraction of cycle from 10 day-Jason-1 periodicity. Envisat's time series are computed by first averaging the data in 2°x2° boxes and then by computing a global average with a weighting depending on the latitude (between 66° N/S) following Dorandeu and Le Traon 1999 [17]. Time series are then smoothed with a 10 points (87.5 days) sliding window. This step enables to smooth the noise and to reduce the SNR (Signal to Noise Ratio) on the slope computation. The Sea Level Anomaly (SLA) formula is given below.

$$SLA = Orbit - Altimeter\ Range - MSS\ CLS01 - \sum_{i=1}^{n} Correction_i$$

with :

$$\begin{aligned}\sum_{i=1}^{n} Correction_i &= Dry\ troposphere\ correction : new\ S1\ and S2\ atmospheric\ tides\ applied \\ &+ Combined\ atmospheric\ correction :\ MOG2D\ and\ inverse\ barometer \\ &+ Radiometer\ or\ ECMWF\ wet\ troposphere\ correction \\ &+ Filtered\ dual\ frequency\ ionospheric\ correction\ /\ GIM\ model\ afterwards \\ &+ Non\ parametric\ sea\ state\ bias\ correction \\ &+ Geocentric\ ocean\ tide\ height,\ GOT\ 2000 :\ S1\ atmospheric\ tide\ is\ applied \\ &+ Solid\ earth\ tide\ height \\ &+ Geocentric\ pole\ tide\ height\end{aligned}$$

Specificities of Envisat:
- The ionospheric correction used in Envisat SSH computation is the filtered dual frequency before 64, the GIM JPL model afterward.
- The USO auxiliary correction distributed by ESA are used in Envisat SSH computation.

According to the periods, the geophysical corrections provided in the GDR products used are not the same. Table 5 details the standards of the different terms used throughout the mission.

	Cycles 9-41	Cycles 41-64	Cycle 65-67	Cycle 68 onwards
Orbit	GDR-A	GDR-B		GDR-C
DAC	Updated	MOG2D-HR Updated		MOG2D-HR
Iono corr	Updated	Dual-Frequency with S-Band SSB	GIM	
MWR Wet tropo	Updated	Corrected from side lobes		
MWR Dry tropo	Updated	S1-S2 atmospheric tides applied		
SSB	Updated	Homogeneous to GDR-B		
Solid Tides	From GDR			
Pole Tides	From GDR			

Table 5: *G*eophysical corrections used following the periods

Unless otherwise stated, the figures have then been plotted after removing annual signal, semi-annual signal, and signals lower than 60 days.

7.1.2.2. MSL time series

Envisat's MSL has various behaviors during its lifetime, including a very odd decreasing trend at the beginning of the mission.
A first look at the raw (unfiltered and with annual, bi-annual and 60 days signal) SLA monitored on the whole time series with a severe selection on purely oceanic data (Lat<50° and oceanic variability lower than 20cm) shows that the series can be split into 2 major parts (Figure 37):
. - Before cycle 22, the annual signal is poorly returned and the slope is clearly negative whereas
- After cycle 22, the annual signal is clearly visible (mainly after cycle 41) and the slope increases again, as expected.

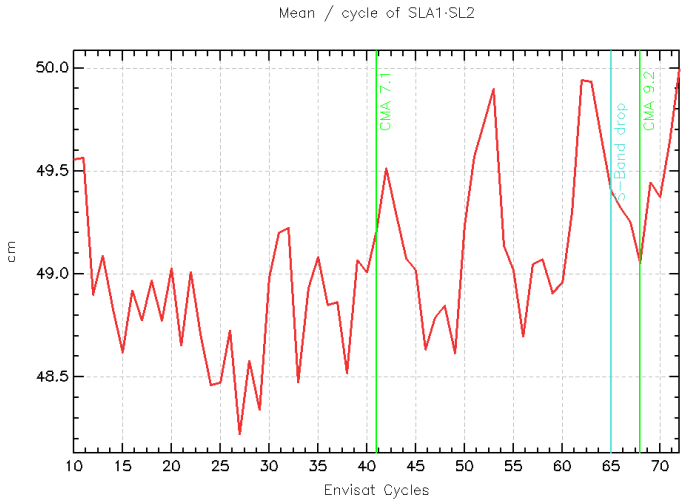

Figure 37: *Envisat MSL per cycle over global ocean for Lat<50° and oceanic variability lower than 20cm with ECMWF Wet tropospheric model.*

This first observation can be refined by a more adapted analysis (see SLA recipe in part 7.1.2.1.), linked to a comparison with Jason-1's MSL (see Figure 38). The period before cycle 22 (January 2004) will be further analyzed afterwards but it is not taken into account in the trends computation.

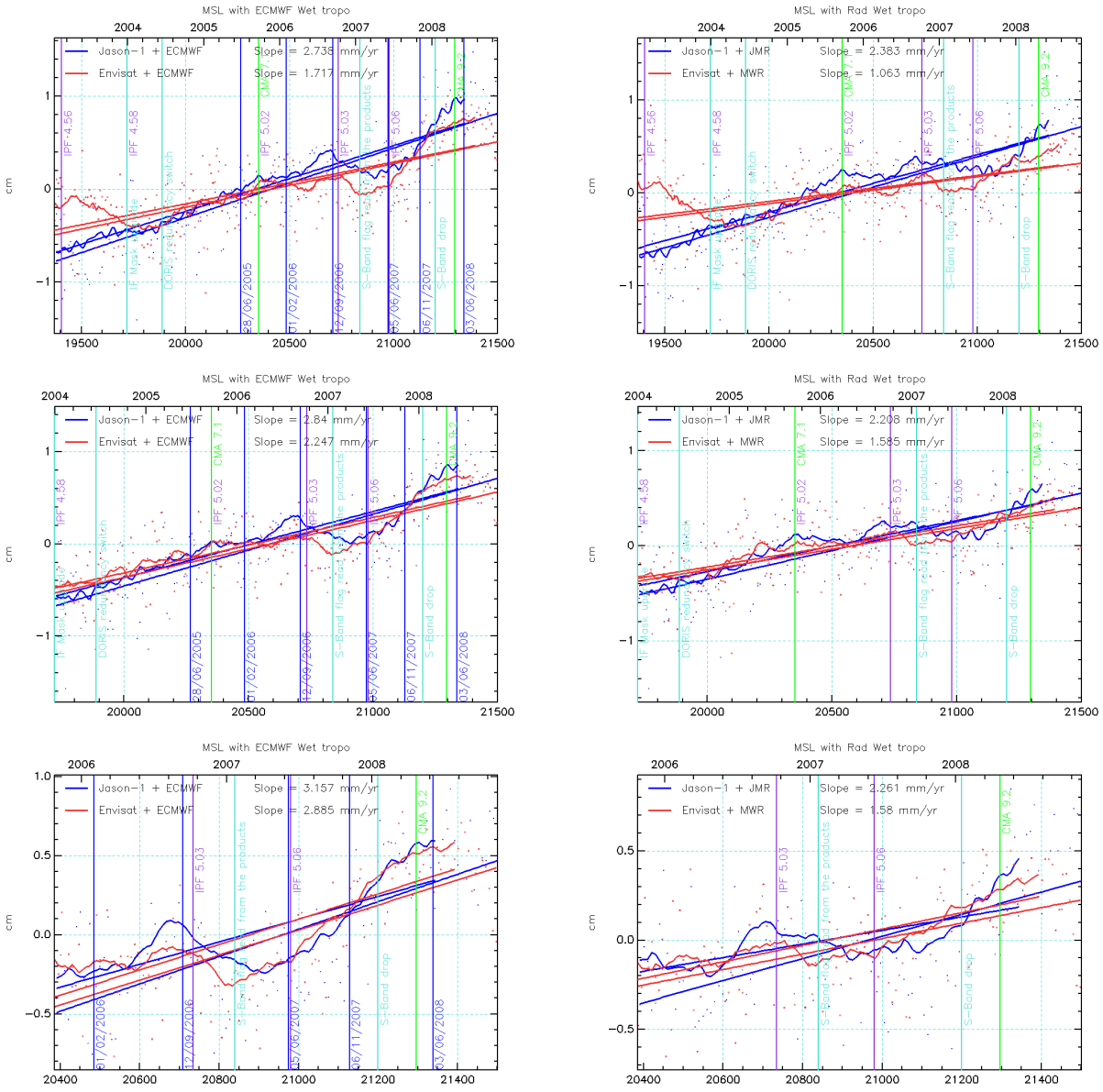

Figure 38: *MSL over global ocean for Envisat and Jason-1 with ECMWF Wet tropospheric model on the left and with the radiometric Wet tropospheric model on the right. TOP: Global shape from the beginning of the mission (cycle 9). MID: Global shape and trend from cycle 22. BOT: Global shape and trend from cycle 41.*

Jason-1's MSL is supposed to be reliable over the whole period because it is consistent with other theoretical climate-orientated studies and the different variations observed during its lifetime can all be explained geophysically (see Ablain et al.2008, [5]). It is plotted in blue on Figures 38, with an ECMWF wet tropospheric correction (left) and its radiometer (JMR) wet tropospheric correction (right). Its shape is very linear (once subtracted annual, semi-annual and 60 days signals) with a slope of:
- Around **2.7mm/year**, with ECMWF wet tropospheric correction.
- Around **2.4mm/year**, with JMR wet tropospheric correction.

Note that at the end of 2006 and during 2007, the MSL slope of Jason-1 shows a flattening also

visible on Envisat's MSL.
Also note that for the 6 upper plots (Figures 38), an annual signal is adjusted on each concerned period, the end of the plots seem slightly different because of this adjustment effect.

Finally, at the end of the period (in 2008), the MSL slope using ECMWF, of Jason-1 shows a large increase, also visible on Envisat's MSL using ECMWF. It will be shown below to be due to a jump in the ECMWF model (part 7.1.4.1.1. and 7.1.2.3.).

Apart from the period before cycle 22, Envisat's MSL plotted in red on Figure 38 middle shows similar behavior to Jason-1 with few discrepancies.
The global slope is slightly underestimated (0.5mm/year lower than Jason-1) compared to Jason-1's:
- Around **2.2mm/year**, with ECMWF wet tropospheric correction.
- Around **1.6mm/year**, with MWR wet tropospheric correction.

After cycle 22 but before cycle 41 (Figure 38 middle), the MSL increases again but with a weaker slope than Jason-1.

After cycle 41 (Figure 38 bottom), the trends are similar but the flattening observed at the end of 2006 and during 2007 is not seen with the same amplitude and duration than on Jason-1 when using ECMWF wet troposphere correction. It is however very similar when considering the MSL using MWR wet troposphere correction.

No clear explanation can be given by now about the strange behavior of the MSL signal on Envisat at the beginning of the mission (before cycle 22) and about the underestimation of the global slope compared to Jason-1. However, many studies were driven around this subject. This documents sums up the different possible causes to be considered.

At the end of 2006 and during 2007, the MSL slope of Jason-1 and Envisat (independently of the wet troposphere correction used) shows a flattening of MSL's slope. Calibration with In-situ data (see more details in the annual report [75]) show no drift of altimetric MSL. Therefore following Commien et al. (personal communication), this flattening might be due to the La Niña currently active (see [7] and below).

7.1.2.3. MSL comparison to in situ tide gauges

Calibration work are performed to compare altimetric missions (including Envisat) to in situ tide gages measurement. The results are detailed in [75]:
- On the first part of the mission (before 41), a strong drift (around -1.5 mm/year) is noticed between altimetric and tide gauges on Envisat (against 0.1mm/year for Jason-1). Meanwhile, Envisat/Jason direct comparison trend difference is around (-2.3mm/year).
- Conversely, from cycles 42 to 67, the evolution of altimeter/tide gauges SLA differences is relatively flat (weak drift close to 0.3 mm/year) for Envisat (against 0.1mm/year for Jason-1). Here as well, this is in agreement with results from the direct comparison with Jason-1 (trend difference around -0.5mm/year).
- Afterward, the version change of November 2007 (cycle 63) in the wet tropospheric correction derived from ECMWF model coincides with a jump (about 2 mm, also noticed in Jason-1's moni-

toring) in the series.
Regarding the error budget of these analysis, these results are in agreement with Envisat/Jason direct comparisons.

7.1.3. Recent updates and sensitivity studies

End of 2007 and beginning of 2008, a fruitful joint work was performed with Remko Scharoo to compare CLS and Altimetrics MSL. In a first step, we had identified the different causes of inhomogeneity between both data sets and updates were performed on both sides (This was already detailed in the Last Envisat Yearly report [6] and [34]). This year, updates on Altimetrics side were also performed, though changing the conclusions and consolidating our confidence in both data sets. Basically:

On CLS Side the following updates had been performed:
- **Dual-frequency ionosphere correction update**: This update consisted in correcting the S-band range from a suitable SSB on cycles 10-41 before computing the dual ionosphere correction. The new MSL trend increases by 0.4mm/year when looking at the whole time series and 0.5mm/year without the first year. This was a positive change: Envisat CLS MSL was now closer to Altimetrics from the one hand and to Jason-1 MSL in the other hand.
- **Radiometer Wet Tropospheric correction**: This update consisted in correcting data from side lobes on the whole mission, as it is done in the GDR-B. This enabled to increase the MSL trend on cycles 23-41 (annual signal removed) by about 0.15mm/year.
- **Other orbits**: Finally, to avoid the inhomogeneous GDRA-B CNES orbit available in the products, we tested 2 homogeneous orbits on the whole time series. But unexpectedly, this evolution decreased the MSL trend (respectively -0.2mm/year and -0.4mm/year for ESOC and Delft orbits).
- Note that unlike in the GDR, the SSB is computed with a homogeneous Sigma0 on the whole series.

On Altimetrics Side the following updates had been performed:
- **Checking SWH** to avoid a jump noticed at cycle 38 on SSB, SWH and on the number of available points. It could come from the lower limit on SWH2 taken by Altimetrics that makes them throw away more than they should, inconsistently with the earlier period for which there was no SWH2.
- Get a homogeneous dry troposphere correction field with the ECMWF DRY (including the S1,S2 fix) and the WET along the track for each record in the GDRs.
- Understanding the jump (7000 points) of **data loss** at cycle 38.
- Changing the method of average by **weighting the data by the size of the 2°x2° boxes** in which you bin the data. The necessity of doing that has been demonstrated for Topex, when the sampling was not global at the end of his life (strong gaps in Indian). Not using a box averaging process would lead to an under-weighting of the Indian ocean MSL trend.
- Applying a **threshold** on the off-nadir pointing value.

After the different updates, both MSL converge. From cycle 22 to cycle 61 (maximum available data at the time of that study), the slopes are:
- CLS with MWR and ECMWF: + 1.5mm/year (consistent)
- Altimetrics with ECMWF: + 1.5mm/year (consistent with CLS using ECMWF)
- Altimetrics with MWR and NCEP: 2.9mm/year (consistent)

Finally, (see Figure 39), the only remaining differences between CLS and Altimetrics come from

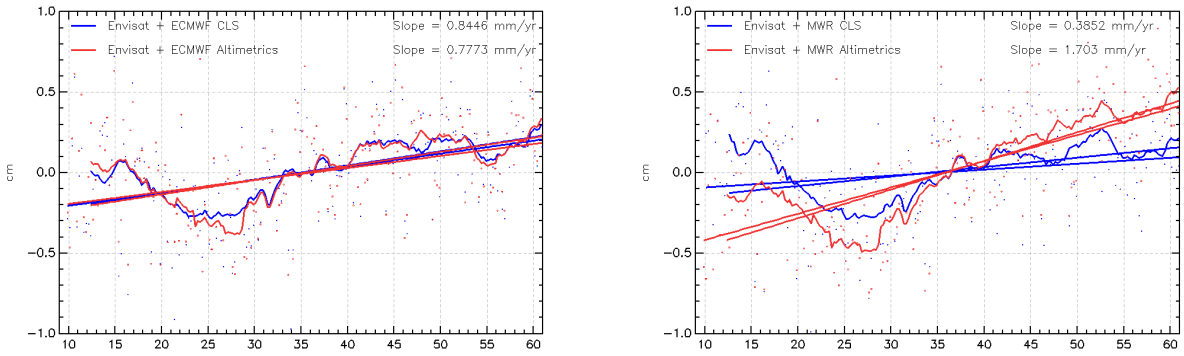

Figure 39: *Comparison of MSL between CLS and Altimetrics using CNES Orbit, updated ionospheric correction ECMWF model (left) and MWR radiometer (right).*

the wet tropospheric correction used. While, CLS's radiometric wet tropospheric correction is homogeneous to ECMWF model, Altimetrics applies a drift on the 23.8GHz channel and is consistent with NCEP model. The reason for that choice is a better confidence into NCEP long term consistency compared to ECMWF which regular updates introduces jumps in the Mean Sea Level (See part). However, at the instrument level, no sign of drift on this channel is observed. Furthermore the use of this correction in the MSL instead of ECMWF would not help reducing the difference between Envisat and Jason-1 (Envisat's trend would be too high then).
This shows another aspect of the uncertainty linked to the wet troposphere correction estimation. Note that before cycle 61, the wet troposphere correction from ECMWF and MWR were in a better agreement because the major changes of the 5th June and 6th November 2007 had not impacted the data yet.

7.1.4. Possible sources of errors

Figure 38 TOP shows that Envisat's MSL can be split into 2 major periods and that globally, the sea level trend is under-estimated by Envisat. These two aspects are unexpected and probably due to an error of processing. This part scans the possible errors inducing: - the strong error before cycle 22 and
- the slight under-estimation between cycle 22 and 41.

7.1.4.1. Errors on geophysical corrections

7.1.4.1.1. Wet tropospheric correction

In order to remove a source of difference and to avoid potential drifts on the radiometer sides, both Jason-1 and Envisat's MSL were computed with the ECMWF wet tropospheric model. Now, and considering the numerous jumps underwent by the model during versions' updates, both radiometer and model correction are analyzed in the MSL studies.
In this part, we focus on the wet tropospheric correction, to underline those changes and their impact on the trends.

Figure 41 shows a monitoring of Envisat MWR and ECMWF wet troposphere corrections difference per cycle from the beginning of the mission with the major changes of ECMWF versions. This highlights a difference of behavior of the difference of troposphere from February to December 2006 on Jason-1 and Envisat. The bump is seen by both missions but it is shorter on Envisat than on Jason-1. This could explain the difference of behavior seen on the MSL Figure 38 (right).

Figure 41 shows a monitoring of different tropospheric correction over 15 years.
The different curves are plotted with a 10 (or 8.75) days sampling, averages by boxe and pondered by latitude as explained above in the MSL recipe. The series is then filtered with a 10day-sliding window and the annual and 60days signals are adjusted and removed.
For the TOPEX period, TOPEX radiometer (TMR) and NCEP correction are available. High values can be noticed, during el Niño event around 1997-1998. Afterward, the different correction are seen to have various behaviors, NCEP showing a very steep slope compared to other corrections. Its drift seems to be slightly too big.
Conversely ECMWF seems stable over the period but with an atypical behavior at the end of the period. Actually, after June 2006, all radiometers as well as NCEP model see a decrease which could be attributed to a physical reduction of the wet tropospheric content. This reduction is not seen by ECMWF and pushes to take this model with care for this particular period.

For mid 2009, a new homogeneous reprocessed version of the ECMWF model is expected to be available. ECMWF is currently producing ERA-Interim, a new global reanalysis of the period since 1989. The ERA-Interim system is based on a recent release of the Integrated Forecasting System (IFS Cy31r2) containing many improvements both in the forecasting model and analysis methodology. The reanalysis will then be continued in near-real time with the same system in order to support climate monitoring. This version will have a degraded resolution (1.5° instead of 0.25°) but this should not matter MSL long term studies. Its impact's analysis on the MSL level will be very interesting.

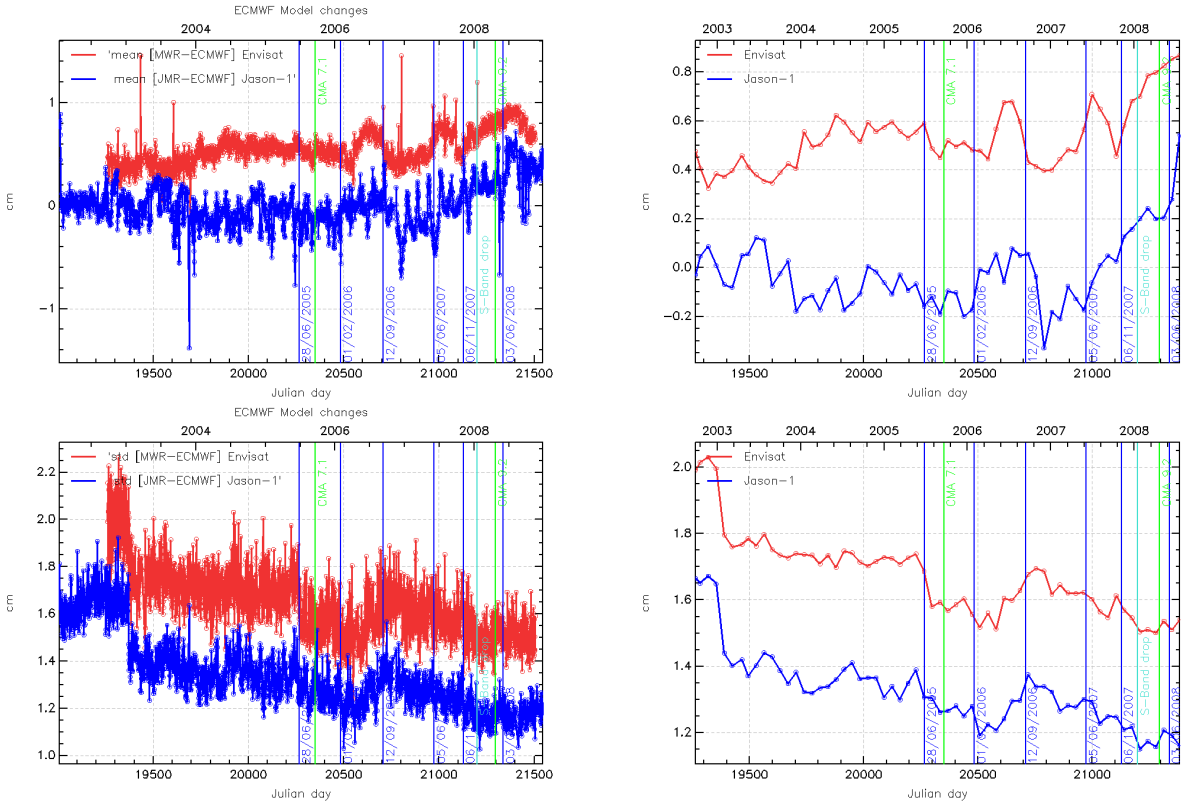

Figure 40: *Comparison of global statistics of Envisat MWR/Jason-1 JMR and ECMWF wet troposphere corrections. Average on top, Standard deviation on bottom. Mean per day (**left**) and mean per cycle (**right**) of the differences of correction.*

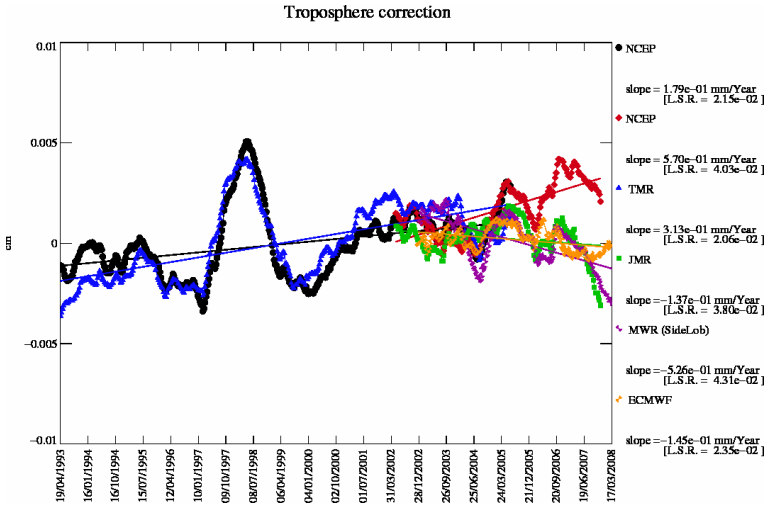

Figure 41: *Wet troposphere from different model/ radiometers over 15 years.*

7.1.4.1.2. Ionospheric correction

The ionospheric correction must be carfully monitored for several reason:
- the dual frequency correction, known as the most accurate correction reflects both S and Ku range behavior and the S-Band on Envisat was rather agitated since the beginning of the mission.
- Moreover, since the S-Band power drop, the dual-frequency ionospheric correction is not available anymore.

As written before, GIM Ionospheric correction is used instead, causing an inhomogeneity on the time series. We call "mix ionospheric correction" the correction made of the befrequency ionospheric correction before cycle 65 and GIM correction afterwards.
While the slope after cycle 22 using a mix ionospheric correction is 2.2mm/year, it jumps down to 1.8mm/year when the GIM correction is used everywhere. The shape of the difference computed with the "a la MSL method" (average per boxe and latitude ponderation + 10days sampling) is plotted on Figure 43, and like on the MSL trend 3 parts can be identified:
- before cycle 22 where the drift is close to -3.2mm/year
- between 22 and 41 where the drift is close to 0.5mm/year
- after 41 where the drift is globally stable .

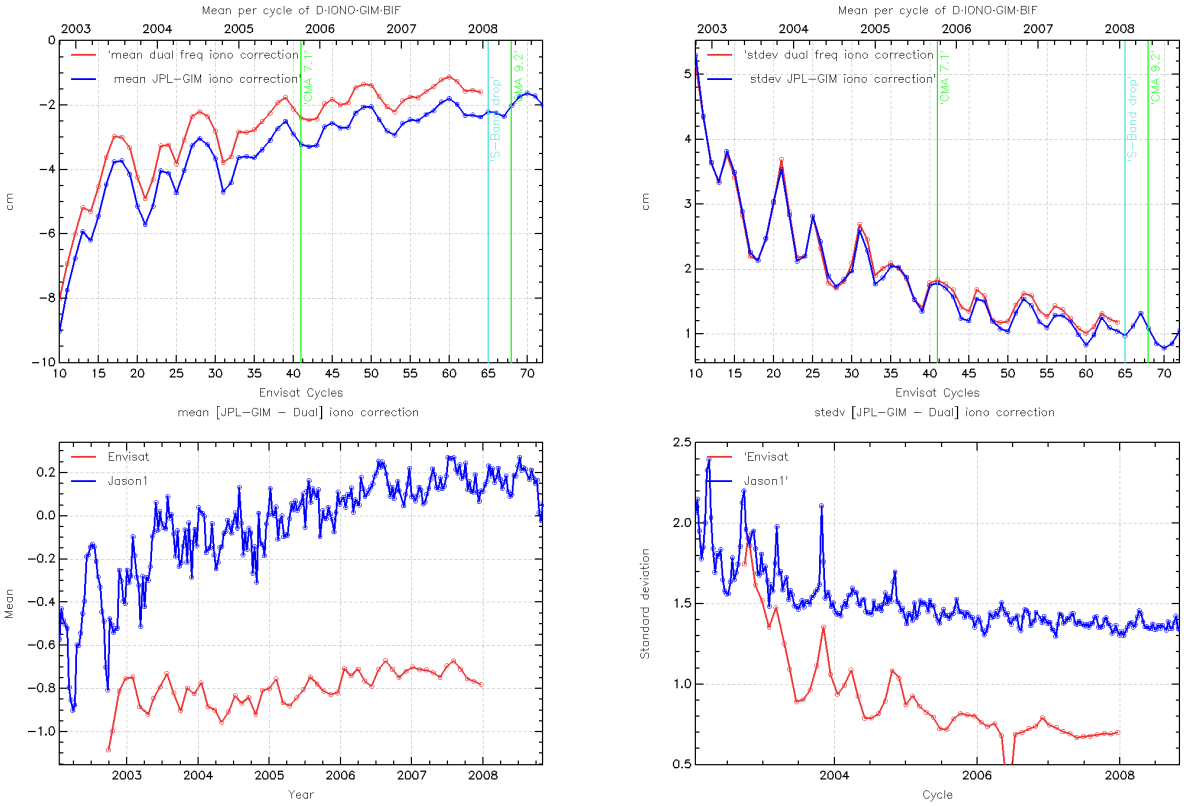

Figure 42: *Comparison of global statistics of Envisat dual-frequency and JPL-GIM ionosphere corrections (cm).* ***top****) Mean and standard deviation per cycle of Dual Frequency and GIM correction.* ***bottom****) Mean and standard deviation of the differences for Envisat and Jason-1*

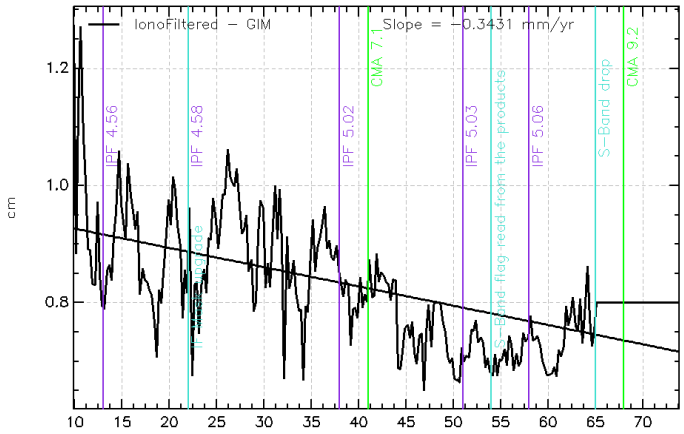

Figure 43: *Difference of ionospheric correction averaged with a "a la MSL" method. Dual-frequency correction - GIM before 64, GIM-GIM afterward.*

To keep on assessing the quality of the ionospheric correction, it is compared to the Jason-1 dual-frequency altimeter based ionosphere correction. The cycle by cycle mean of dual-frequency and JPL GIM ionosphere correction are plotted in figure 42. This shows that the ionospheric correction at the beginning of the mission is wrongly estimated by one or the other of the methods (GIM or dual-frequency). Therefore, this could be a source of error that has to be analyzed further. For instance, to take into account Envisat's sun-synchronism, a study could consist in plotting Jason-1's ionospheric correction for the same local time range (9 to 11 am and pm) corresponding to Envisat measurements.

7.1.4.1.3. Tides correction

Envisat mission has a sun-synchronous orbit (also called a heliosynchronous orbit) (from [25]). It combines altitude and inclination in such a way that the satellite passes over any given point of the Earth's surface at the same local solar time. Envisat, for instance, crosses the equator fourteen times a day, always around 10:00 local time. With a sun-synchronous orbit, observation of the ground is always illuminated at the same Sun angle when viewed from the satellite. However, as 24 hours is the period of some tidal constituents, these will thus always be observed at the same stage of their cycle.

This particularity of Envisat implies that some tides components cannot be solved by Envisat's sampling. The aliasing of these uncorrected components can therefore potentially have an impact on the MSL.

This aspect was underlined by Richard Ray Hobart OSTST presentation: « Sun-Synchronous satellite aliases diurnal errors. It maps diurnal errors (on ionosphere, pressure, ocean tide) to undesirable periods. Diurnal errors look like climate signal ». However, no estimation of this error could be made yet.

7.1.4.1.4. Error on day/night measurement: ascending descending discrepancies

Recent studies ([6]) showed that strong discrepancies were observed between ascending and descending passes. While around 0.6mm/year differences are observed on ascending/descending Jason-1's tracks (2.37mm/year on Descending (day) tracks versus 2.99mm/year on Ascending (night) tracks), the discrepancies on Envisat are around 2.26mm/year (3.16mm/year on Descending (night) tracks versus 0.90mm/year Ascending (day) tracks). Furthermore, note that for TOPEX, these discrepancies are close to zero.

The MSL shape separating ascending and descending tracks (Figure 44) are seen to be similar after cycle 41 and very different before.
On Envisat, this discrepancy was seen to be very depending on the orbit standard used and will be further detailed in part .

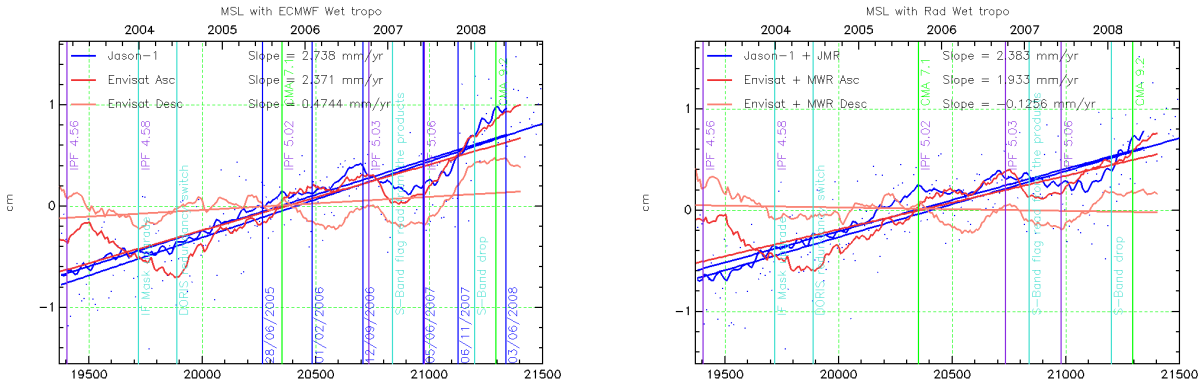

Figure 44: *Ascending/descending Jason-1 MSL compared to Envisat MSL with ECMWF Wet tropospheric model on the left and with the radiometric Wet tropospheric model on the right.*

Other ascending/descending discrepancies can be observed on geophysical correction:
- ionospheric correction (explained by the difference night/day of enlightenment). Figure 45 (left) shows that following the models (Dual-frequency or GIM). They are similar on Ascending passes (for low ionosphere correction but reach up to 1.2mm/year (4mm between cycle 10 and 44) on Descending passes.
- tropospheric correction. Figure 45 (right) also show that the differences between ECMWF model and MWR correction are different following the track's parity.

The sun-synchronous character of Envisat is one of its major differences with Jason-1 mission. The strong asymmetry between ascending and descending tracks could be related to this:
- by a geophysical correction error on one (or both) of the track's parity
- and more probably by a disymetry of the orbit computation as seen further.

7.1.4.2. Errors on instrumental drifts corrections?

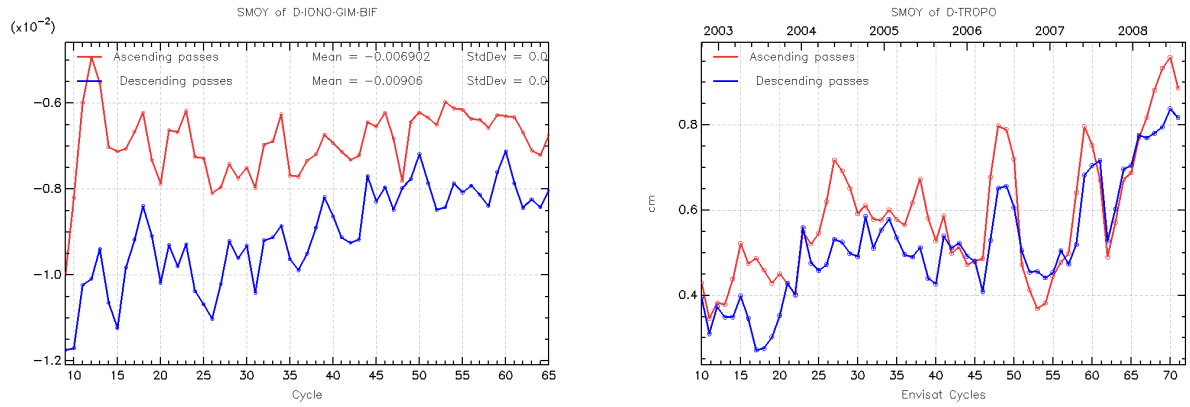

Figure 45: *Comparison of global statistics of Envisat dual-frequency and JPL-GIM ionosphere corrections (cm). Mean difference per cycle of Dual Frequency ionospheric correction with GIM correction (left). Mean differences per cycle of MWR - ECMWF troposphere corrections (right)*

A strong change of behavior was noticed on the MSL shape and trend after cycle 41, when GDR processing was updated to its B version. The improvements concerned many aspect, most of which could actually be updated on the whole time series. It was notably the case for geophysical corrections. But even with homogeneous geophysical correction on the data series, the change of behavior before and after 41 remains. Therefore, non geophysical drifts are suspected. This part scans all the possible sources of errors on instrumental correction.

7.1.4.2.1. USO

A previous study (Faugere et al. 2005, [27]) suspected the odd behavior at the beginning of Envisat mission as a consequence of a bad monitoring of the USO drift.
For other purpose, a new method of computation was developed in July 2006 (see part 3.2.1. and 2006 Envisat yearly report [6]).
It is recalled that the USO range correction is computed with the equation:

$$Corr_{USO} = Range.\frac{Period(t) - Period_{used}}{Period(t)} \quad (1)$$

Where the period is calculated by finite difference between the OBDH Clock and the USO count with a step of respectively 100 and 86400 seconds.

$$Period(t) = \frac{OBDH(t - step/2) - OBDH(t + step/2)}{USO_{count}(t - step/2) - USO_{count}(t + step/2)} \quad (2)$$

This method enables a monitoring of the correction with an increased time resolution (finite difference with a 100sec step instead of 86400sec step, see Figure 46).

But the new computation method does not change the estimated USO drift at the beginning of the period. Thus, the USO drift undergoes a change of behavior around cycle 22, like the MSL.

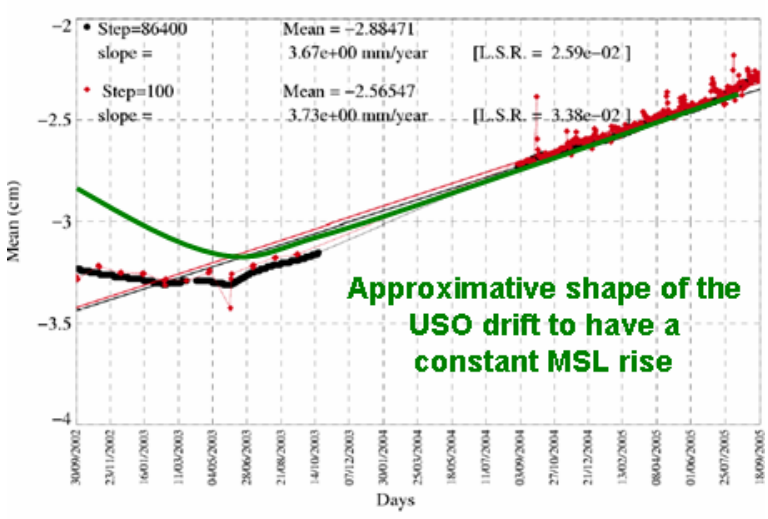

Figure 46: *USO correction computed with two methods compared to the expected trend of the correction to correct the MSL at the beginning of the mission (green). Finite difference with a 100sec step (red) instead of 86400sec step (black).*

However, no obvious reason is known to suspect any link between both drifts on that period.

7.1.4.2.2. Intermediate Frequency Filter (IF Mask)

The monitoring of the IF (Intermediate Frequency) filter or mask is seen to go through various behaviors (cf. Envisat FDGDR cyclic report ECAR [23]). The processing chain also changes various times with some impact on the data, see part and 47.
- After cycle 22: IF mask auxiliary data file was upgraded
- After IPF 5.02 evolution, cycle 41: IF estimation is performed monthly instead of the single constant filter applied before

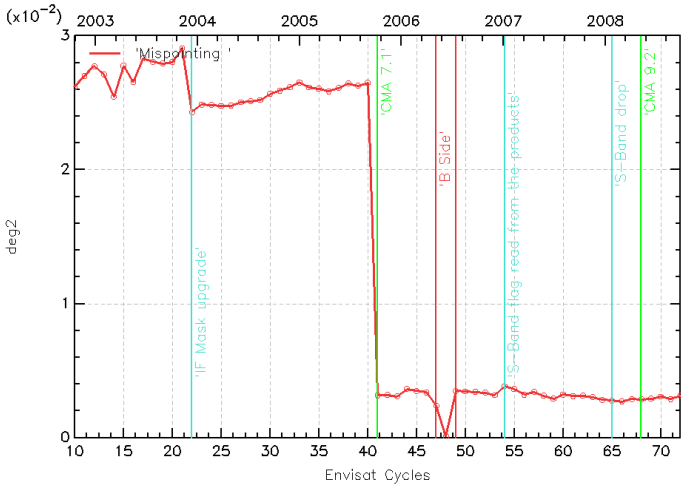

Figure 47: *Mean per cycle of the square of the off-nadir angle deduced from waveforms (deg2).*

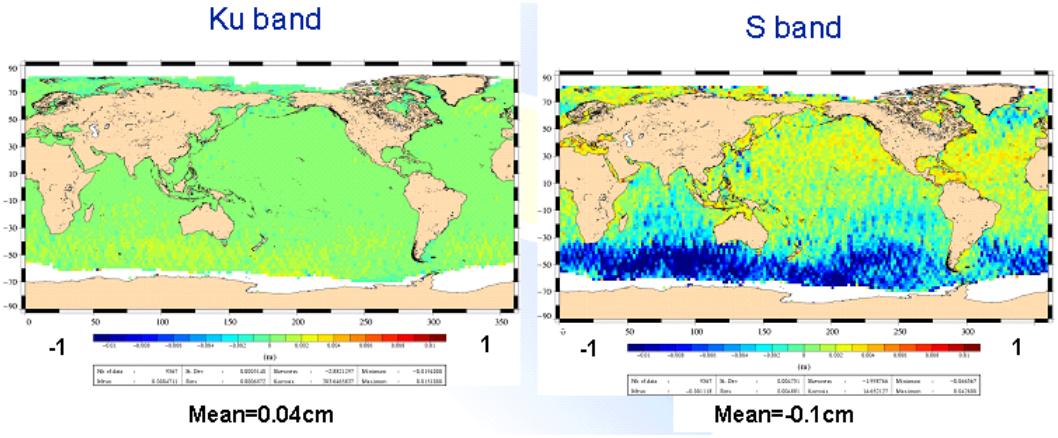

Figure 48: *Impact of IF mask drift between cycle 40 and 41 on Envisat's SLA (new -old). On Ku band (left) and S Band (right).*

Before cycle 41, the filter was constant, avoiding the monitoring of its drift. A study was performed concerning the impact of this drift on the SSH data. Figure 48 shows that the impact of the IF

drift is millimetric on Ku band and reaches 5mm for S-Band:

Considering the following formula of the ionospheric correction, a quick calculation shows that even 0.1cm on the S-Band (observed at high latitudes) is converted into a 5.88.10-2mm bias on the ionospheric correction which is negligible.

$$\text{Iono(Ku)=Coef(Ku)[Range(Ku)-Range(S)], with Coef(Ku) = 0.0588}$$
$$\text{Iono(S)=Coef(S)[Range(Ku)-Range(S)], with Coef(S) = 1.0588}$$

(see http://envisat.esa.int/handbooks/ra2-mwr/CNTR2-7-1-13.htm and [37]).

Therefore, the IF Mask does have an impact on the SSH data through the Ionospheric correction but its impact on the MSL seems to be rather negligible at least concerning the CMA 7.1 (cycle 40-41) evolution. However, it could be checked by analyzing its impact in terms of SLA drift.
The jump noticed for cycle 22 (IF mask upgrade) also has an impact on the mispointing estimation and might be related to the weird behavior described at the beginning of the mission. The test performed on cycle 40 could be performed for cycle 22 transition.

The weird behavior described in [26] was no more present. According to the In-Flight Tests performed on cycle 62, 63, 64 and 65 this problem, present since the beginning of the mission, seems to be related to the AGC used for the calibration mode.

7.1.4.2.3. In Flight Time Delay / PTR drift

Recent studies were carried out concerning the Point Target Response's drift (PTR) monitored and corrected by the In Flight Time Delay calibration factor. The PTR (more or less a "sinc" signal) was found to be too poorly sampled to enable a meaningful drift analysis. Monica Roca shows in [64] that "the resolution that can be provided by performing the FFT with the 128 samples of the nominal RA-2 filter bank is not enough to appreciate the real PTR variability". She also shows that a better sampling of the PTR could highlight a 4.5mm drift over the whole mission (around 0.8mm/year drift).
Studies are on going and need further analysis.

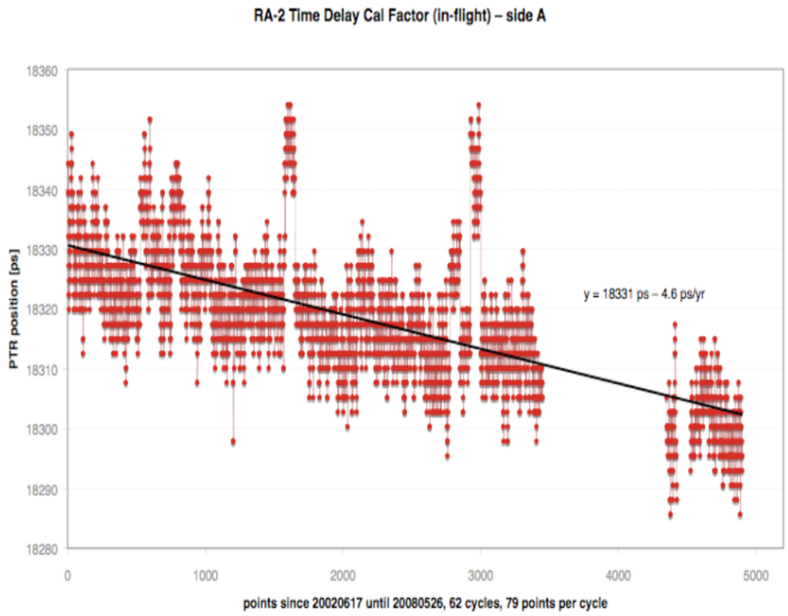

Figure 49: *Time calibration factor trend analysis with the PTR's better sampling (with a 128 zero padding).from M. Roca [64]*

7.1.4.2.4. UTC/ICU clock

A significant part of an eventual error in the RA-2 products dating could result from imperfect synchronization between the Satellite Binary Time and the UTC Time due to a drift of the ICU clock period. A correlation between those two times is performed at every Kiruna orbit dump and then extrapolated for the four non-Kiruna orbits (cf. Envisat FDGDR cyclic report ECAR [23]).

The behavior of this parameter goes through various behaviors slightly related to the MSL periods. In Figure 50 the differences between the extrapolated UTC values and the corresponding real UTC values measured at the next Kiruna dump, are reported for data from cycle 14 (day 1180) to cycle 32 (day 1800).

- On the bottom plot:
* before cycle 17 (before abscissa 1220), an important jump of 20ps within 1 cycle is noticed.
* Afterwards, the values stay within the warning thresholds.
- On the top plot:
* few anomalous events can be observed at the beginning of the period (cycles 16/17) for which the difference rises above the 20 microseconds warning threshold.
* Starting from cycles 22/23, the trend is stabilized but the number of small differences (10 microseconds plus or minus) increases a lot.
* Finally, during the last ten days of the cycle 32 and for all cycle 33 and 34, the variability of the deviations has increased reporting many peaks just over the 20 microseconds threshold.

The strong variability of these time related monitoring are now fixed [23]. On recent cycles the variation is around + or - 1ps per cycle.

Converted into range, these differences are negligible (20 microseconds are equivalent to less than 0.5mm jumps (using a radial speed of 25m/s) however the whole time series is not available and it could be interest to have the values concerning the cycles prior to cycle 17.

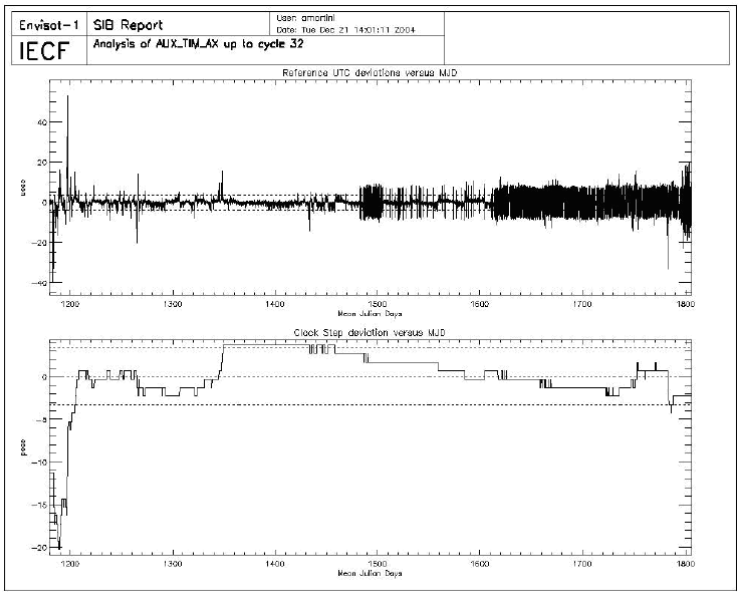

Figure 50: *UTC deviations and ICU clock period up to cycle 32.*

7.1.4.3. Errors on orbit determination

On cycle 41 (and for cycles 38 to 40 also afterwards), a new CNES POE (Precise Orbit Estimation) orbits standard was implemented in the products. Between GDR A and B orbit standards, one of the main evolutions is the use of the GRACE gravity model EIGEN CG03C. This new model implies a strong reduction of the geographically correlated radial orbit errors. However, this inhomogeneity in the data set can have a serious impact on the global MSL trend. This year, studies were performed with solutions coming from other orbit production centers in order to homogenize the data. The results are analyzed hereafter.

7.1.4.3.1. Different orbits

Different homogeneous orbits could be used in comparison with the current CNES POE orbit:
- the first one (Delft POE), from the Department of Earth Observation and Space Systems of the Delft University of technology was analyzed last year and the main results are detailed in 2007 yearly report ([6]).
- the second one (ESOC POE), from the European Space Operations Center (collaboration with Michiel Otten) was analyzed in a first version (V2) last year at the same time as (Delft POE). This year, the study was carried on, thanks to 3 new versions of the orbit (V3, V3_CR and V4 versions).

The characteristics of theses orbits are detailed in Appendix . Basically, the 4 ESOC POE versions are using ITF2005 (unlike CNES POE GDR-B which is refered to ITRF 2000):
- Between V2 and V3 versions the changes are mainly model changes like gravity field (using time varying gravity, and annual and semi-annual variation) plus updated ocean tides

- V3 CR includes a complementary testing on the solar radiation modeling of Envisat. In this version, the classic modeling Solar Radiation coefficient (fixed at 1) is relaxed and replaced by an estimated Solar Radiation coefficient (constrained at 2%).
- V4 uses the same standards as the GDR-C standards. Note that after cycle 71, the GDR's orbit standards are actually GDRC' (see part GDRC).

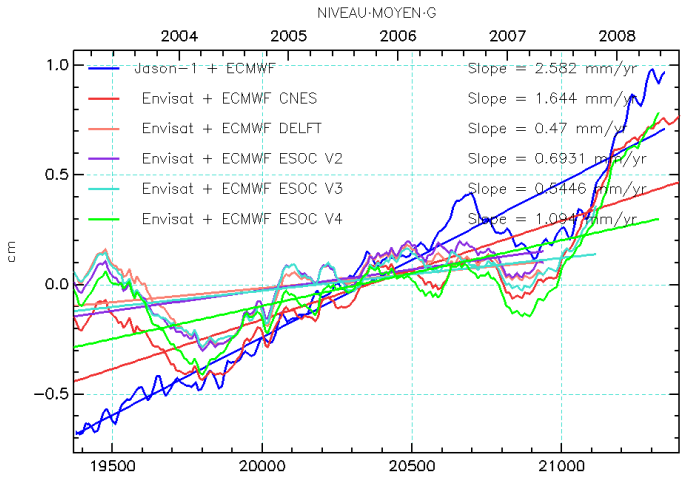

Figure 51: *Centered (averaged removed) Envisat's MSL with different orbits solutions CNES, DELFT, ESOC V2,V3,V4 compared to Jason-1's.*

Figure 51 shows the MSL computed with the different orbits. ESOC V4 uses GDR-C standards, similarly to the future reprocessed data. The reprocessed data are therefore expected to have a similar behavior. Let's first focus on CNES POE orbit (red curve) and on ESOC V4 (green curve):
- After cycle 41 (day 20350 in abscissa): The shape and trend of the ESOC V4 MSL is very similar to CNES GDR-B standard period
- Before 41, however, the ESOC V4 MSL is different and situated above the one using CNES orbit (by a few mm).
- Globally the trend over cycles 22 to 71 (day 20350 to 21400 in abscissa, plot not shown here) is 1.7mm/year, reduced by 0.4mm/year compared to the CNES POE orbit

To compare the trends using the other orbits, the trend must be computed on the same period (13 to 58 only). On this period (see Figure 52):
- ESOC V3 (turquoise) and V4 (green) version are almost superimposed everywhere
- ESOC V2 (purple) is superimposed to V3 and V4 before cycle 44 and stands above them afterwards
- CNES (red) is superimposed to V3 and V4 before cycle 38 and stands above them afterwards
- DELFT (orange) is above all the other orbits before cycle 41 and superimposed to CNES afterwards

This study also evidenced a difference of behavior on ascending and descending tracks, whatever the 4 orbits standard used and compared to CNES POE Orbit (53 (top)).
- DELFT orbit is the most homogeneous from this point of view with only 0.4mm/year ascending/descending difference (between cycles 13 and 58) see Figure 53 (top left)
- ESOC V2 orbit is, similarly to CNES POE, very inhomogeneous: with 1.9mm/year ascend-

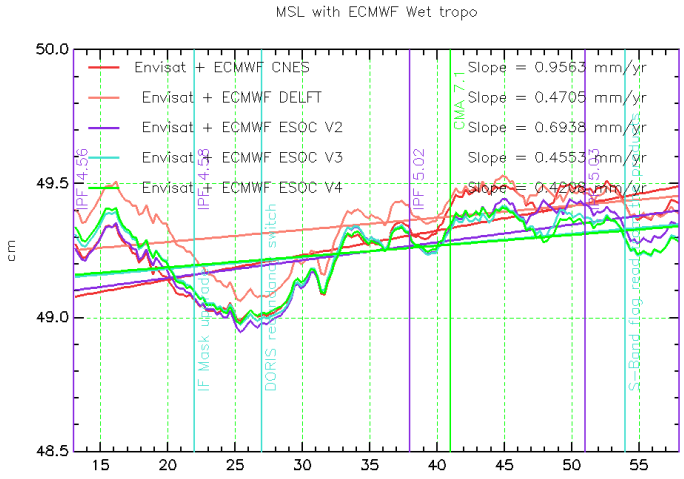

Figure 52: *Envisat's MSL with different orbits solutions CNES, DELFT, ESOC V2,V3,V4 on the period concerning the cycles 13 to 58 only.*

ing/descending difference (between cycles 13 and 58) see Figure 53 (top right)
- ESOC V3 orbit is very homogeneous before cycle 41 and diverges afterwards totalizing a 1.2mm/year ascending/descending difference (between cycles 13 and 63) see Figure 53 (top left)
- ESOC V4 orbit, similarly to ESOC V3, very homogeneous before cycle 41 and diverges afterwards. Note that a bias (around 3 mm) is also introduced between the ascending and descending tracks. The total ascending/descending difference see Figure 53 (top left) is around 1mm/year (between cycles 13 and 69).

In terms of crossover SSH standard deviation the different between V3 and V4 are negligible but ascending/descending discrepancies are sensitive to the type of orbit chosen (see Figure 53 and Table 6).
They are mainly very sensitive for the ESOC V3 case before cycle 38 (compared to V2).
Concerning the ESOC V4 case, the bias introduced bias remains unexplained. The global trend difference is however smaller than the others.

Note that the V3_CR including the complementary testing on the solar radiation modeling of Envisat is not conclusive. Actually, its effect on the MSL is totally minor.

Between cycles 22 and the last cycle (plot not shown here), the trends are sum up in the Table below:

	DEFLT	ESOC V2	ESOC V3	ESOC V4	CNES
Last Cycle	58	58	63	69	71
Asc	1.23	2.3	1.6	2.2	3.13
Desc	0.7	-0.08	-0.03	0.8	0.91
					.../...

	DEFLT	ESOC V2	ESOC V3	ESOC V4	CNES
Asc and Desc	1.1	1.2	0.96	1.7	2.6

Table 6: MSL trends from cycle 22 (in mm/year)

The Table 6 highlights that descending tracks trends are very low compared to the ascending tracks ones, which are in a good agreement with Jason's trend. Therefore, the descending tracks are particularly suspected. Figure 54 shows the difference of orbits (ESOCV2, CNES and DELFT) for ascending tracks only (left) and for descending tracks only (right). This shows that the different orbits have similar behaviors on the descending tracks and that the model evolutions are mostly impacting the ascending tracks.
Unlike the stable right hand plot. Three periods are noticed on the left hand plot:
- After cycle 23: Reduction of noise and annual signal appearing?
- After cycle 31: another reduction of noise is noticed, could be due to the DORIS chained mode evolution (see part 7.1.4.3.3.)
- After cycle 41: Change of behavior of all missions (not only evolution of CNES Orbit (GdrB))

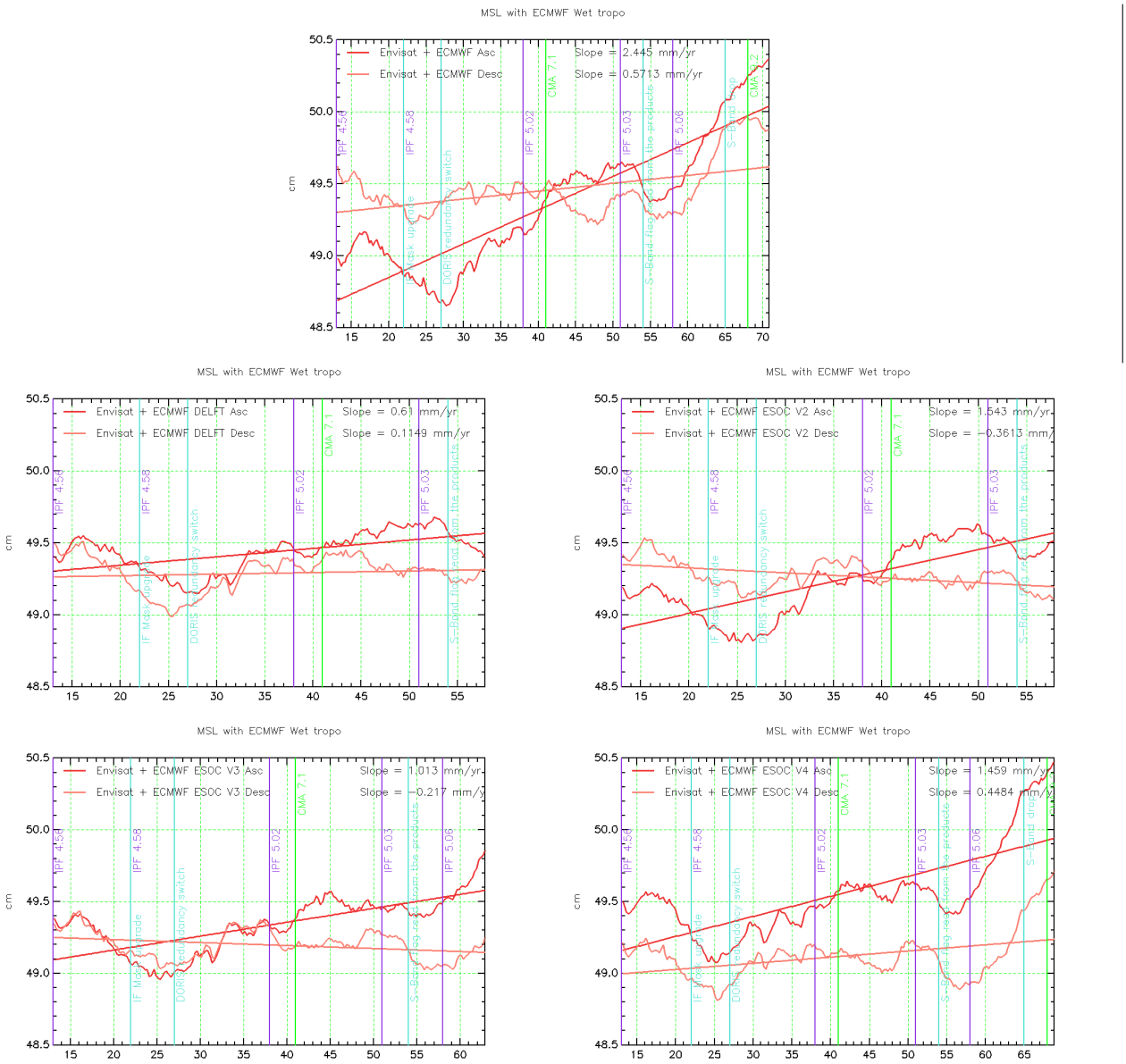

Figure 53: *MSL over global ocean for Envisat with ECMWF Wet tropospheric model and with various orbits. TOP: CNES, MIDDLE: DELFT (left) ESOC V2 (right), BOTTOM: ESOC V3 (left) ESOC V2 (right).*

Finally, this study enables to conclude that the different orbit standards have:
- an impact on the MSL trend, surprisingly the global trend using a homogeneous orbit using the GDR-C standards is reduced compared to the inhomogeneous orbit set (actual CNES POE in a mixed GDR-A,B and C standards). On the cycles 13 to 58 (plot not shown here), the reduction is estimated to around 0.5mm/years).
- a significant impact on the long term drift ascending/descending discrepancies, mainly due to an impact on the ascending tracks.
Therefore, the orbit remains one of the major error source in the MSL trend estimation.

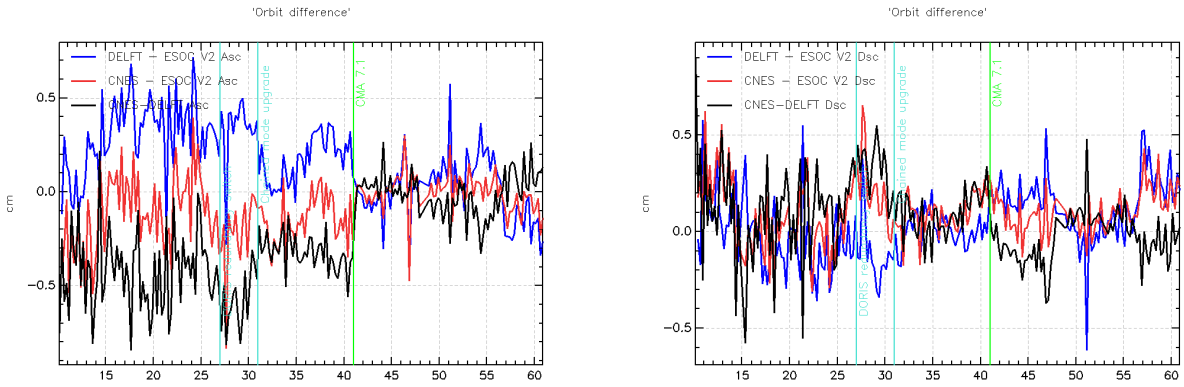

Figure 54: *Difference of orbits solutions for Ascending tracks only (left) and for Descending tracks only (right).*

7.1.4.3.2. DORIS availability

The use of homogeneous orbit on the data set show that the change of behavior on cycle 22 and 41 do not disappear when using other solutions. However, it is important to notice that all this solutions were computed from the same bi-technique method using the DORIS web coverage as well as Laser stations.
Therefore, the evolution concerning DORIS coverage and availability has a direct impact on the data quality as shown in *from F. Mercier et al. Venice 2006 [54]*. The impact on the MSL trend is not well known. Furthermore, this evolution is independent from the orbit computation itself and will have an impact on the reprocessed data as well.

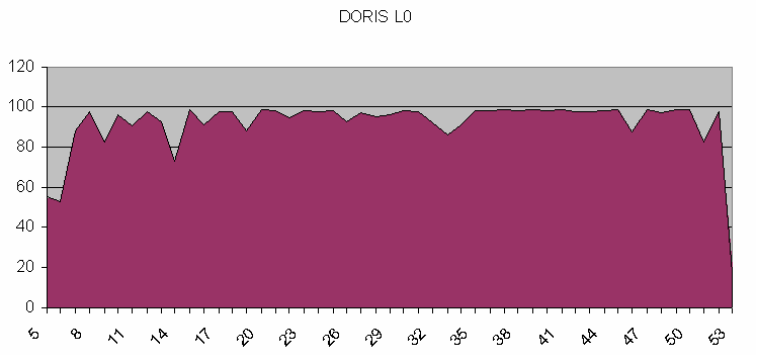

Figure 55: *Doris Level 0 data coverage from cycle 5 to 53. From FPAC team, POD Reprocessing status, November 2008*

Figure 55 shows that (apart from cycles 5 to 9 which are not considered in our studies), DORIS data coverage is rather stable. However, the number of Envisat DORIS measurement changes during the mission. (Figure 56) shows the monitoring of the number of measurements (top) directly linked to the rms of the estimation (bottom). The orbit estimation's rms undergoes several changes. Directly linked to the SLA quality, the orbit quality variation would be likely to have an

impact on the MSL quality. The different jumps or behaviors observed are listed hereafter:
- At the beginning of the mission (before Orbital cycle 20: Envisat cycle 10) a trend is noticed on the number of values: the number of valid data keeps increasing, though reducing the rms. This is probably due to the weak number of Doris Level 0 data but do not impact our data
- Cycle 22 (Orbital cycle 78): another jump is noticed with no particular explanation.
- Cycle 31 (Orbital cycle 122): the introduction of the chained mode improved greatly the number of measurements as well as the rms of the orbit (0.5 mms/s to 0.43 mms/s).
- Cycle 41 (Orbital cycle 172): finally, a jump is explained due to the introduction of a pre-processing allowing no elevation limitation. The global rms is slightly increased by this evolution.

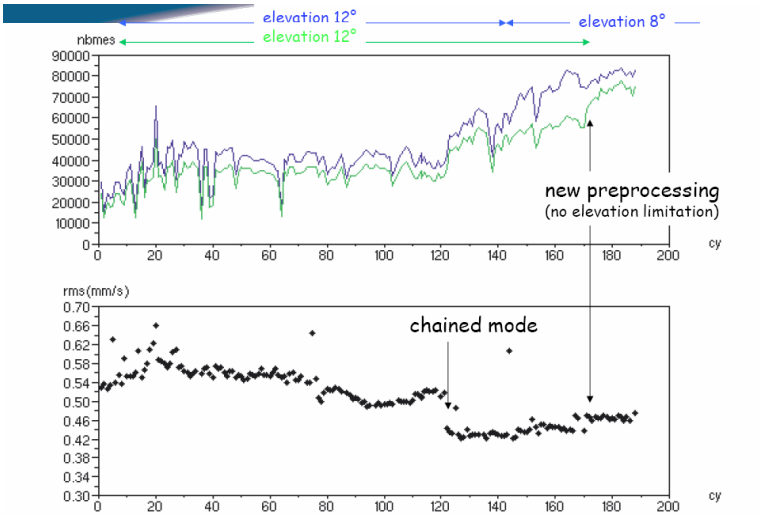

Figure 56: *Envisat DORIS measurement around the chained mode evolution.from F. Mercier et al. Venice 2006 [54].Top Blue: initial number of measurements, Top Green: validated number of measurements, Bottom Black: weighted rms values for each POE arc*

7.1.4.3.3. Analysis of a Doris pure solution on the ascending/descending MSL discrepancies

Doris and Laser data are used in the Envisat POE orbit computation. Beside the nominal Doris/Laser solution production a Doris pure solution is also produced. It would be interesting to test this solution to see the impact of the Laser data. Moreover, as shown on Figure 57, the number of Laser measurements is twice as much important at night time than during daytime. This could potentially induce an inconsistency between ascending and descending passes.

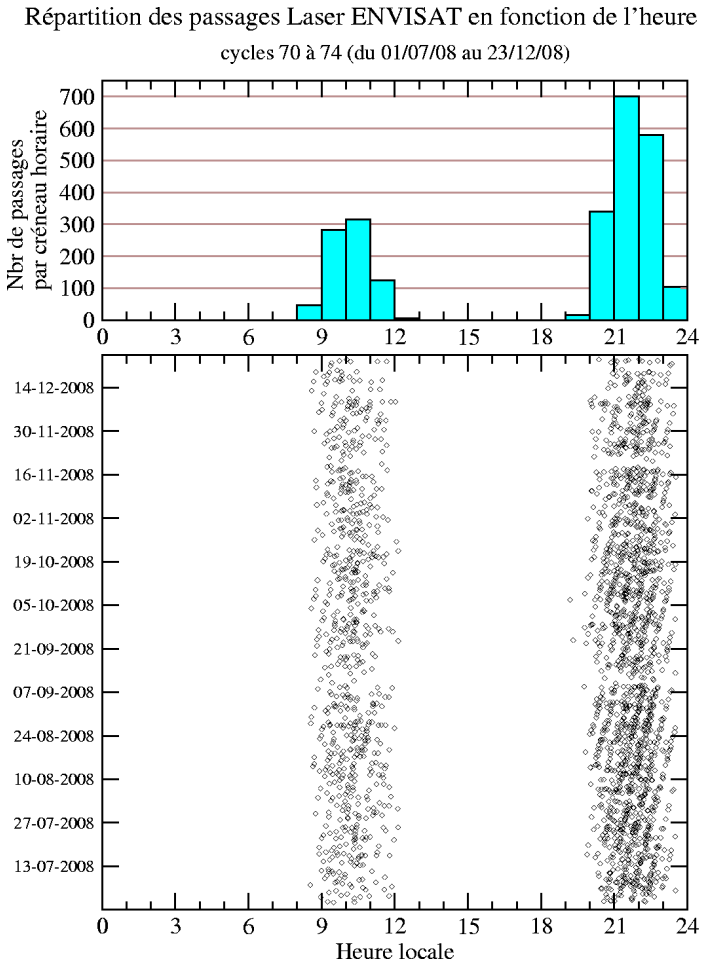

Figure 57: *Envisat's LASER station visibility as a function of local time.*

7.1.5. Conclusion

This year, updates and sensitivity studies were performed on Envisat's MSL.
After many improvements and updates over the whole time series, its similarity to Jason-1's MSL and to tide gauges after cycle 22 and even more significantly after cycle 41 is very encouraging.

All the geophysical corrections improved in the GDRB version were updated on the whole period (Sea-State bias, ionospheric correction, MOG2D Dynamic atmospheric correction...). Therefore, the remaining differences are likely to be due to an orbit inhomogeneity and/or to instrumental updates (PTR drift, IF Mask, ...) and/or to a processing .

The biggest differences concerns the beginning of the mission (before Envisat's cycle 22) were a steep decrease is noticed: this non-physic trend is likely to be due to an instrumental/processing anomaly which seems to be solved afterward. Working tracks were listed to explain it. Note that the ionospheric correction can also be suspected regarding the shape of the difference between the JPL GIM model and the dual-frequency ionospheric correction. Further studies should be carried to understand this correction better.

Another difference is the slight under estimation of slope observed before cycle 41. However, for Envisat, the major discontinuities existing in our data-set are between cycle 40 and 41 due to the gravity model of the orbit. Unfortunately, studies using homogeneous orbits on the whole time series seem to decrease the slope instead of increasing it. The difference of slope shall therefore be due to a combination of errors.

Most geophysical correction were scanned and compared to Remko Scharoo's results from Altimetrics. This study enabled to agree on a new MSL trend and to conclude that the only remaining differences between CLS and Altimetrics come from the wet tropospheric correction used. While, CLS's radiometric wet tropospheric correction is homogeneous to ECMWF model (before 2 major updates during 2007), Altimetrics applies a drift on the 23.8GHz channel and is consistent with NCEP reanalysis fields. For various reasons presented in this document, that choice is not followed at CLS but this discrepancy shows the uncertainty linked to the wet troposphere correction estimation.

That wet troposphere correction is in fact suspected to explain a difference of shape noticed on the end of 2006 and 2007 flattening attributed to a La Niña event. Its model version from ECMWF is also suspected to introduce a erroneous jump at the end of the series. This should be solved by a homogeneous reprocessed ECMWF ERA-INTERIM correction expected for 2009. By now, the use of radiometer corrections is recommended in the MSL computations.

Remaining differences are likely to be due to an orbit inhomogeneity and/or to instrumental updates (PTR drift, IF Mask, ...).

Finally, the sun-synchronous character of Envisat is one of its major differences with Jason-1 mission. The strong asymmetry between ascending and descending tracks could be related to this:
- by a geophysical correction error on one (or both) of the track's parity.
- and/or by an asymmetry of the orbit computation as seen when using different types of orbit.

The table 7 sums up the different suspected terms involved in Envisat's MSL errors.

Term/Correction	Suspected period (cycles)	Expected changes with the reprocessing /Versus GDR products	Expected changes with the reprocessing /Versus CLS altimetric database
Geophysical			
SSB model	Before 41 (+2cm shift due to the GDR-A/B evolution) and Everywhere (-0.5cm additional shift)	Yes (+1.5cm before 41, -0.5cm elsewhere)	No (Update already performed) -0.5cm shift not yet updated
MOG2D High frequency	Before 41	Yes but negligible impact	No (Update already performed)
Dual-frequency Ionosphere corrected from S-Band SSB	Before 41	Yes (around 0.4mm/year)	No (Update already performed)
Dual-frequency Ionosphere Odd behavior/GIM	Everywhere, especially before 22	No	Idem
GIM Ionosphere	Jumps at every solar coefficient update (<1mm jumps every 2 years)	Yes	Idem
MWR Wet Troposphere Side Lobe correction	Before 41	Yes, around 0.15mm/year	No (Update already performed)
MWR Wet Troposphere 36.5GHz drift	Everywhere	No	No but could be corrected in the future
MWR Wet Troposphere New instrumental calibration	Everywhere	Possibly	Idem
MWR Dry Troposphere S1 S2 update	Before 41	Yes	No (Update already performed)
ECMWF Wet Troposphere	At every ECMWF change of version	No	Possibly with ERA-Interim solution
Tides	Everywhere through the aliasing of diurnal errors	No	No

.../...

Term/Correction	Suspected period (cycles)	Expected changes with the reprocessing /Versus GDR products	Expected changes with the reprocessing /Versus CLS altimetric database
Orbital			
DORIS on board processing wait/chained mode	Before 30	No	No
DORIS ground pre-processing	Before 40 (TBC)	Possibly	Idem
CNES POE	Before 41	Possibly	Idem
CNES POE	After 41	Possibly	Idem
Instrumental			
USO	Everywhere especially during anomaly periods	Yes	No (Update already performed with Auxiliary files)
UTC/ICU clock	?	?	Idem
IF Mask	Before 41 especially before 22	Probably negligible	Idem
PTR drift	Everywhere	Possibly (+0.7mm/year TBC)	Idem

Table 7: *S*uspected terms in Envisat's MSL errors

Envisat MSL behavior should be further studied and better understood next year, thanks to the full mission reprocessing planned for 2009. The aim of such study should be to be sufficiently confident in the trend to make it available for climate-oriented studies.

7.2. Orbit comparison analysis

7.2.1. Introduction

The aim of this study is to compare the orbit included in the product (CNES POE) to three other solutions developed in the European Space Operations Centre (ESOC POE): version V3, V3_CR and version V4. These three solutions use recent standards, and are available over a long period, cycles 10-60 for V3 version, cycles 10-71 for the V4 version. This allows us, first, to assess the quality of the GDR orbit through a cross comparison study over the GDR-B period (41 to 60). Then, V4 version gives us a first idea of the reprocessed data as far as it is very close to GDR-C standards. Finally, this allows us to produce homogeneous SLA time series over the whole Envisat period, which is of interest for the analysis of MSL trend for exemple.

7.2.2. Orbit configuration

The different orbit configurations are available in the Appendix at the end of this document.

7.2.3. Processing

The reprocessed ESOC V3 and V4 orbits have been studied for respectively cycles 41-66 and cycles 10-71. Before using these orbits the editing used for CNES orbit has been applied to the ESOC orbits in order to remove wrong measurements, mainly around maneuvers. A criteria base on differences between CNES and orbits studied has also been applied.

Criteria	Min	Max
SSH	-130m	100m
SLA	-2m	2m

Table 8: *E*diting based on threshold on SSH

Criteria	Maximum autho-rized $\|Mean/pa$	Maximum autho-rized Stdev/pass
Differences between CNES and orbits studied	5cm	5cm
SLA ($Bathy < -1000m$,$Var < 30cm$)	30cm	30cm
SLA ($Bathy < -1000m$,$Var < 10cm$, Nbr of points¿200)	15cm	15cm

Table 9: *E*diting based on statistics per pass

7.2.4. Orbit differences

Figure 58 shows the mean orbit differences over cycles 41 to 66 (V3) and cycles 41 to 71 (V4). Starting from cycle 41, the strong difference due to the well known GDR-A/GDR-B improvement is avoided. The differences are quite small in both cases, lower than 1.5cm.

- ESOC V3/CNES: The global bias is about -1.3mm with a East West pattern clearly visible. ESOC V3 is lower than CNES orbit in the Atlantic and in the East Pacific Ocean whereas it is higher in the Indian and West Pacific oceans.

- ESOC V4/CNES: The global bias is about -1mm as well. The geographical differences are similar to the ones observed with V3 but slighly weaker mainly in the south Brasilian zone.

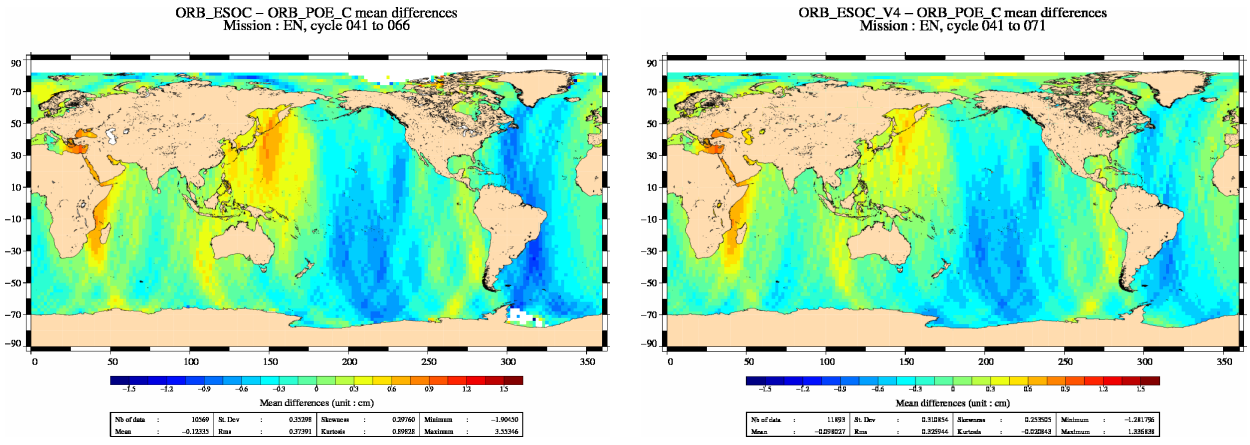

Figure 58: *ESOC V3-CNES (left) and ESOC V4-CNES (right) mean differences from cycles 41*

Figure 59 (top) shows the mean of differences per cycle.

- ESOC V3/CNES: The global bias is about -1.3mm with an increase of the bias (2mm) for cycles 54 to 57 were ESOC V3 is lower than CNES orbit during this period for an unexplained reason.

- ESOC V4/CNES: The global bias is about -1mm as well but the time series is split into 3 periods: before cycle 41 where the bias increases from 0 (cycle 10) to -1.5mm (cycle 40). Afterwards (the rupture could also be done around cycle 34), the series is quite stable around -1.5mm with no particular jump for cycles 54-57. Finally, after cycle 68 (and actually not for cycle 71), the bias is around 0 again. The impact of this jump on the change from GDR-B to C reaches around 1mm which could have a non negligible impact on the MSL trend. Note that for GDR-C' (cycle 71), the bias is reduced (0.5mm) compared to GDR-C.

In terms of Crossover Variance gain Figure 59 (bottom), we have:

- ESOC V3/CNES: Equivalent performances are observed for both orbits because the gain is alternatively positive and negative during the GDR-B period (between +1cm2 and -1cm2). A particular variance difference is however noticed for cycle 51 and cycle 61 signing a lower performance for ESOC V3 than for CNES orbit.

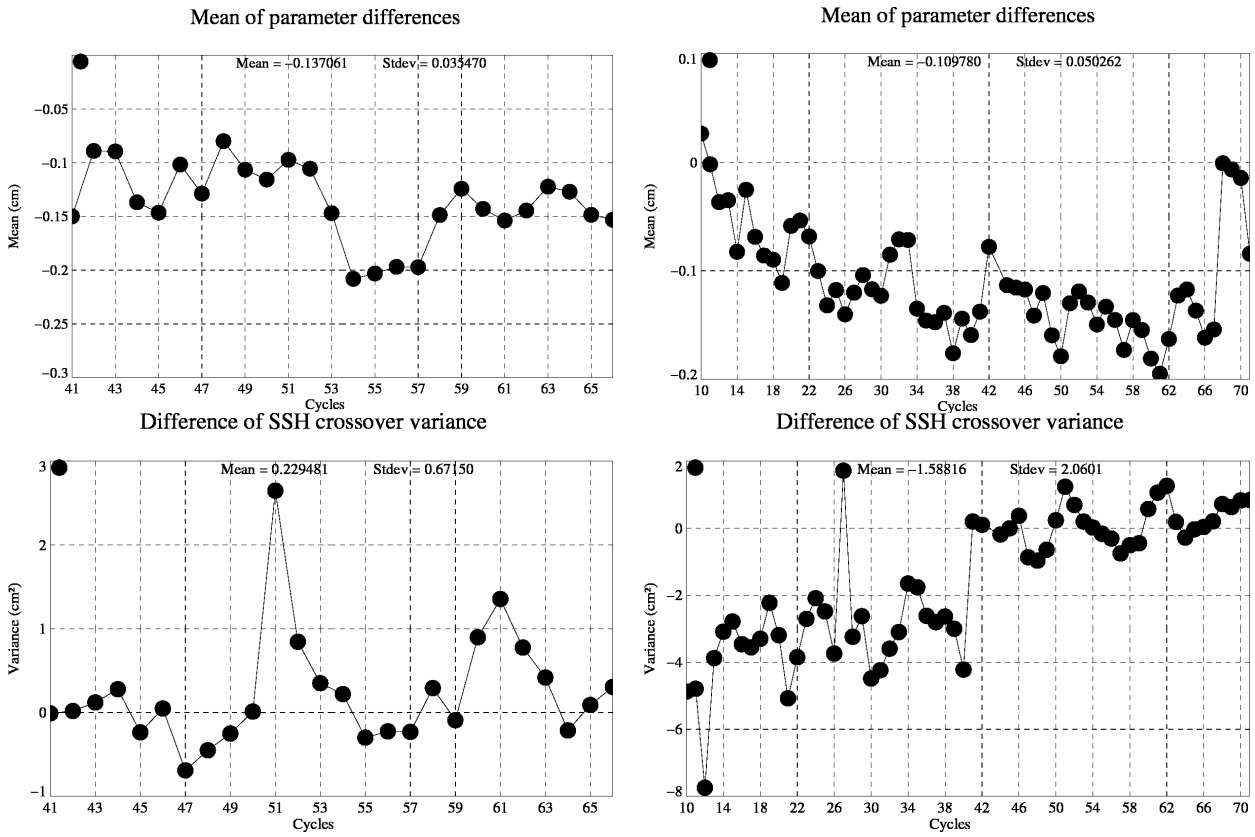

Figure 59: *ESOC V3-CNES (left) and ESOC V4-CNES (right) Mean differences (top) and Crossover Variance gain (bottom)*

- ESOC V4/CNES: The time series is also split into 3 periods: As expected, before cycle 41 ESOC V4 performance is much better than the GDR-A standard CNES orbit (around 3cm2 variance gain observed). Afterwards, the variance gain is less obvious (centered signal) and an annual signal is noticed with alternative positive and negative variance gain. Finally, after cycle 68, the variance gain becomes unexpectedly positive (around 0.6cm2), meaning that ESOC V4 degrades slighly the quality of the data compared to the CNES POE version available from this cycle.

Finally, the study was completed by a comparison of SLA variance gain (see Figure 60). As expected, a variance gain is observed before cycle 41 on the comparison between ESOC V4 and CNES. But, this criteria also shows that, for both comparisons, an annual signal can be observed on the gain after cycle 41. This is explained by the introduction of a time varying gravity field in both ESOC V3 and V4 solutions. This annual signal could also be observed on Jason-1 with the new GDR-C orbit.

7.2.5. Conclusion

In this study, the quality of ESOC V4, based on the GDR-C orbit was found to be good but with similar performances than the older version ESOC V3 and no evidence of a spurious drift could be noticed. However, a 1mm bias is observed when comparing GDR-B to GDR-C. This kind of study

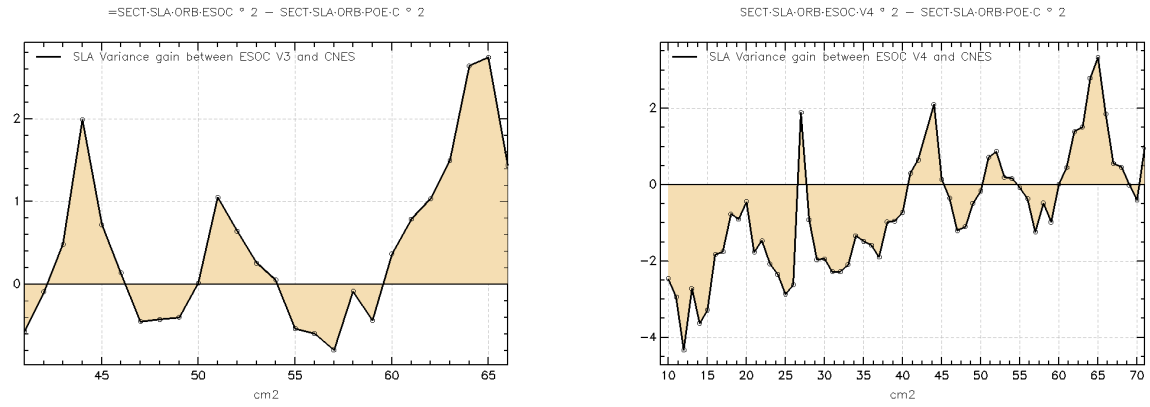

Figure 60: *ESOC V3-CNES (left) and ESOC V4-CNES (right) SLA Variance gain*

enable to evidence such small jumps which could hardly be seen on the SLA itself and that could have a non negligible impact on the MSL trend.

7.3. Study on ENVISAT Jason-1 crossovers: geographical biases

7.3.1. Introduction

This study aims at describing the geographical features of the Envisat/Jason-1 differences. Using this cross calibration technique we are able to observe the sum of the geographically correlated errors of the two satellites. These errors can have a similar or a different signature on the ascending and descending passes of each satellite. In the first case, they can be observed using a single crossover analysis on each mission separately, but in the other case, they are only visible with a cross calibration or an external calibration. The use of Grace gravity model in the orbit solution has almost completely cancelled the first type whereas the second one, though reduced are still significant.
Envisat and Jason-1 altimetry systems are not completely independent (Doris technique for the orbit computation, same geophysical corrections...) but they have strong differences in terms of instruments, processing and of course orbit plan. The fact notably that Envisat is sunsynchroneous might cause particar errors. Using a dual crossover analysis is thus particularly interesting to investigate these errors.

7.3.2. Data used and processing

Since the GDR "version b", Grace gravity models are used in the POE orbit computation which dramatically reduces the differences. Long time series are thus necessary to observe these fine signals. Cycles 10 to 64 are used for this analysis. The full reprocessing of Jason-1 products in b version was completed mid-2007 whereas Envisat products have not been reprocessed yet. Most of the Envisat GdrB upgrade has been implemented in the CLS altimetry data-base but the CNES POE orbit, one of the SSH component that strongly changes in the GDR product, can't be updated for cycles lower than 41. Orbit solutions from the ESOC center have thus been used in order to work on a longer homogeneous time series (cycles 10-60). The V3 version has been used (see standards description in a dedicated part). Several periods of time will be thus considered:
-Cycles 10-41 corresponding to Envisat GDRA data
-Cycles 41-64 corresponding to Envisat GDRB data
-Cycles 10-60 corresponding to the ESOC V3 orbit availability

The baseline for the SSH formulae used in this study is described in the SSH assessment part. The ECMWF model is used for the wet tropospheric correction. The sensitivity to the type of wet troposphere correction (radiometer instead of model), ionosphere correction (dual frequency versus GIM model) and tide correction (GOT 2000 versus FES 2004) has also been analysed.

The processing is the following:
-Computation of cyclic 10-day dual crossovers
-Average in 2°x2° geographical bin for each cycle
-smoothing of the 2x2° individual maps using a loess filter with an approximately 2500km wave length in order to remove the effect of the mesoscale variability
-computation of the temporal mean of the 2x2° raw map time series
-computation of the temporal standard deviation of the smoothed 2x2° map time series

The temporal mean differences will show the local biases whereas the standard deviation will

inform on the variability of these biases. As an example the effect of the filtering of the individual maps is shown in figure 61. On the top figures the standard deviation map is dominated by the mesoscale variability, whereas on the bottom, the map shows expected structures. Note that the global mean difference has been removed in order to have differences centred around zero.

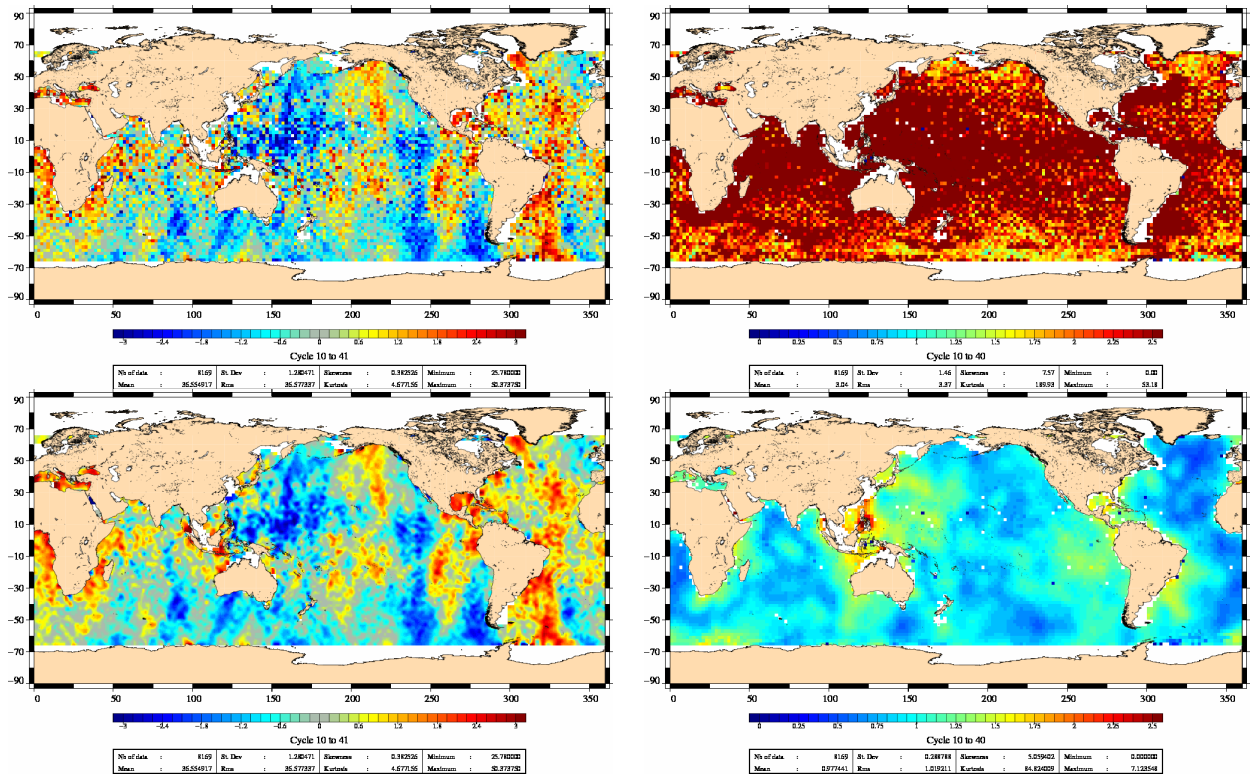

Figure 61: *Envisat-Jason-1 average (left) and standard deviation(right),raw (top) and smoothed (bot)*

7.3.3. Impact of the GDR version

The impact of the GDR version is shown in Figure 62. Mean differences ups to +/-3 cm are observed on several areas for the GDRA version. Using GDRB data the differences strongly change. The differences related to the gravity model errors have disappeared. There are now slight East/West differences. The standard deviation is globally reduced. Both mean and variable geographically correlated errors have been reduced, only a slight basin scale difference remains.

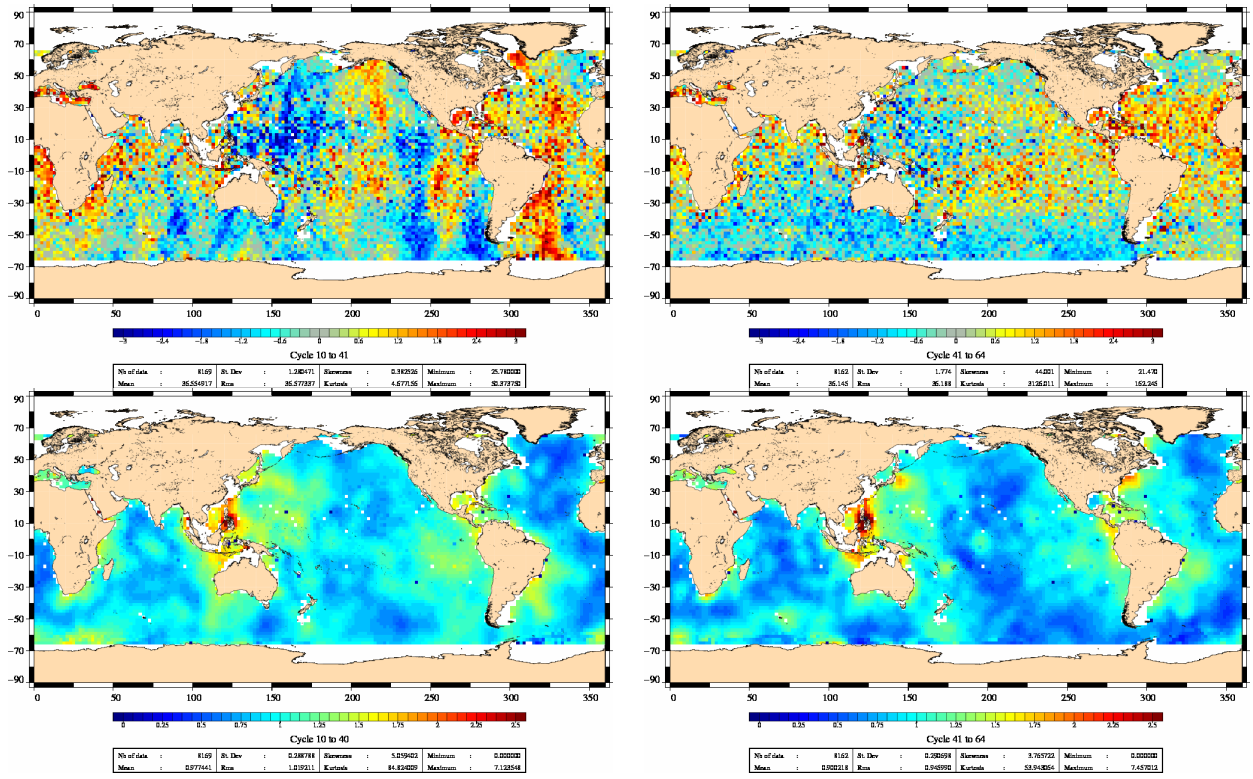

Figure 62: *Envisat/Jason-1 Average (top) and Standard deviation (bottom) at Crossovers with Envisat GdrA (left), and with Envisat GdrB (right)*

Note that using the Jason-1 data in GDRb version without updating a SSB model compatible with the MLE4 retracking, we obtain much stronger differences as seen on 63 on the left. Note that such an updated SSB is available in the GDRc version of Jason-1.

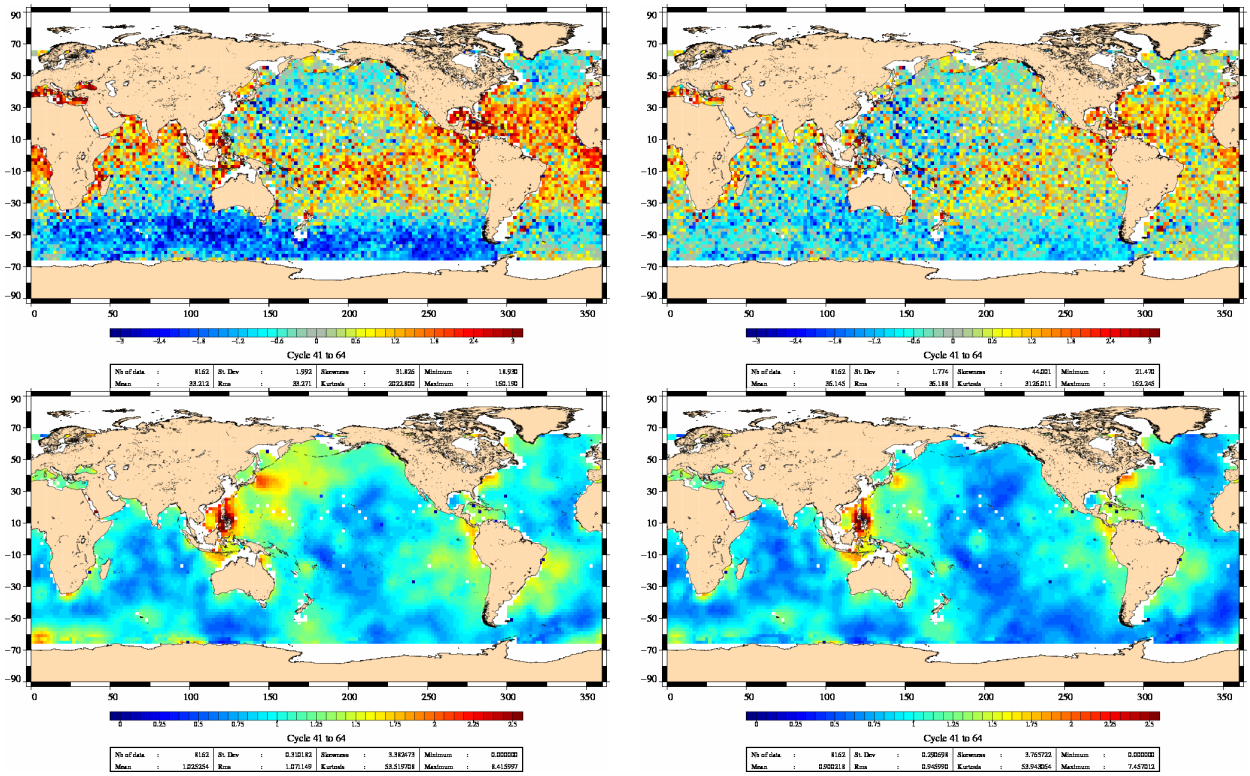

Figure 63: *Envisat/Jason-1 Average (top) and Standard deviation (bottom) at Crossovers with Envisat GdrB exept for the SSB (GdrA) (left), and with Envisat GdrB SSB included (right)*

7.3.4. Impact of the Orbit solution

The map of statistics of the SSH differences at crossovers using the ESOC orbit on the period 10-60 are shown in figure 64. The mean differences are much less noisy than those previously obtained over a shorter period. Using the ESOC orbit, a North/South structure now dominates the difference: negative differences are observed in the Southern Hemisphere at high latitudes. Relatively strong (2cm) positive patterns around central America are noticed. Note that on the left hand side, both orbits from J1 and Envisat come from a CNES standard whereas onthe right hand side, orbits don't come from the same orbit center (CNES/ESOC), introducing a relative inhomogeneity mostly in the Pacific ocean. The Standard deviation is on the contrary slightly higher using the ESOC orbit.

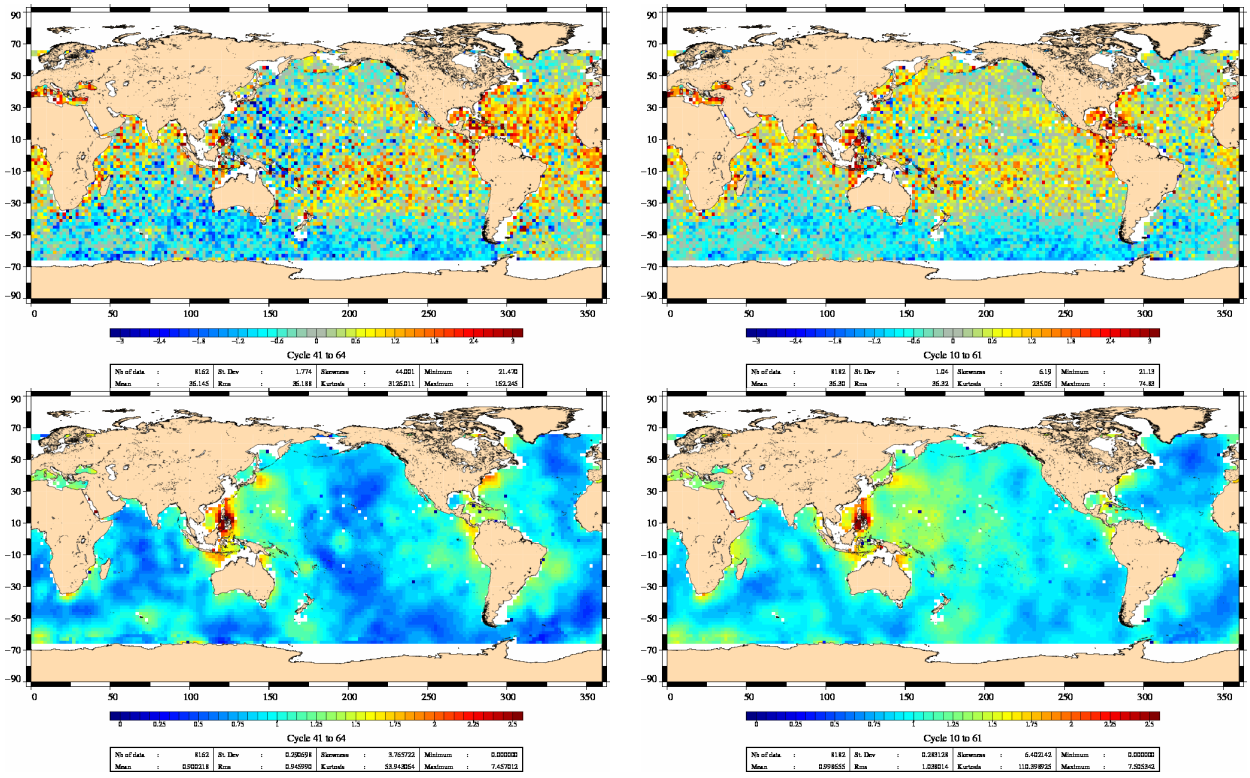

Figure 64: *Envisat/Jason-1 Average (top) and Standard deviation (bottom) at Crossovers with Envisat GdrB with CNES POE and ECMWF wet tropo (left), and with Envisat GdrB with ESOC POE and ECMWF wet tropo (right)*

7.3.5. Impact of the corrections

The impact of several geophysical corrections on the mean differences are also analysed in the following figures. Using the radiometer correction instead of the model increases the inconsistency. Note that the Envisat MWR correction with the side lobe correction has been updated on the whole whole mission . Using the GIM correction instead of the dual frequency ionosphere correction has little impact. Using the FES2004 model instead of the GOT00 model changes the differences in Indonesia and West Madagascard. It increases the biases and variability almost everywhere.

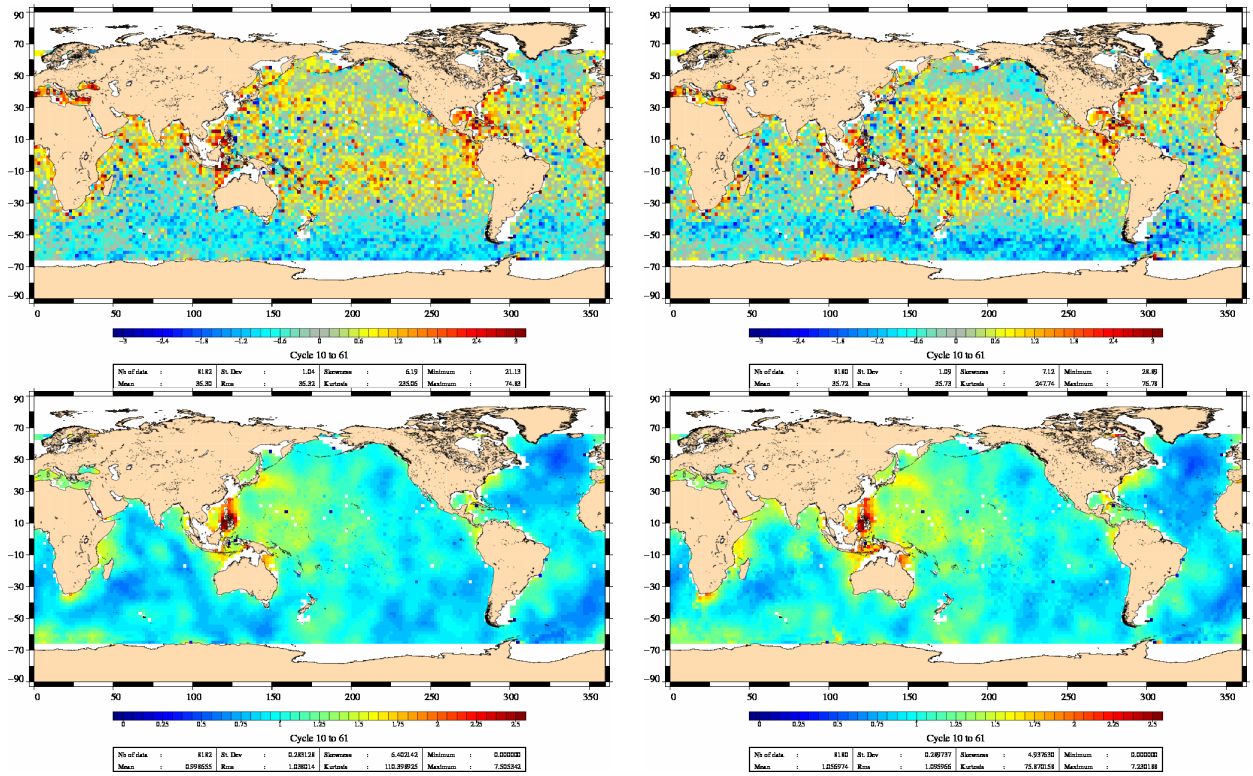

Figure 65: *Envisat/Jason-1 Average (top) and Standard deviation (bottom) at Crossovers with Envisat GdrB with ESOC POE and ECMWF wet tropo (left), and with Envisat GdrB with ESOC POE and Radiometer wet tropo (corrected from Side Lobe) (right)*

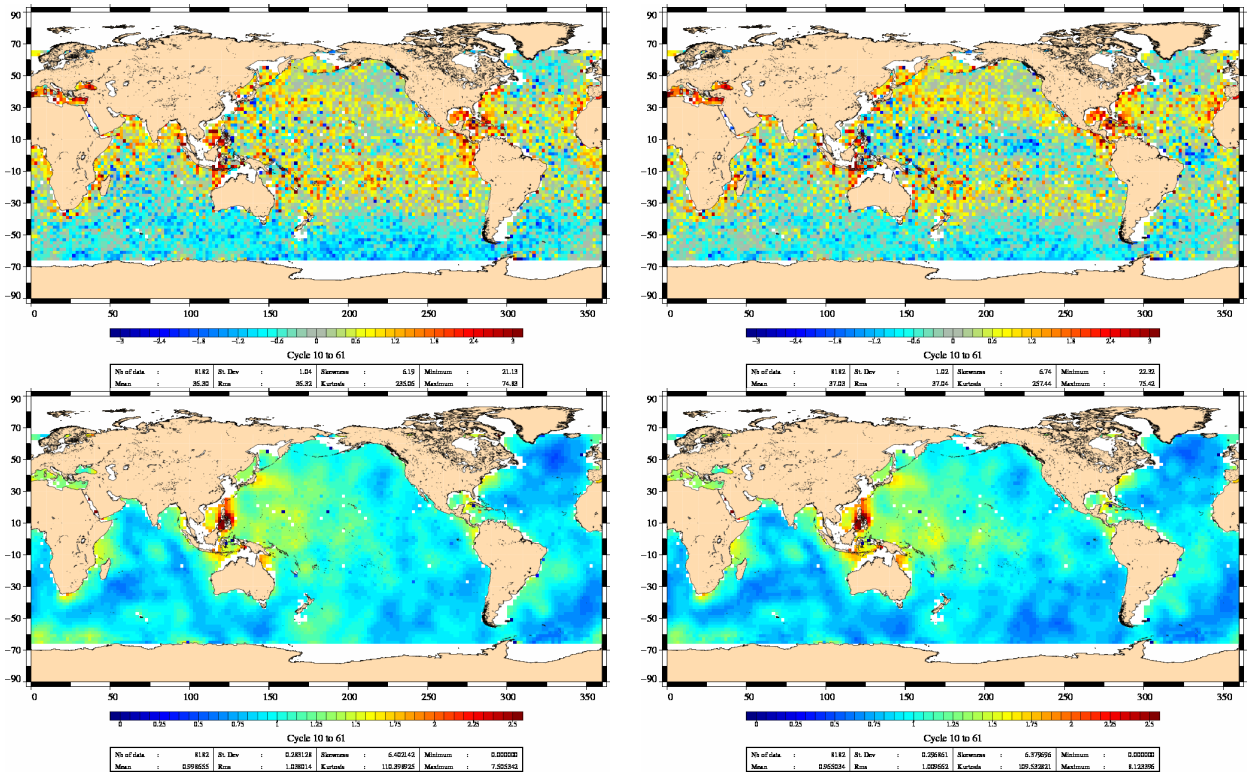

Figure 66: *Envisat/Jason-1 Average (top) and Standard deviation (bottom) at Crossovers with Envisat GdrB with ESOC POE and ECMWF wet tropo and Mixte Ionosphere (Bifr+ GIM) (left), and with Envisat GdrB with ESOC POE and ECMWF wet tropo and GIM Ionosphere (right)*

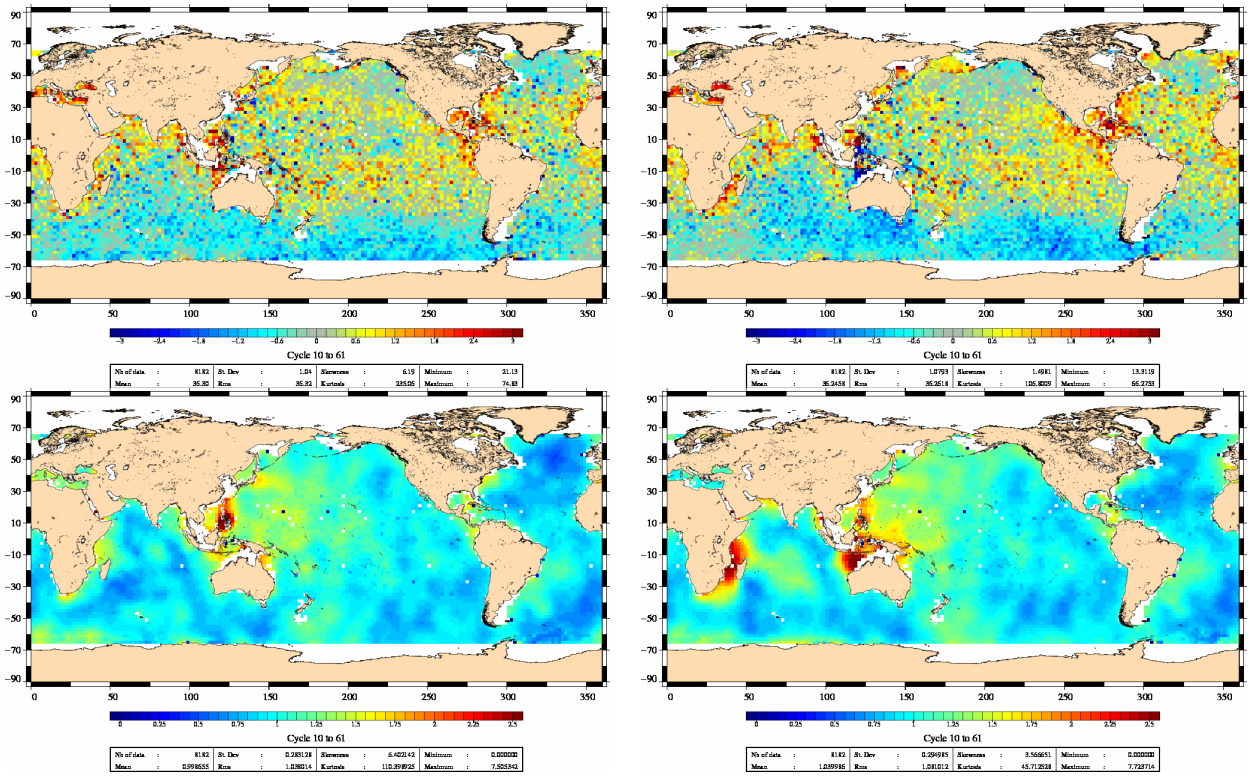

Figure 67: *Envisat/Jason-1 Average (top) and Standard deviation (bottom) at Crossovers with Envisat GdrB with ESOC POE and ECMWF wet tropo and GOT00 tide model (left), and with Envisat GdrB with ESOC POE and ECMWF wet tropo and FES04 tide model (right)*

7.3.6. Impact of the ascending descending separation

The map of statistics of the SSH differences at crossovers using ESOC orbit on the period 10-60 and separating ascending and descending Envisat passes are shown in Figure 68. The main comment is that Jason-1 is more consistent with Envisat descending passes than ascending passes in terms of geographically correlated biases.

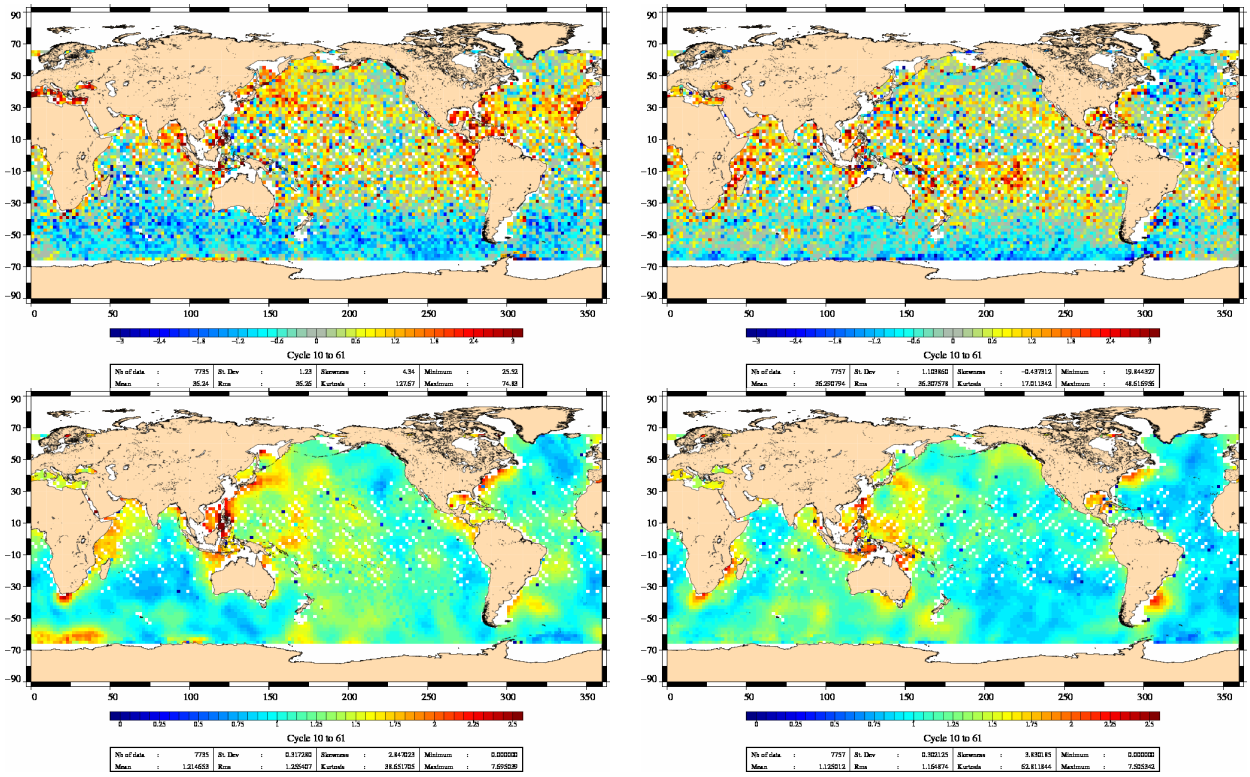

Figure 68: *Envisat/Jason-1 Average (top) and Standard deviation (bottom) at Crossovers with Envisat GdrB with ESOC POE and ECMWF wet tropo (Asc) (left), and with Envisat GdrB with ESOC POE and ECMWF wet tropo (Desc) (right)*

7.4. Improvements of the GDR with GDR-C Orbit and DAC

A **reprocessing** of the whole Envisat altimetric mission is expected for 2009. The major evolutions will be a new precise orbit based on recent Grace data and new ITRF model, better ECMWF meteo fields, new geophysical and instrumental (USO) corrections, new SSB correction, updated wet tropospheric correction. Besides it is planned to re-process ERS-2 data with similar algorithms. Then, performances and comparisons will be carried out again using these new data in order to assess the consistency between Envisat and ERS-2 parameters.
These new products will further improve the high quality level of the Envisat altimetric mission and will make easier the data fusion for multi-mission altimetry, as it is essential for oceanography and applications.

By now two evolutions occurred from cycle 68 onwards:

- On cycle 68: the GDR C Orbit was implemented for Envisat (see part) and Jason-1, but extensive studies were done for Jason-1 GDR-C orbit (see [7] or [10]), evidencing that one of the trend modelled in the time gravity field could introduced some long term errors. A new GDR-C' standard was therefore implemented and computed agan from cycle 68 on Jason-1 (not for Envisat). Another refined version (GDR-C") that will be used for Envisat's reprocessing was also computed.

- On cycle 71: the GDR C' Orbit was implemented for Envisat. For this mission, CNES GDR-C (nore GDRC') standard were not analysed yet, but an homogeneous orbit from ESOC in a similar standard configuration was checked on Envisat (see part).
- On cycle 68, introduction of a new High resolution Dynamic atmospheric correction: this correction was studied for both Jason-1 and Envisat missions. The main results are detailed hereafter.

The map of SSH at crossovers difference between the new and old correction is shown on Figure 69. It shows that in coastal areas (less than 200km from the shore), DAC's high resolution is mostly similar to the low resolution version. However, in some zones such as around England, Ireland and near the Hudson bay (North Canada, blue on the map), a strong improvement is noticed. It is also the case in the Baltic sea, Black sea, Red sea, as well as in the Persian Gulf : This improvement is due to the fact that those closed seas are not included in the MOG2D model griding that generates the DAC. Therefore, in these zones the low frequency DAC contains the invert barometer values.
Finally, a significant improvement is noticed in the open ocean near Bellingshausen basin, South from Australia, North Atlantic and North Pacific.

Moreover, the variance gain is plotted Figure 70. It is higher when approching the coasts and reaches up to 3cm (once converted into standard deviation) at less than 100km from the coasts. Elsewhere, it also improves the data quality (of 1cm for Jason-1 and around 1.5cm for Envisat).

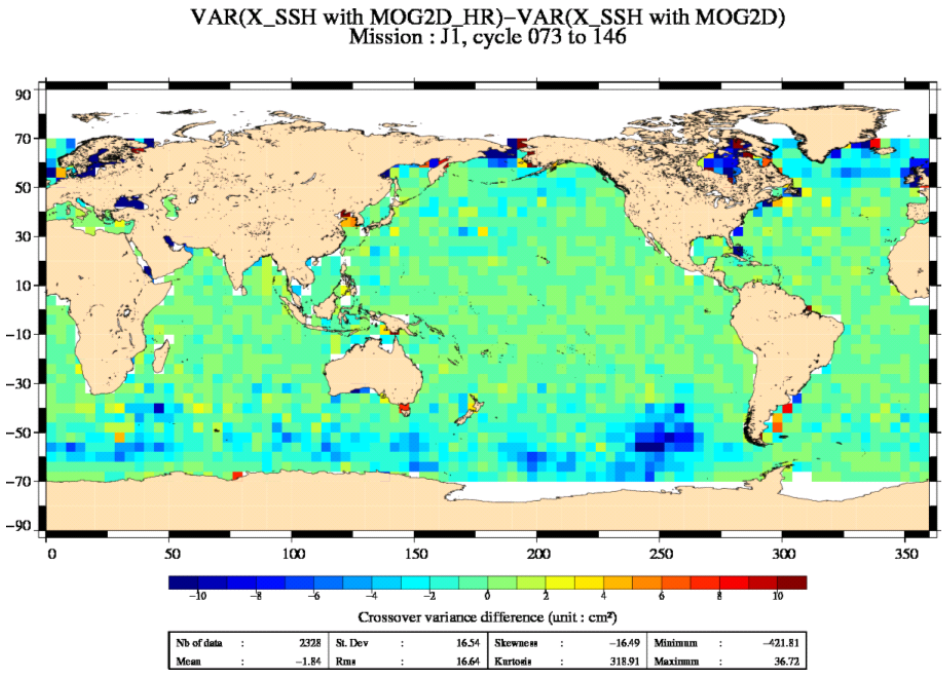

Figure 69: *Difference of the SSH at crossovers with high resolution DAC for Jason-1 mission Jason-1 during 2004-2005.*

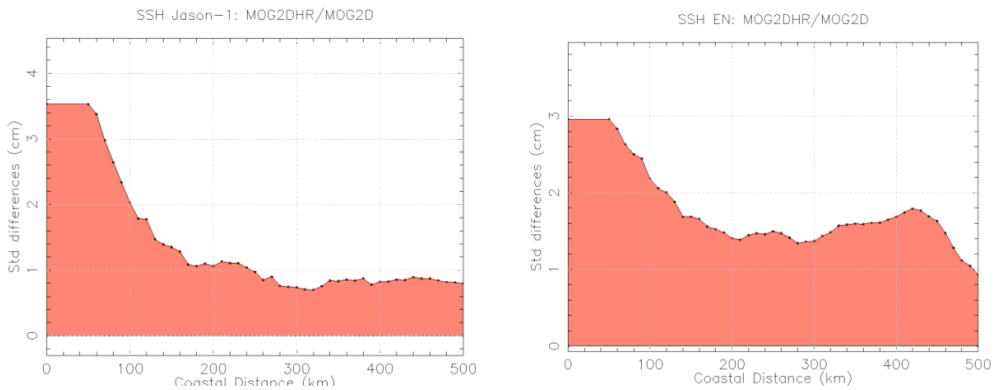

Figure 70: *Square root of the SSH at crossovers' variance gain versus the distance to the coast for 2004-2005 and for Jason-1 (left) and Envisat (right).*

7.5. Cross-Calibration with Jason-2

7.5.1. Introduction

The OSTM/Jason-2 (Ocean and Surface Topography mission) satellite was successfully launched on 20th of June, 2008. Since 4th of July Jason-2 is on its final orbit, and flew in tandem with Jason-1 up to when Jason-1 was moved to a different orbit (shifted from 5 days) on the 26-28th of January 2009. Extensive Jason-1/Jason-2 comparisons have been performed since both missions were on the same orbit spaced out by 55 seconds during the tandem phase.

In this study, the use of Envisat, the other flying precise altimetric mission, is considered. This is shown to complete the cross-calibration and validation of the Jason-2 mission by giving a 3rd point of comparison to explain discrepancies between Jason-1 and Jason-2.

A global cross-calibration analysis between Envisat and Jason-2 data has been carried out as part of the SALP/CalVal activities, completing both Envisat/Jason-1 and Jason-2/Jason-1 cross-calibrations. Over the life period of Jason-2 the two missions have been compared in terms of geographically correlated SSH differences, high frequency content of the SSH signal and monitoring of relevant parameters. Results are given for IGDR products and completed with the POE precise differed time orbit. These results are setting the basis of a long term monitoring on differed time Geophysical Data Record (GDR) products.

7.5.2. Conclusion

Envisat /Jason-2 are very consistent
standard deviation of cross-over differences = 4,5 cm (IGDR) and 3.4 cm (GDR), which enables a precise cross calibration

Envisat is a useful third point of comparison between Jason-1 and -2
- The geographically correlated biases between Envisat and Jason-2 are lower than with Jason-1.
- High frequency content for Envisat Jason-1 and Jason-2 are very consistent at 1Hz and 20Hz, independently from the tracker used on Jason-2.
- Concerning the 20Hz content, the comparison with other missions enables to notice a light coloration of the noise above 3Hz (see [59]).

Jason-1 and -2 comparisons with Envisat GDR are very consistent
This is encouraging for insuring a good continuity on the long term monitoring already initiated with Jason-1 since 2002.

This cross calibration shows that precise analysis can be performed even if the satellites are not on the same tracks, so paving the way to the calibration of Cryosat and/or Sentinel 3 missions that will use new repetition ground tracks.

7.5.3. Whole OSTST presentation

Jason-1/2 cross-calibration with Envisat

A. Ollivier, Y. Faugère - CLS
N. Picot - CNES, P. Femenias - ESA

Introduction

- Since Envisat was launched, Cross Calibration studies with the Jason-1 mission are performed to assess the data quality and performances of both missions.
- A precise altimetric mission as Envisat can help to understand the observed differences between Jason-1 and Jason-2 by giving a third reference
- This presentation aims at showing the cross-calibration between Jason-2 and Envisat, enlightened by 6 years of cross calibration with Jason-1.

Overview

In this presentation, we will focus on :

1. Short overview Envisat / Jason-1 GDR : *How close are they today?*
   - ➔ Comparisons using GDR products on the whole period
2. Envisat / Jason-2 : *Envisat, a useful third point of comparison between the Jasons*
   - ➔ Comparisons using IGDR products on the 110 days of Jason-2 life time
   - ➔ Engaging results concerning comparisons using GDR products on the 60 days of data
3. Envisat / Jason-2 / Jason-1 : *A specific comparison analysis*
   - ➔ High frequency content comparison.

1. Envisat / Jason-1 GDR : *How close are they today?*

Envisat GDR status

- 6 years of data availability

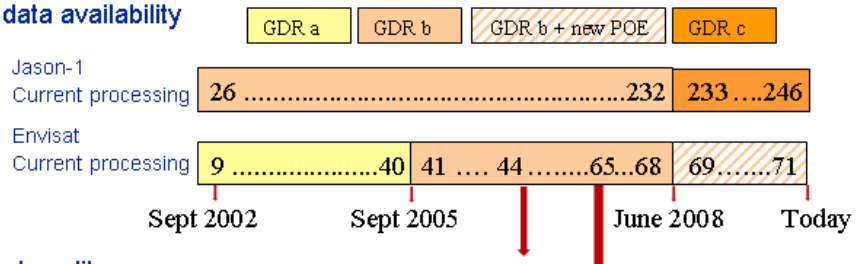

- Good general quality :
  - Very good availability of data.
  - **USO anomaly**: In February 2006, the RA-2 Ultra Stable Oscillator (USO) clock frequency underwent, for an unknown reason, a strong change of behavior.
    → Altimeter range can be corrected from this anomaly by users, thanks to **auxiliary files** distributed by ESA since mid 2006
  - **Loss of the S-Band**: On the 17 January 2008, a drop of the RA2 S-band transmission power occurred. There is thus no more dual frequency altimeter both in A and B-Sides.
    → GIM ionospheric correction is available in the IGDR and GDR products
- **Reprocessing** of the whole Ra-2 Envisat GDR in version C will be done in 2009

Jason-1 / Envisat consistency

- Good consistency between the two missions.

Envisat –Jason-1 dual cross-overs on cycles 10 to 61 with a homogenised dataset

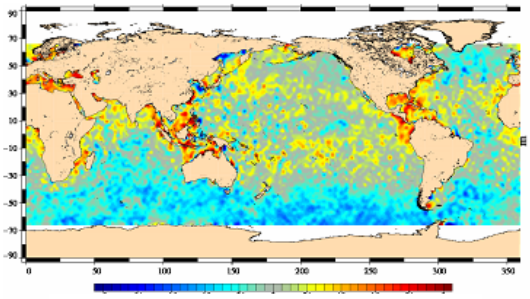

→ **Consistency in terms of geographically correlated biases**

Mean Sea Level trend from cycle 41

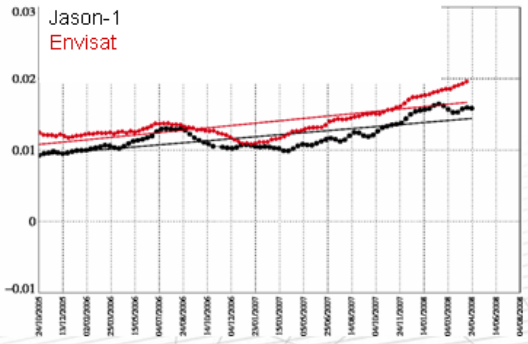

→ **Consistency in terms of MSL on mid-2005/2007**

- More details in Poster "Envisat /Jason-1 Cross-Calibration" (Faugère et al.)

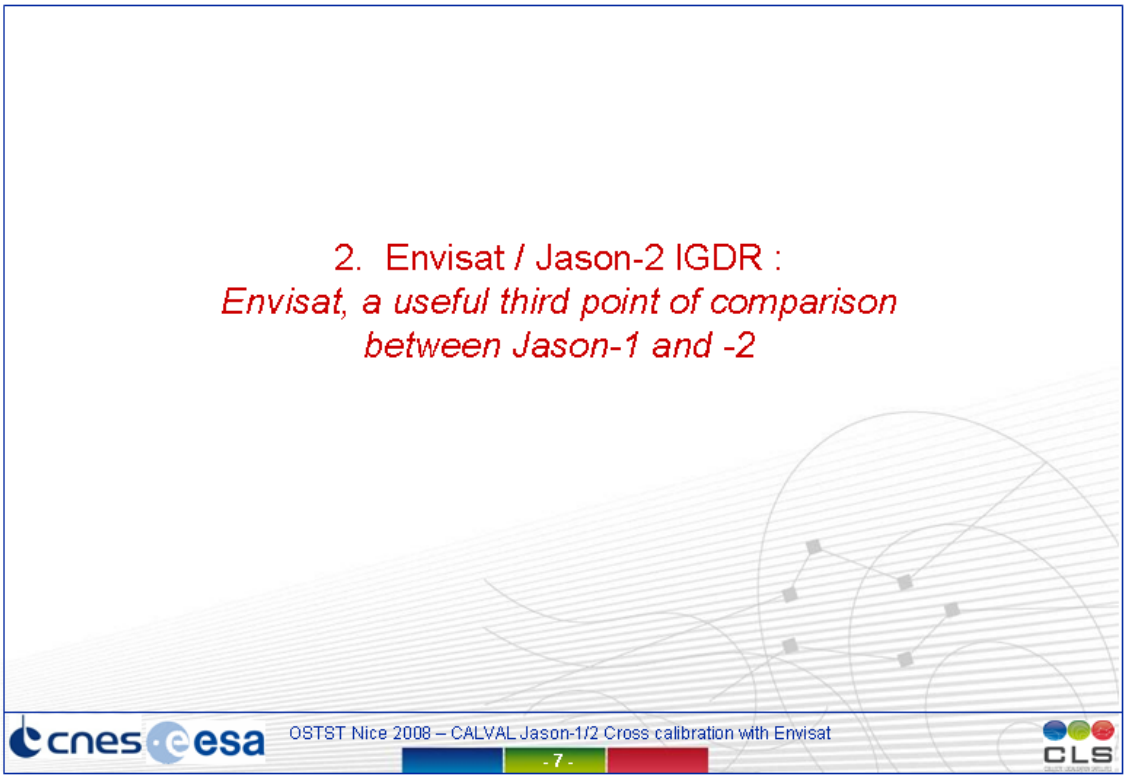

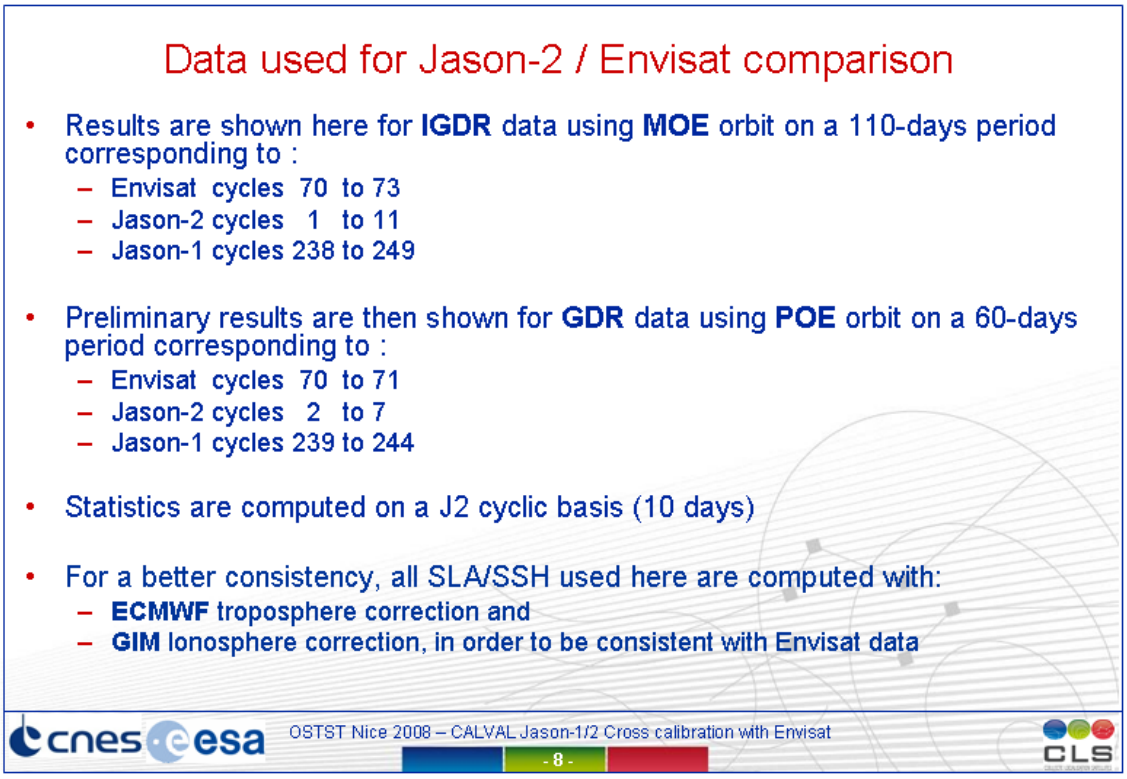

Differences of along track SLA

J2- J1 SLA using MOE

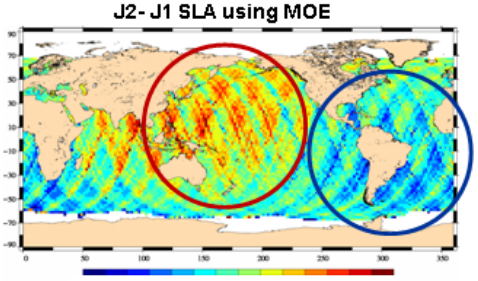

EN- J2 SLA using MOE

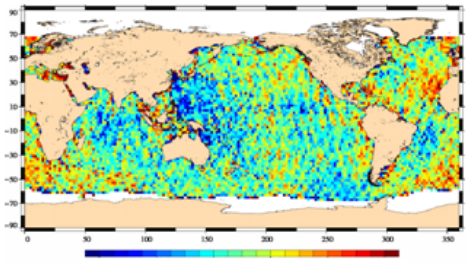

EN- J1 SLA using MOE

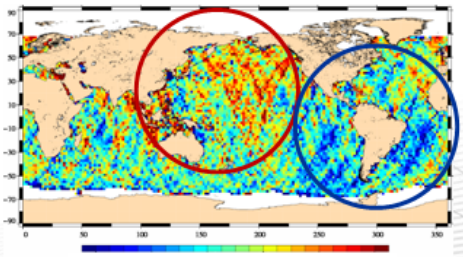

- Differences of averaged IGDR SLA averaged per boxe on the whole period show:
  - ➔ East/ West bias seen on J1/J2 and EN/J1 comparison is no more visible on EN/J2 comparison.

Differences at dual crossovers using MOE

- Averaged SSH crossover difference on the whole period show:
  - ➔ East/ West bias seen on J1/J2 and EN/J1 comparison is no more visible on EN/J2 comparison.
  - ➔ J2 is much closer to Envisat than J1
  - ➔ Balanced by the fact that the differences are small. Standard deviation at dual crossovers = 4.5 cm : enables a precise detection of potential anomalies

J1/EN using MOE

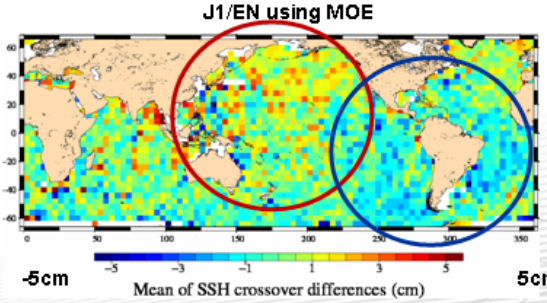

J2/EN using MOE

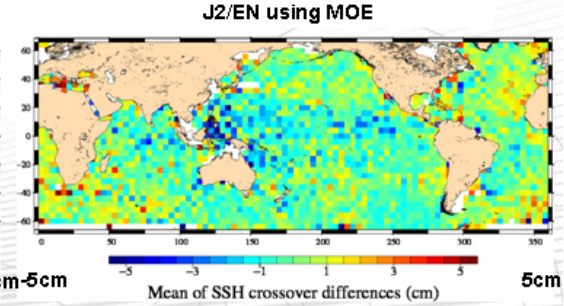

Monitoring of the standard deviation at crossovers

- Standard deviation of monomission SSH crossover difference cycle per cycle show:
  - ➔ slightly better performances for Jason-2 (4.4cm), Jason-1 (4.7cm) and Envisat (5cm).
  - ➔ Good consistency for the three missions

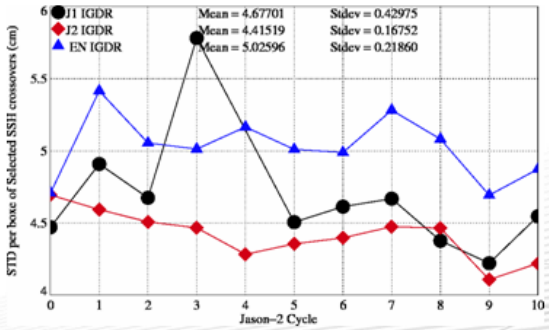

Envisat higher standard deviation is due to a different sampling (reference = J2 cycle → Envisat cycles are not complete).

An average per boxes is performed, prior to the statistics in order to allow us to have homogeneous sampling of the ocean for the 3 satellites.

Engaging preliminary results using POE

- Averaged SSH crossover difference on the whole period show:
  - ➔ No more East/ West bias seen on Jason-1 related comparison (see M. Ablain presentation)
  - ➔ Jason-2 and Jason-1 are very similar seen from Envisat
  - ➔ Standard deviation at dual crossovers = **3.4cm** (< 4.5 cm with MOE) : enables an even more precise detection of potential anomalies than in NRT (IGDR)
- Standard deviation of monomission SSH crossover difference cycle per cycle show for GDR (with POE):
  - ➔ As for NRT (IGDR): good consistency for the three missions

    slightly better performances for Jason- 1 and -2 (4.2cm) and Envisat (5cm). The best improvement between IGDR and GDR is noticed for J1.
  - ➔ Engaging results consistent and slighly better than NRT

3. Envisat / Jason-2 / Jason-1 comparison : *High frequency content*

High frequency content

- **Spectral analysis are performed (Mean spectrogram) on SSH along tracks with an ocean editing criteria**
  - On 10 days cut into 160 seconds samples for 1Hz data
  - On 1 day cut into 15 seconds samples for 20Hz data

➔ **1Hz data high frequency content show a complete agreement for the three missions, independently from the tracker used on Jason-2**

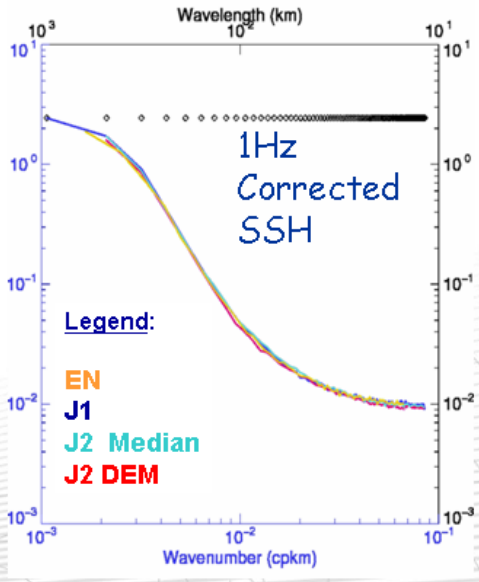

20Hz High frequency content

- Envisat and Jason-1 and -2 spectral content have a similar shape, with a first slope, a small bump around 20-70km and a noise plateau at :
  - 9.2cm white noise for Envisat
  - 7.9cm white noise for Jason-1 and Jason-2
- High frequency content for Jason-1 and Jason-2 are very consistent, exept that Jason-2 presents an unexplained coloration for frequencies above 3Hz.

➔ Slight coloration under investigations :
- Unchanged by selections on data (distance to coast, 20 valid data per second, selection on mispointing, waves or MQE criteria…)
- Present for any tracker (remains for the SGT mode, although it is the same as Jason-1)

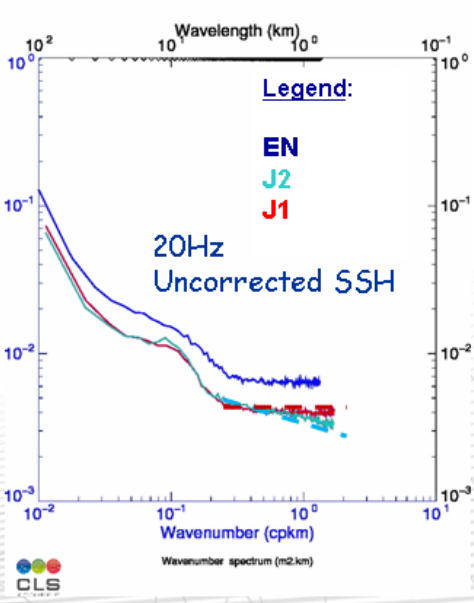

Conclusion

- **Envisat /Jason-2 are very consistent**
  - standard deviation of cross-over differences = 4,5 cm (IGDR) and 3.4 cm (GDR), which enables a precise cross calibration
- **Envisat is a useful third point of comparison between the Jason-1 and -2**
  - The geographically correlated biases between Envisat and Jason-2 are lower than with Jason-1.
  - High frequency content for Envisat Jason-1 and Jason-2 are very consistent at 1Hz and 20Hz, independently from the tracker used on Jason-2.
  - Concerning the 20Hz content, the comparison with other missions enables to notice a light coloration of the noise above 3Hz.
- **Jason-1 and -2 comparisons with Envisat GDR are very consistent**
  - This is encouraging for insuring a good continuity on the long term monitoring already initiated with Jason-1 since 2002.
- **This cross calibration shows that precise analysis can be performed even if the satellites are not on the same tracks**

Envisat / Jason-2 cross calibration

A. Ollivier, Y. Faugère - CLS
N. Picot - CNES, P. Féménias - ESA.

Introduction

Cross calibration of Jason-1/2 measurements with other flying precise altimetric missions is essential to assess data quality and performances. Cross calibration with Envisat is important for data quality assessment but also for allowing combination of altimeter datasets as required by applications and operational oceanography. This poster is complementary to the ***Envisat/Jason-1 Cross calibration*** poster where the whole set of Envisat and Jason-1 data are studied.

Cross calibration using Envisat

Years of experience enables to develop various methods to Cross calibrate the Jason's mission with Envisat. Concerning short time series, two methods are presented here:

-Differences of SLA averaged by boxes over the globe

-Differences at cross-overs with monitoring of the statistics and maps of averages over several cycles.

The second method (cross over analysis) enables to reduce the ocean variability effect seen on the unsmoothed SLA differences.

For a better consistency between missions, all SLA/SSH used for the study are computed with **ECMWF** tropospheric correction and the **GIM** Ionospheric correction, in order to be consistent with Envisat data for which the S-band is no longer available (since January 2008).

Envisat mission gives a 3rd point of comparison to explain discrepancies between Jason-1 and Jason-2's IGDR Geographically correlated biases.

Jason-1 – Envisat SLA using MOE: Est West bias

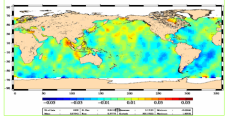

Jason-2 – Envisat SLA using MOE: Homogeneous map

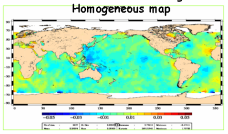

Jason-1 – Jason-2 SLA using MOE: East West bias

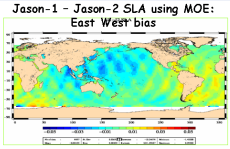

Both analyses show that Est-West Geographically correlated biases for the comparisons concerning J1/EN and J1/J2 are higher than for J2/EN. This enables to show that J2/EN are very consistent.

Mean cross-overs for IGDR products using MOE orbit :

-**Geographically correlated bias** are observed between the three missions. Like for SLA differences,

-East-West biases observed for the comparisons concerning J1/EN unlike for J2/EN.

Jason-1 /Envisat X_SSH using MOE: East West bias

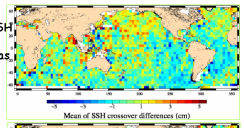

Jason-1 /Envisat X_SSH using POE

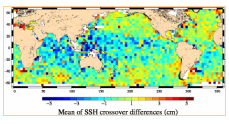

Mean of SSH crossover differences (cm)

Jason-2 /Envisat X_SSH using MOE : homogeneous data

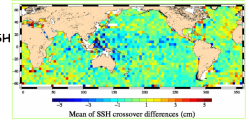

Jason-2/Envisat X_SSH using POE

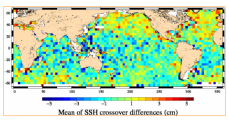

Mean of SSH crossover differences (cm)

GDR products using POE orbit :

- Higher noise due to a smaller time series but

-The biases repartition changes: J1/EN and J2/EN maps are now consistent.

This is in agreement with the improved quality of Jason-1 POE compared to its MOE (cf poster ***"Assessment of Jason-2 and Jason-1 orbit quality from SSH analysis"***)

Comparison between IGDR and GDR products show a good consistency of data. Performances using POE orbit are better as expected but the calval and cross calibration with IGDR data already show a good consistency between missions.

In terms of geographically correlated bias, using POE instead of MOE changes the patches repartition.

IGDR products using MOE orbit :

Monitoring of the standard deviation at cross overs is performed. An average per boxes is performed, prior to the statistics in order to allow us to have homogeneous sampling of the ocean for the 3 satellites. The statistics are very similar for the three missions, with slightly better performances for Jason-2 (smaller Standard deviation at cross overs (4.4cm), in front of Jason-1 (4.7cm) and Envisat (5cm).

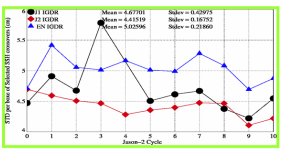

GDR products using POE orbit:

Monitoring of the standard deviation at cross overs is performed with the same average per boxe than for NRT study. The statistics are very similar for the three missions, around 4.2cm for the Jasons missions, that is to say, better than using NRT products and 5cm for Envisat.

On longer periods, such monitorings on independant missions enables to enlight/explain drifts, caused by processing/instrumental anomalies. This is largely developped in the poster ***Envisat/Jason-1 Cross calibration***.

Conclusion 1

Differences of SLA and standard deviation at Cross-over show that the three missions have **very good and very similar performances**. Geographically correlated biases are observed between the three missions, high-lighting a better consistency between Jason-2 and Envisat than between Jason-1 and the two other missions when using the MOE. On the other hand, biases concerning Jason-1 and 2 are very week concerning the POE Orbit. Although Envisat's sampling is different from the two Jasons, cross calibration with its data enables to provide a precise quality assessment of the Jasons's data, thanks to a set of several Cross calibration methods.

Spectral analysis of the HF content

The following study is based on user products and aims at analysing the high frequency (HF) part of the Sea Surface Height (SSH) signal of Jason-1, Jason-2 and Envisat. This signal includes instrumental noise, processing noise, correction noise, residual geophysical signals... Comparing the HF content of several missions enables to compare the performances but also to better understand the physical content of each signal. The spectral analysis allows us to quantify accurately the global SSH HF for 1Hz and 20Hz data. Comparison are performed for Envisat and Jason-1 **GDR** data and Jason-2 **IGDR** data.

Method

A plateau on a power spectrum can be the signature of a white noise. The standard deviation of its distribution can be obtained by :

$$\sigma = \sqrt{\frac{\alpha}{2.\Delta t}}$$

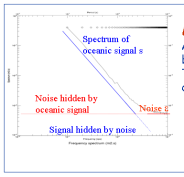

1Hz spectra

• 1Hz spectra are computed from 10 days of data

•High frequency content is compared for Jason-1, Envisat, and concerning Jason-2 using its two tracker modes: Median and DEM (Digital Elevation Model). The shape of the high frequency content is, as expected very similar for the three missions. When using uncorrected SSH, Envisat SSH is slightly above the others in terms of noise. This effect is cancelled when the SSH is corrected from instrumental and geophysical corrections.

20Hz spectra

•20Hz spectra are computed from 2 days of data

•On 20Hz data, at frequencies higher than 3Hz, the Envisat signal is hidden by a plateau at $10^{-3}m^2s$. This plateau is the signature of a **9.2 cm white noise**. Assuming uncorrelated 20 Hz noise, it is equivalent to 2.1 cm for the 1 Hz averages. The Jason-1 spectra has a similar shape as Envisat but with a lower plateau (**7.9cm**). Unlikely, on Jason-2, the spectrum does not behave as a white noise. A weak slope is noticed for the frequencies higher than 3Hz, showing a coloration on the noise at these frequencies. This effect is seen for all the tracker modes including SGT one (chosen for Jason-2's Cycle 1) which is identical to the one used on Jason-1. This different behavior is currently under investigations. By now, it was seen to be unchanged by selections on data (distance to coast, 20 valid data per second, selection on mispointing, waves or MQE criteria...) Elsewhere, the spectrum is similar to the other missions. Note that a higher energy in the 0.1-0.4 Hz (20-50km) bandwidth is noticed for the three missions.

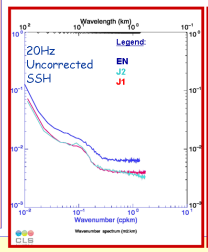

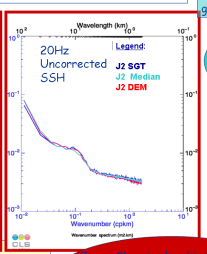

1Hz data high frequency content show a complete agreement for the three missions, undependently from the tracker used on Jason-2

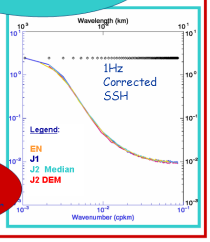

Conclusion 2

The high frequency content of the mission is another way of quantifying the data quality.

At 1Hz, the three missions compared have a complete agreement. On the other hand, an unexplained coloration of the noise above 3Hz is noticed for Jason-2. This coloration is particularly evidenced when the spectrum is compared to other missions 's spectra (here Jason-1 and Envisat) who present a white noise at these frequency, consistently to the theory.

Jason-2's noise level is the same as Jason-1's. However, high frequency content of Jason-2 presents an unexplained coloration for frequencies above 3Hz

Collecte Localisation Satellites
8-10 rue Hermes
31526 Ramonville Saint Agne - France

OSTST meeting Nice, November 2008

8. Conclusion

A statistical evaluation of Envisat altimetric measurements over ocean has been presented in this report. With more than six years of data now available in Geophysical Data Record (GDR) products, Envisat altimetric measurements show good general results:

- A very good **availability** of Envisat data on the last 6 months was noticed thanks to an improvement of the data dissemination since May 2008.

- The **S-Band loss** is considered to be permanent and all the S-band parameters MUST NOT be used anymore. The dual ionospheric correction could efficiently be replaced by the JPL GIM Ionospheric correction with no visible impact on the data quality, presumably thanks to the low solar activity period when it occured. However, this could be problematic for MSL studies regarding the instabilities noticed on the GIM correction.

- Before the S-Band power drop, the **S-Band anomaly** had been solved. This should allow reprocessed data free from that anomaly.

- The **USO anomaly** is not affecting Ra-2 data anymore since January the 23th 2008. Auxiliary files correction allows Envisat Ra-2 data to recover their nominal quality during anomaly period. They are also recommended to be used in non anomaly periods as well in order to take into account the long term aging drift.

- The **SLA performance** is very good, at the same level as Jason-1 with geographical differences between Envisat and Jason-1 reaching the cm level using recent (September 2005's IPF/CMA update) orbit and geophysical correction. The current standards (orbit configuration, instrumental and geophysical correction) used since September 2005 in the IPF/CMA, allow Envisat products to have a high geophysical quality.

- The ocean-1 **altimeter and radiometer parameters** are consistent with expected values. However, differences between MWR and ECMWF wet troposphere correction were noticed this year due to version changes of the ECMWF Model and having strong impact on the MSL trend. Homogeneous model time series would be very useful.

- Very good consistency was found between Envisat and new available **Jason-2** data which is encouraging for insuring a good continuity on the long term monitoring already initiated with Jason-1 since 2002.

- The Envisat **Mean Sea Level trend** is still an issue because it is unusable at the beginning of the mission (until cycle 22), and shows some unexplained ascending/descending inconsistencies on the SSH. This year, extensives studies were perfomed to better understand the MSL behaviors and discrepencies with Jason-1. Though on the last two years, Envisat and Jason-1 have the same MSL trend, which is encouraging.

- A **reprocessing** of the whole Envisat altimetric mission is expected in 2009. The major evolutions will be a new precise orbit based on recent Grace data and new ITRF model, better ECMWF meteo fields, new geophysical and instrumental (USO) corrections, new SSB correction, updated wet tropospheric correction. Besides it is planned to re-process ERS-2 data with similar

algorithms. Then, performances and comparisons will be carried out again using these new data in order to assess the consistency between Envisat and ERS-2 parameters.
These new products will further improve the high quality level of the Envisat altimetric mission and will make easier the data merging for multi-mission altimetry, as it is essential for oceanography and applications.

9. Bibliography

References

[1] Abdalla, S., "A wind retrieval algorithm for satellite radar altimeters", ECMWF Technical Memorandum, in preparation, 2006.

[2] Ablain, M., G. Pontonnier, B. Soussi, P. Thibaut, M.H. de Launay, J. Dorandeu, and P. Vincent. 2004. Jason-1 GDR Quality Assessment Report. Cycle 079. SALP-RP-P2-EX-21072-CLS079, May.

[3] M. Ablain., S. Philipps, Dorandeu J., 2006: Jason-1 validation and cross calibration activities. Yearly report. Technical Note CLS.DOS/NT/06-302, Contract N° 03/CNES/1340/00-DSO310 - lot2.C http://www.jason.oceanobs.com/documents/calval/validation_report/annual_report_j1_2006.pdf

[4] M. Ablain., S. Philipps, 2007: Jason-1 validation and cross calibration activities. Yearly report. Technical Note CLS.DOS/NT/06-302, Contract N° 03/CNES/1340/00-DSO310 - lot2.C http://www.jason.oceanobs.com/documents/calval/validation_report/annual_report_j1_2007.pdf

[5] Ablain M., Cazenave A., Guinehut S., Valladeau G., (submitted for publication), A new assessment of global mean sea level from altimeters highlights a reduction of global slope from 2005 to 2008 in agreement with in-situ measurements, submitted to Ocean Sciences.

[6] Faugere Y., Granier N., Ollivier A., 2007: Envisat RA-2/MWR ocean data validation and cross-calibration activities. Yearly report. Technical Note CLS.DOS/NT/08.006, Contract N° SALP-RP-MA-EA-21516-CLS http://www.aviso.oceanobs.com/fileadmin/documents/calval/validation_report/EN/annual_report_en_2007.pdf

[7] Commien L., S. Philipps, M. Ablain., 2008: Jason-1 validation and cross calibration activities. Yearly report. Technical Note CLS.DOS/NT/09-006, Contract N° 60453 - lot2.C http://www.jason.oceanobs.com/documents/calval/validation_report/annual_report_j1_2008.pdf

[8] Beckley, B. D., F. G. Lemoine, S. B. Luthcke, R. D. Ray, and N. P. Zelensky A reassessment of global and regional mean sea level trends from TOPEX and Jason-1 altimetry based on revised reference frame and orbits, Geophys. Res. Lett., 34, L14608, 2007, doi:10.1029/2007GL030002.

[9] Carrère, L., and F. Lyard, Modeling the barotropic response of the global ocean to atmospheric wind and pressure forcing - comparisons with observations. 2003. Geophys. Res. Lett., 30(6), 1275, doi:10.1029/2002GL016473.

[10] Commien, L., 2009. Différences entre l'orbite des GDR-C et GDR-B Jason-1, NT08.338

[11] Commien, L., S. Philipps, M. Ablain, and N. Picot, 2008. SSALTO CALVAL Performance assessment Jason-1 GDR "C" / GDR "B". Poster presented at OSTST meeting, Nice, France, 09-12 November 2008. Available at: http://www.aviso.oceanobs.com/fileadmin/documents/OSTST/2008/commien.pdf

[12] Legeais JF. and Carrere L, July 2008, Complement de validation de la DAC_HR par rapport à la DAC , en zone cotiere, Technical Note CLS.DOS/08.189.

[13] Cazenave, A., et al.,1999: Sea Level Change from Topex/Poseidon altimetry and tide gauges, and vertical crustal motions from DORIS, G. Res. Let., 26, 2077-2080.

[14] Celani C., B. Greco, A. Martini, M. Roca, 2002: Instruments corrections applied on RA-2 Level-1B Product. 2002: Proceeding of the Envisat Calibration Workshop.

[15] Chambers, D., P., J. Ries, T. Urban, and S. Hayes. 2002. Results of global intercomparison between TOPEX and Jason measurements and models. Paper presented at the Jason-1 and TOPEX/Poseidon Science Working Team Meeting, Biarritz (France), 10-12 June.

[16] Dedieu M., L. Eymard, E. Obligis, N. Tran, F. Ferreira, 2005: ENVISAT Microwave Radiometer Assessment Report Cycle 039, Technical Note CLS.DOS/NT/05.147 Available at http://earth.esa.int/pcs/envisat/mwr/reports/

[17] Dorandeu, J. and P.Y. Le Traon, 1999: Effects of Global Atmospheric Pressure Variations on Mean Sea Level Changes from TOPEX/Poseidon. J. Atmos. Technol., 16, 1279-1283.

[18] Dorandeu J., Y. Faugere, F. Mertz, F. Mercier, N. Tran, 2004a: Calibration / Validation Of Envisat GDRs Cross-calibration / ERS-2, Jason-1 Envisat and ERS Symposium, Salzburg, Austria.

[19] Dorandeu, J., M. Ablain, Y. faugere, F. Mertz, B. Soussi, 2004b, Jason-1 global statistical evaluation and performance assessment. Calibration and cross-calibration results Mar. Geod. 27(3-4): 345-372.

[20] Doornbos E., Scharroo R., 2005: Improved ERS and Envisat precise orbit determination, Proc. of the 2004 Envisat and ERS Symposium, Salzburg, Austria.

[21] ECMWF, The evolution of the ECMWF analysis and forecasting system Available at: http://www.ecmwf.int/products/data/operational_system/evolution/

[22] EOO/EOX, October 2005, Information to the Users regarding the Envisat RA2/MWR IPF version 5.02 and CMA 7.1 Available at http://earth.esa.int/pcs/envisat/ra2/articles/

[23] EOP-GOQ and PCF team, 2005: Envisat Cyclic Altimetric Report, Technical Note ENVI-GSOP-EOPG-03-0011 Available at: http://earth.esa.int/pcs/envisat/ra2/reports/pcs_cyclic/

[24] Eymard L., E. Obligis, N. Tran, February 2003, ERS2/MWR drift evaluation and correction, CLS.DOS/NT/03.688

[25] http://earth.esa.int/brat/html/alti/dataflow/processing/pod/orbit_choice_en.html

[26] Envisat RA-2 Range Instrumental correction: USO clock period variations and associated auxiliary file, ENVI-GSEG-EOPG-TN-03-0009

[27] Faugere Y., Mertz F., Dorandeu J., 2003: Envisat GDR quality assessement report (cyclic), Cycle 015. SALP-RP-P2-EX-21072-CLS015, May. Available at http://www.aviso.oceanobs.com/html/donnees/calval/validation_report/en/welcome_uk.html

[28] Faugere Y., Mertz F., Dorandeu J., 2003: Envisat validation and cross calibration activities during the verification phase. Synthesis report. Technical Note CLS.DOS/NT/03.733, ESTEC contract N°16243/02/NL/FF WP6, May 16 2003 Available at http://earth.esa.int/pcs/envisat/ra2/articles/Envisat_Verif_Phase_CLS.pdf

[29] Faugere Y., Mertz F., Dorandeu J., 2004: Envisat RA-2/MWR ocean data validation and cross-calibration activities. Yearly report. Technical Note CLS.DOS/NT/04.289, Contract N° 03/CNES/1340/00-DSO310 Available at http://earth.esa.int/pcs/envisat/ra2/articles/Envisat_Yearly_Report_2004.pdf

[30] Faugere Y., Estimation du bruit de mesure sur jason-1, December 2002, CLS.ED/NT.

[31] Y.Faugere, J.Dorandeu, F.Lefevre, N.Picot and P.Femenias, 2005: Envisat ocean altimetry performance assessment and cross-calibration. Submitted in the special issue of SENSOR 'Satellite Altimetry: New Sensors and New Applications'

[32] Faugere Y., Mertz F., Dorandeu J., 2005: Envisat RA-2/MWR ocean data validation and cross-calibration activities. Yearly report. Technical Note CLS.DOS/NT/04.289, Contract N° 03/CNES/1340/00-DSO310 http://www.jason.oceanobs.com/documents/calval/validation_report/en/annual_report_en_2005.pdf

[33] Faugere, Y., J. Dorandeu, N. Picot, P. Femenias. 2007. Jason-1 / Envisat Cross-calibration, presentation at the Hobart OSTST meeting

[34] Faugere, Y., Ollivier, A., 2007, Investigation on the differences between CLS and Altimetrics Envisat MSL trend, CLS.DOS/NT07-261

[35] Faugere, Y., Ollivier, A., 2008, Investigation on the High frequency content of Jason and Envisat, CLS.DOS/NT08-119

[36] Dibarbour, G., Bruit Jason et Analyse spectrale, March 2001, CLS.ED/NT

[37] Imel, D., Evaluation of the TOPEX/POSEIDON dual-frequency ionosphere correction, J. Geophys. Res., 99, 24,895-24,906, 1994

[38] Labroue, S. and P. Gaspar, 2002: Comparison of non parametric estimates of the TOPEX A, TOPEX B and JASON 1 sea state bias. Paper presented at the Jason 1 and TOPEX/Poseidon SWT meeting, New-Orleans, 21-12 October.

[39] Labroue S. and E. Obligis, January 2003, Neural network retrieval algorithms for the ENVISAT/MWR, Technical note CLS.DOS/NT/03.848

[40] Labroue S., 2003: Non parametric estimation of ENVISAT sea state bias, Technical note CLS.DOS/NT/03.741, ESTEC Contract n°16243/02/NL/FF - WP3 Task 2

[41] Labroue S., 2004: RA-2 ocean and MWR measurement long term monitoring, Final report for WP3, Task 2, SSB estimation for RA-2 altimeter, Technical Note CLS-DOS-NT-04-284

[42] Labroue S., 2005: RA2 ocean and MWR measurement long term monitoring 2005 report for WP3, Task 2 SSB estimation for RA2 altimeter, Technical Note CLS-DOS-NT-05-200

[43] Labroue S., 2006: Estimation du Biais d'Etat de Mer pour la mission Jason-1, Technical note CLS-DOS-NT-06-244

[44] Laxon and M. Roca, 2002: ENVISAT RA-2: S-BAND PERFORMANCE, S., Proceedings of the ENVISAT Calibration Workshop, Noordwijk

[45] Le Traon, P.-Y., J. Stum, J. Dorandeu, P. Gaspar, and P. Vincent, 1994: Global statistical analysis of TOPEX and POSEIDON data. J. Geophys. Res., 99, 24619-24631.

[46] Le Traon, P.-Y., , F. Ogor, 1998: ERS-1/2 orbit improvement using TOPEX/POSEIDON: the 2 cm challenge. J. G. Res., VOL 103, p 8045-8057, April 15, 1998.

[47] Lefèvre, F., and E. Sénant, 2005: ENVISAT relative calibration, Technical Note CLS-DOS-NT-05.074.

[48] Lillibridge J, R. Scharroo and G. Quartly, 2005: rain and ice flagging of Envisat altimeter and MWR data, Proc. of the 2004 Envisat and ERS Symposium, Salzburg, Austria

[49] Luthcke. S. B., N. P. Zelinsky, D. D. Rowlands, F. G. Lemoine, and T. A. Williams. 2003. The 1-Centimeter Orbit: jason-1 Precision Orbit Determination Using GPS, SLR, DORIS, and Altimeter Data. Mar. Geod. 26(3-4): 399-421.

[50] Martini A. and P. Féménias, 2000: The ERS SPTR2000 Altimetric Range Correction: Results and Validation. ERE-TN-ADQ-GSO-6001. 23 November 2000.

[51] Martini A., 2003: Envisat RA-2 Range instrumental correction : USO clock period variation and associated auxiliary file, Technical Note ENVI-GSEG-EOPG-TN-03-0009 Available at http://earth.esa.int/pcs/envisat/ra2/articles/USO_clock_corr_aux_file.pdf http://earth.esa.int/pcs/envisat/ra2/auxdata/

[52] A. Martini, P. Feminias, G. Alberti, M.P.Milagro-Perez, 2005: RA-2 S-Band Anomaly: Detection and waveform recontruction. Proc. of 2004 Envisat & ERS Symposium, Salzburg, Austria. 6-10 September 2004 (ESA SP-572, April 2005).

[53] Mertz, F., Y. Faugere and J. Dorandeu, 2003: Validation of ERS-2 OPR cycle 083-086. CLS.OC.NT/03.702 issue 083-086.

[54] Mercier, F., L.Cerri, S. Houry, A. Guitart, P. Broca, C. Ferrier, J-P. Berthias, 2006: DORIS 1b Product evolution, Symposium 15 Years of progress in radar altimetry, Venice.

[55] Mertz F., J. Dorandeu, N. Tran, S. Labroue, 2004, ERS-2 OPR data quality assessment. Long-term monitoring - particular investigations, Report of task 2 of IFREMER Contract n° 04/2.210.714. CLS.DOS/NT/04.277.

[56] Mitchum, G., 1994: Comparison of TOPEX sea surface heights and tide gauge sea levels, J. Geophys. Res., 99, 24541-24554.

[57] Mitchum, G., 1998: Monitoring the stability of satellite altimeters with tide gauges, J. Atm. Oceano. Tech., 15, 721-730.

[58] Obligis E., L. Eymard, N. Tran, S. Labroue, 2005: Three years of Microwave Radiometer aboard Envisat: In-flight Calibration, Processing and validation of the geophysical products, submitted

[59] Ollivier A.,Y. Faugere, P. Thibaut, G. Dibarboure, J. Poisson, 2008: Investigation on the high frequency content of Jason-1 and Jason-2, Technical note CLS-DOS-NT-09-027

[60] Ollivier, A., Y. Faugere and N. Picot, P. Femenias 2008. ENVISAT Jason-2 Cross calibration. Poster presented at OSTST meeting, Nice, France, 09-12 November 2008. Available at: http://www.aviso.oceanobs.com/fileadmin/documents/OSTST/2008/ollivier.pdf

[61] Product disclaimer available on http://earth.esa.int/dataproducts/availability/

[62] R D Ray and R M Ponte, 2003: Barometric tides from ECMWF operational analyses, Annales Geophysicae, 21: 1897-1910.

[63] Roca M., A. Martini, 2003: Level 1b Verification updates, Ra2/MWR CCVT meeting, 25-26 March 2003, ESRIN, Rome

[64] Roca M., A. Martini, PTR Study, QWG meeting, November 2008, ESRIN, Rome

[65] Rudolph A., D.Kuijper, L.Ventimiglia, M.A. Garcia Matatoros, P.Bargellini, 2005: Envisat orbit control - philosophy experience and challenge, Proc. of the 2004 Envisat and ERS Symposium, Salzburg, Austria

[66] R. Scharroo and P. N. A. M. Visser, 1998: Precise orbit determination and gravity field improvement for the ERS satellites, J. Geophys. Res., 103, C4, 8113-8127

[67] Scharroo R., A decade of ERS Satellite Orbits and Altimetry, 2002: Phd Thesis, Delft University Press science

[68] Scharroo R., December 12, 2002, Routines for iono corrections, internet communication to the CCVT community

[69] Scharroo R., J. L. Lillibridge, and W. H. F. Smith, Cross-Calibration and Long-term Monitoring of the Microwave Radiometers of ERS, TOPEX, GFO, Jason-1, and Envisat, **Marine Geodesy, 27:279-297**, 2004.

[70] Scharroo, R., RA-2 USO Anomaly: predictive correction model, Tech. Rep. N1-06-002, Altimetrics LLC, Cornish, New Hampshire, May 2006.

[71] Stum J., F. Ogor, P.Y. Le Traon, J. Dorandeu, P. Gaspar and J.P. Dumont, 1998: "An intercalibration study of TOPEX/POSEIDON, ERS-1 and ERS-2 altimetric missions", Final report of IFREMER contract N_97/2 426 086/C CLS.DOS/NT/98.070.

[72] Tran, N., D. W. Hancock III, G.S. Hayne. 2002: "Assessment of the cycle-per-cycle noise level of the GEOSAT Follow-On, TOPEX and POSEIDON." J. of Atmos. and Oceanic Technol. 19(12): 2095-2117.

[73] Tran N. and E. Obligis, December 2003, Validation of the use of ENVISAT neural algorithm on ERS-2. CLS-DOS-NT-03.901.

[74] Tran N., E. Obligis and L. Eymard, 2006, Envisat MWR 36.5 GHz drift evaluation and correction. CLS-DOS-NT-05.218.

[75] Valladeau G., Ablain M., Validation of altimetric data by means of tide gauge measurements for TOPEX/Poseidon, Jason-1 and Envisat, Reference : CLS.DOS/NT/08-256, Nomenclature : SALP-NT-MA-EA-21589-CLS

[76] Vincent, P., S. D. Desai, J. Dorandeu, M. Ablain, B. Soussi, P. S. Callahan, and B. J. Haines 2003. Jason-1 Geophysical Performance Evaluation. Mar. Geod. 26(3-4): 167-186.

[77] Witter, D. L., D. B. Chelton, 1991: "A Geosat altimeter wind speed algorithm development", J. of. Geophys. Res. (oceans), 96, 8853-8860, 1991.

[78] Zanife, O. Z., P. Vincent, L. Amarouche, J. P. Dumont, P. Thibaut, and S. Labroue, 2003. Comparison of the Ku-band range noise level and the relative sea-state bias of the Jason-1, TOPEX and Poseidon-1 radar altimeters. Mar. Geod. 26(3-4): 201-238.

10. Appendix 1: Instrument and plateform status

10.1. ACRONYMS

The main acronyms used to described the events are explained below.
CMA: Centre Multimission Altimetrique
CTI tables: Configuration Table Interface. They Contain the setting of the instruments and are uploaded on board after a switch off, a reset
HTR Refuse: Heater Refuse
ICU: Instrument Control Unit, a part of the distributed command and control function implemented on ESA spacecraft. The unit receives, decodes and executes high-level commands for its instrument, and autonomously performs health-checking and parameter monitoring. In the event of anomalies it takes autonomous recovery actions.
IPF: Instrument Processing Facilities
MCMD: Macrocommand
OBDH: On Board Data Handling
OCM: Orbit Controle Mode/maneuvre
P/L SOL: Payload Switch Off Line
SEU: Single Event Upset
SM-SOL by PMC: SM Switch Off Line by Payload Main Computer
SW: Software
TM: Telemetry
USO: Ultra Stable Oscillator

10.2. Cycle 010

- RA-2 went to STBY/Refuse (2002/10/09 09 13:34:22 to 2002/10/10 08:56:53)

10.3. Cycle 011

- Ra2 switch-down - Planned SM-SOL by PMC1 (2002/11/18 04:38:00 to 2002/11/19 19:19:21,Pass 382-429)
- DORIS Navigator switch-down - Planned SM-SOL by PMC1 (2002/11/18 04:38:02 to 2002/11/22 12:40:00, Pass 382-505)
- MWR switch-down - Planned SM-SOL by PMC1 (2002/11/18 04:37:59 to 2002/11/20 12:20:06, Pass 382-448)
- Orbit Maintenance Maneuver (2002/11/07 18:15:51 to 2002/11/07 21:06:17,Pass 83-85)
- Orbit Maintenance Maneuver (2002/11/29 03:35:30 to 2002/11/29 06:25:57,Pass 696-698)

10.4. Cycle 012

- RA-2 went to HTR-0 Refuse (2002/12/21 04:31:26 to 2002/12/21 12:52:00, Pass 325-333)
- Orbit Inclination Maneuver (2002/12/18 04:28:18 to 2002/12/18 06:36:46, Pass 238-240)

- Orbit Maintenance Maneuver (2002/12/18 22:17:22 to 2002/12/19 00:17:34, Pass 259-261)

10.5. Cycle 013

- RA-2 went to HTR-0 Refuse (2003-01-16 01:52:36 to 2003-01-17 17:00:35)
- RA-2 went to suspend mode (2003-01-25 23:56:36 to 2003-01-27 19:54:02)
- Orbit Maintenance Maneuver (2003/01/14 00:55:17 to 2003/01/14 03:45:42 TAI)
- Orbit Maintenance Maneuver (2003/02/11 23:04:49 to 2003/02/12 01:04:57 TAI)

10.6. Cycle 014

- SEU's caused a Software Anomaly (2003/03/02 02:46:44 to 2003/03/03 16:46:35).
- Subsystems unavailable - Autonmous P/L switch-off (2003/03/15 04:21:08 to 2003/03/17 19:00:13)
- RA2 in HTR0/Refuse due to HPA primery bus undercurrent (2003/03/17 21:09:32 to 2003/03/18 18:50:40)
- Orbit Maintenance Maneuver (2003/02/21 03:42:57 to 2003/02/21 05:53:24)
- Orbit Maintenance Maneuver (2003/03/03 23:51:14 to 2003/03/04 01:51:22)

10.7. Cycle 015

- Wrong setting of Ra2 parameters (no CTI tables have been up-loaded on-board) from 18 Mar 2003 18:50:40 to 9 Apr 2003 17:12:24, Pass 1 to 452
- RA-2 unavailability (Format Header Error forcing ICU to RS/WT/INI) from 8 Apr 2003 15:08:57.000 to 9 Apr 2003 17:12:24.000, Pass 437 to 452
- RA-2 unavailability (Format Header Error forcing ICU to RS/WT/INI) from 8 Apr 2003 15:08:57.000 to 9 Apr 2003 17:12:24.000, Pass 613 to 624
- RA-2 unavailability: Multiple SEU caused ICU switchdown (2003/04/24 13:20:09 to 2003/04/25 09:15:36,879 to 901)
- Orbit Maintenance Maneuver (2003/04/04 00:40:48 to 2003/04/04 02:40:56 TAI)

10.8. Cycle 016

- RA2 unavailability (known SEU failure) (from 5 May 2003 12:30:17.000 to 6 May 2003 10:01:10.000, Pass 191 to 215)
- RA-2 unavailability (ICU in SUSPEND due to TM FMT Error when a Reduced FMT was requested) (from 11 May 2003 11:06:33.000 to 12 May 2003 10:14:35.726, Pass 361 to 387)
- Orbit Maintenance Maneuver (from 2003/05/14 22:40:13 to 2003/05/15 00:40:19 TAI, Pass 460 to 462)

- RA-2 unavailability (Switch-down for PMC SW upgrade and OCM) from 18 May 2003 06:25:17.000 to 19 May 2003 15:59:28.000, Pass 548 to 602)
- MWR unavailability (Switch-down for PMC SW upgrade and OCM) from 18 May 2003 06:25:24.000 to 19 May 2003 14:45:40.000, Pass 548 to 602)
- DORIS unavailability (Switch-down for PMC SW upgrade and OCM) from 18 May 2003 06:25:25.000 to 19 May 2003 13:21:28.000, Pass 548 to 602)
- Orbit Inclination Maneuver (from 2003/05/20 04:11:53 to 2003/05/20 06:23:31 TAI, Pass 610 to 612)
- RA-2 unavailability (ICU went to RS/WT/INI) from 1 Jun 2003 14:36:40.000 to 2 Jun 2003 09:20:35.000, Pass967 to 987

10.9. Cycle 017

- Orbit Maintenance Maneuver (from 2003/06/07 01:08:16 to 2003/06/07 03:08:23 TAI, Pass 119 to 122)

10.10. Cycle 018

- Orbit Maintenance Maneuver (from 2003/07/11 0:58:45 to 2003/07/11 03:49:08 TAI, Pass 90 to 94)
- RA2 unavailability (RA-2 in STBY/REF due to MCMD timeout) (from 26 Jul 2003 15:28:11 to 26 Jul 2003 17:25:35, Pass 538)
- RA2 unavailability (RA-2 picked up Mission Planning schedule) (from 31 Jul 2003 16:11:02 to 31 Jul 2003 18:06:30, Pass 682)
- Orbit Maintenance Maneuver (from 2003/07/11 0:58:45 to 2003/07/11 03:49:08 TAI), Pass 91 to 94)

10.11. Cycle 019

- Orbit Maintenance Maneuver (from 2003/08/15 1:31:29 to 2003/08/15 03:31:35 TAI, Pass 91 to 93)
- RA-2 went to STBY/Refuse due to Individual Echoes MCMD Timeout (from 2003-08-15 16:40:21 to 2003-08-15 18:35:35, Pass 110)
- RA-2 went to STBY/Refuse due to Individual Echoes MCMD Timeout (from 2003-08-30 15:28:00 to 2003-08-30 20:47:35, Pass 538 to 543)
- PLSOL . Instrument Switch OFF/ON (from 2003-09-04 22:52:52 to 2003-09-06 16:41:09, Pass 689 to 738)

10.12. Cycle 020

- RA-2 in STANDBY / REFUSE MODE (from 2003-09-21 15:36:40 to 2003-09-21 17:33:30, Pass 166 to 167)

- RA-2 is in RS/WT/INT mode (from 2003-09-27 00:28:08 to 2003-09-27 12:52:00, Pass 320 to 333)
- Wrong setting of Ra2 parameters (no CTI tables have been up-loaded on-board) (from 2003-09-27 12:52:00 to 2003-09-30 12:45:00, Pass 334 to 407)
- Orbit Maintenance Maneuver (2003/09/30 00:40:53 to 2003/09/30 02:41:00 TAI, Pass 405 to 407)

10.13. Cycle 021

- Orbit Inclination Maneuver (2003/10/28 04:56:18 to 2003/10/28 07:09:44 TAI, Pass 210 to 212)
- RA-2 is in RS/WT/INT mode. 29 Oct 2003 06 :47 :04 to 29 Oct 2003 12 :58 :35, Pass 242 to 247)
- Orbit Maintenance Maneuver (2003/10/31 01:13:10 to 2003/10/31 03:13:25 TAI, Pass 291 to 293)
- RA-2 is in RS/WT/INT mode. TM format header error (02 Nov 2003 15 :16 :56 to 03 Nov 2003 12 :08 :35, Pass 366 to 389)
- Orbit Maintenance Maneuver (2003/11/18 23:02:30 to 2003/11/19 01:52:55 TAI, Pass 833 to 835)

10.14. Cycle 022

- RA-2 is in RS/WT/INT mode (2003-11-26 13:31:20 to 2003-11-26 19:39:35, Pass 49 to 54)
- RA-2 PLSOL . Instrument Switch OFF/ON (2003-12-03 07:18:43 to 2003-12-05 16:35:05, Pass 241 to 308)
- MWR PLSOL . Instrument Switch OFF/ON (2003-12-03 07:18:43 to 2003-12-04 18:45:41)
- RA-2 is in RS/WT/INT mode. (2003-12-06 15:55:52 to 2003-12-10 19:16:36, Pass 338 to 455)
- Orbit Maintenance Maneuver (2003/12/15 21:02:28 to 2003/12/15 23:02:36, Pass 601 to 603)
- Orbit Maintenance Maneuver (2003/12/26 21:03:30 to 2003/12/26 23:03:34, Pass 916 to 918)

10.15. Cycle 023

- Orbit Maintenance Maneuver (2004/01/21 23:54:27 to 2004/01/22 01:54:37))
- Orbit Maintenance Maneuver (2004/01/26 22:26:07 to 2004/01/27 00:26:11))

10.16. Cycle 024

- Orbit Inclination Maneuver (2004/02/04 04:46:39 to 2004/02/04 06:58:05)

- Orbit Maintenance Maneuver (2004/02/05 11:17:21 to 2004/02/05 13:17:23)
- Orbit Maintenance Maneuver (2004/02/24 11:48:39 to 2004/02/24 13:48:45)

10.17. Cycle 025

- Orbit Maintenance Maneuver (2004/04/07 20:05:30 to 2004/04/07 22:05:34)

10.18. Cycle 026

- RA-2 in STANDBY/REF DUE TO MCMD H202 FAILURE (2004-22-04 15:15:36 2004-22-04 17:07:05)
- RA-2 Switch down to RESET/WAIT due to too many SEU's reported. (2004-05-10 02:06:31 2004-05-10 11:27:30)
- Orbit Inclination Maneuver (2004/04/14 04:43:02 2004/04/14 06:55:00)
- Orbit Maintenance Maneuver (2004/05/07 01:08:56 2004/05/07 03:09:04)

10.19. Cycle 027

- RA2 went to suspend owing to repeated type 10 entries in report format (2004/05/31 02:45:27 to 2004/05/31 12:01:50)
- No DORIS data from 2004/06/06 13:00:00 to 2004/06/14 14:52:00. Following an onboard incident, Doris instrument has been switched to the redundant chain. Doris data are unavailable from June, 6th to June, 14th. To allow GDR production, POE with laser only data have been produced during this period.
- RA2 in SUSPEND Mode (2004/06/21 14:47:51 to 2004/06/21 19:24:30, Pass 995 to 999)

10.20. Cycle 028

- RA2 in ICU rs/wt/ini (2004/07/18 13:47:03 to 2004/07/18 19:59:00, Pass 765 to 771)
- Orbit Maintenance Maneuver (2004/06/30 08:08:29 to 2004/06/30 10:08:35, Pass 242 to 244)

10.21. Cycle 029

- RA2 in ICU RS/WT/INI. (SDU problem in RAM) (2004/08/10 15:00:39 to 2004/08/11 10:59:30, Pass 423 to 445)
- Orbit Maintenance Maneuver (2004/08/17 02:04:20 to 2004/08/17 04:04:26 , Pass 607 to 609)

10.22. Cycle 030

- RA2 in ICU RS/WT/INI. (SDU problem in RAM) (2004/09/26 13:39:50 to 2004/09/27 16:23:30, Pass 765-795)

- Abnormal behaviour of the RA-2 sensor (2004/09/27 16:23:30 to 2004-09-29 10:21:07, Pass 796-846)
- Collision avoidance Maneuver (2004/09/01 22:52:27 to 2004/09/02 00:52:37, Pass 60-62)
- Collision avoidance Maneuver (2004/09/02 23:44:27 to 2004/09/03 01:44:37, Pass 89-91)
- Orbit Inclination Maneuver (2004/09/21 04:14:37 to 2004/09/21 06:29:19, Pass 610-612)
- Orbit Maintenance Maneuver (2004/09/24 03:53:38 to 2004/09/24 05:53:46, Pass 695-697)

10.23. Cycle 031

- Collision avoidance Maneuver (2004/10/22 03:20:22 to 2004/10/22 07:00:41, Pass 495-498)
- High solar activity (Pass 974-1002)

10.24. Cycle 032

- RA2 in RS/WT/INI. 2004/11/23 13:25:58 to 2004/11/24 14:10:10, Pass 421-449
- RA2 Format header error. 2004/12/01 10:22:30 to 2004/12/01 15:34:29, Pass 647-651
- Orbit Maintenance Maneuver (2004/11/12 01:07:57 to 2004/11/12 03:08:06,Pass 91-93)

10.25. Cycle 033

- RA-2 went to RS/WT/INI due RBI (2004/12/27 02:49:10 to 2004/12/27 13:49:30, 380 to 391)
- Orbit Maintenance Maneuver (2004/12/17 01:03:48 to 2004/12/17 03:03:52, 91 to 93)
- Orbit Maintenance Maneuver (2005/01/05 23:10:28 ro 2005/01/06 01:10:36, 661 to 663)
- Orbit Inclination Maneuver (2005/01/07 04:25:17 to 2005/01/07 06:38:53, 696 to 698)

10.26. Cycle 034

- RA-2 went to RS/WT/INI Mode (2005/01/26 15:50:30 to 2005/01/26 21:07:30, 252 to 257)
- Orbit Maintenance Maneuver (2005/02/18 01:23:24 to 2005/02/18 03:23:28, 893 to 894)

10.27. Cycle 035

- RA-2 went to RS/WT/INI Mode (2005/03/18 04:35:34 to 2005/03/18 12:58:00, 697 to 705)
- Orbit Maintenance Maneuver (2005/03/17 04:51:26 to 2005/03/17 07:06:31, 668 to 669)

10.28. Cycle 036

- RA-2 went to RS/WT/INI mode (2005/04/18 05:01:10 to 2005/04/18 13:22:32, 583 to 591)

- RA-2 went to RS/WT/INI mode (2005/04/18 37:58:10 to 2005/04/24 11:42:30, 742 to 761)

10.29. Cycle 037

- RA-2 went to ICU in RS/WT/INI (RBI ERR 71) (2005/05/14 23:56:37 to 2005/05/15 10:53:45, 348 to 359)
- RA-2 went to ICU in RS/WT/INI (2005/05/21 00:10:45 to 2005/05/21 10:55:35, 520 to 531)

10.30. Cycle 038

- RA-2 went to ICU in RS/WT/INI (2005/07/04 04:41:10 to 2005/07/04 11:19:39, 783 t0 789)

10.31. Cycle 039

- RA-2 went to ICU in RS/WT/INI (2005/07/16 13:32:21 to 2005/07/16 19:58:52,135 to 141)
- RA-2 went to ICU in RS/WT/INI (2005/07/17 14:43:49 to 2005/07/17 19:20:30,165 to 169)
- RA-2 went to ICU in RS/WT/INI (2005/07/29 00:41:41 to 2005/07/29 09:58:30,492 to 501)
- Orbit Maintenance Maneuver (2005/08/09 22:45:44 to 2005/08/10 00:45:50 TAI)

10.32. Cycle 040

- RA-2 went to ICU in RS/WT/INI (2005/08/16 16:41:57 to 2005/08/16 20:22:30,24 to 27)
- RA-2 went to ICU in RS/WT/INI (2005/08/30 16:01:25 to 2005/08/30 19:43:00,424 to 427)
- RA-2 went to ICU in RS/WT/INI (2005/09/12 15:53:09 to 2005/09/12 19:47:00,796 to 799)
- Orbit Maintenance Maneuver (2005/09/07 05:19:53 to 2005/09/07 07:36:31 TAI)

10.33. Cycle 041

- RA-2 went to ICU in RS/WT/INI (2005/09/20 12:19:17 to 2005/09/20 18:56:00,19 to 25)
- RA-2 went in RS/WT/INI (2005/10/04 12:47:33 to 2005/10/04 16:35:30,420 to 423)
- Orbit Maintenance Maneuver (2005/10/06 02:19:10 to 2005/10/06 02:19:14 TAI)

10.34. Cycle 042

From this cycle onward, the Orbit Maintenance Maneuvers (having no impact on data) are not listed anymore.

- RA-2 went in RS/WT/INI following Uncontrolled S/W Action (2005/10/28 05:34:13 to 2005/10/28 10:39:00,97 to 101)

10.35. Cycle 043

RA-2 went in RS/WT/INI following Uncontrolled S/W Action (2006/01/02 12:56:35 2006/01/02 18:09:30,993 to 997)

10.36. Cycle 044

- RA-2 went in RS/WT/INI following Multiple SEU Anomaly (ref AR-614) (2006/01/12 14:20:35 to 2006/01/12 19:12:30,279 to 283)
- RA-2 went in RS/WT/INI(2006/01/30 02:07:15 to 2006/01/30 11:29:00,780 to 789)
- RA-2 went in RS/WT/INI following Uncontrolled S/W Action (2006/02/01 05:17:56 to 2006/02/01 12:04:30,841 to 847)
- RA-2 went in RS/WT/INI following Uncontrolled S/W Action (2006/02/01 16:30:28 to 2006/02/01 18:36:30,854 to 855)
- Orbit Inclination Maneuver (2006/01/10 05:54:24 to 2006/01/10 06:11:24)

10.37. Cycle 045

- RA-2 went in RA2 back to operations following TM format anomaly (2006/03/13 09:36:51 to 2006/03/13 17:40:00,989 to 997))

10.38. Cycle 046

- RA-2 switch to STBY and back to measurement to get useful telemetry related to USO (2006/03/17 12:04:00 to 2006/03/17 13:26:00,104 to 107)
- Orbit Inclination Manoeuvre (2006/03/28 05:33:20 to 2006/03/28 05:52:11 TAI)
- Payload anomaly DORIS MVR switch off (no data from) (2006/04/06 02:09:00 to 2006/04/08 12:40:00 TAI)
- RA2 back to operations following TM format anomaly (2006/04/06 12:31:00 to 2006/04/08 12:31:00,664 to 735)
- Doris Doppler Instrument nominal mode with median frequency bandwith pre-positionning (required for DORIS incident recovery) (2004/04/08 12:40:00 to 2006/04/14 09:00:00 TAI)
- Payload anomaly DORIS Reset (2006/04/14 09:00:09)

10.39. Cycle 047

- On 12th-13th May, a special operation was executed to limit RA-2 Chirp Bandwidth to 80MHz (starting from 12/05/2006 at 15:51:37, pass 710) and then 20 MHz (starting from 13/05/2006 at 03:57:57, Pass 724). The instrument was returned to 320MHz on 13/05/2006 at 15:10:17, Pass 738. Users are strongly advised not to use passes 710-738

- The instrument sub-system Radio Frequency Module (RFM) was switched to its B-side on 15 May 2006 at 14:21:50, Pass 790
- RA-2 BACK TO OPERATIONS AFTER 2 CONSECUTIVE SEU ANOMALIES (19 May 2006 09:24:32 and 19 May 2006 19:13:00)

10.40. Cycle 048

- RFM switched to its nominal configuration side (A-side) on the 2006/06/21 at 13:20:15, Pass 850
- RA-2 Back to Measurement following Uncontrolled S/W Action (2006/06/25 15:01:36 to 2006/06/25 19:46:00, passes 967-971)

10.41. Cycle 049

- none

10.42. Cycle 050

- RA-2 Back to Measurement following Multiple SEU Anomaly (2006/08/01 01:14:40 to 2006/08/01 08:54:30,6 to 13)
- Foccserver have been re-booted and is up and running. The problem was probably due to a HW failure at ESRIN (IECF) which caused all the user slots to be occupied(2006/08/17 00:00:41 to 2006/08/17 11:10:00,TAI)

10.43. Cycle 051

- RA-2 Back to Measurement following a Service Module Anomaly (2006/09/7 16:40:30 to 2006/09/10 15:47:30,80 to 166)
- Orbit Inclination Maneuver (2006/09/13 05:22:17 to 2006/09/13 05:40:29)
- Interruption of the Envisat data transmission via the ESA Data Relay Satellite Artemis (anomaly with Envisat Ka-band antenna) from 2006/09/26 until 2006/10/1,630 to 641, 658 to 669, 686 to 697, 716 to 725, 744 to 755)

10.44. Cycle 052

- RA-2 Back to Measurement following a Service Module Anomaly (2006/10/26 04:02:43 to 2006/10/26 10:32:00,467 to 473)
- RA-2 Back to Measurement following a Service Module Anomaly (2006/11/02 15:20:19 to 2006/11/02 20:07:00,681 to 685)

10.45. Cycle 053

- RA-2 Back to Measurement following Multiple SEU Anomaly (2006/11/26 08:01:06 to 2006/11/26 17:32:00, 358-367)
- Available again in Measurement after SM Memory Maintenance (2006/11/28 07:40:00 to 2006/11/29 17:23:00,413-469)
- The entire payload switched off (Due to a LVL 3 PROTOCOL ERROR AND INTERRUPT) (2006/12/12 18:02:17 to 2006/12/15 15:54:00,826-909)

10.46. Cycle 054

- HSM input reset (2006/12/27 14:18:50 to 2006/12/28 10:51:48)

10.47. Cycle 055

- Orbit Inclination Maneuver (2007/01/23 04:33:06 to 2007/01/23 04:51:50; 9)
- RA-2 recovered from STANDBY / REFUSE MODE and back to MEASUREMENT (2007/02/01 15:15:30 to 2007/02/01 17:11:30, 280-281)
- RA-2 return to operation from RESET/WAIT due to MCMD Transfer Acknowledge Error (2007/02/16 00:47:49 to 2007/02/16 11:07:00, 692-703)
- RA-2 return to operation from HT0/REF due to low HPA PBC current (2007/02/17 00:45:47 to 2007/02/19 11:11:00, 721-789)

10.48. Cycle 056

- No event

10.49. Cycle 057

- Orbit Inclination Maneuver (2007/04/03 04:34:42 to 2007/04/03 04:50:14)
- RA-2 Return to Mesurement from HEATER 0 / REFUSE MODE due to HPA bus current OOL (2007/04/03 12:37:27 3 to 2007/04/03 13:48:00)
- RA-2 Return to Measurement after HEATER 0 / REFUSE MODE due to HPA bus current OOL (2007/04/04 09:49:12 to 2007/04/04 11:30:00)
- RA-2 back to measurement from STBY/REFUSE following HTR0/REFUSE MODE (2007/04/09 05:08:51 to 2007/04/09 10:36:30)

10.50. Cycle 058

- The MWR instrument switched into Stand-by/Refuse mode following an on-board anomaly (2007/05/26 13:20:29 to 2007/05/30 13:41:06, 535-649)

10.51. Cycle 059

- RA-2 recovered back to measurement from HTR1/REF0 (2007/06/30 00:37:55 to 2007/06/02 09:51:00,520-587)

10.52. Cycle 060

- RA-2 returned to Measurement from HTR1/REF due to a Telemetry error.(2007/07/19 01:08:026 to 2007/07/19 07:38:00,63-69)
- Orbit Inclination Maneuver (2007/07/17 04:41:26 to 2007/07/17 04:43:42,9)

10.53. Cycle 061

- Payload switch-off due to Service Module Anomaly (Global AOCS Surveillance triggered) (24 Sep 2007 12:27:00 to 27 Sep 2007 11:13:30,993-1002)

10.54. Cycle 062

- Payload switch-off due to Service Module Anomaly (Global AOCS Surveillance ered).(24 Sep 2007 12:27:00 to 27 Sep 2007 11:13:30,1-7)
- Orbit Inclination Maneuver (27 Sep 2007 05:16:25 to 27 Sep 2007 05:31:15)
- MCMD Transfer Acknowledge Error caused the ICU to be put into Reset/Wait Mode. This is one of the expected anomalies and RA-2 was back to measurement on the same day. (2 Oct 2007 16:15:55 to 2 Oct 2007 20:09:30,224-227)

10.55. Cycle 063

- The instrument was switched to Suspend by the PMC following consecutive TM format errors, the mode was commanded back to Measurement on the same day.(8 Nov 2007 13:31:47 to 8 Nov 2007 17:24:30)

10.56. Cycle 064

- Planned payload unavailability for OCM and Maintenance (3 Dec 2007 22:00:00 to 4 Dec 2007 13:50:00, passes 2 to 21)
- Orbit Inclination Maneuver (4 Dec 2007 04:34:54 to 4 Dec 2007 04:49:55)
- RA-2 Back to Measurement following TM Format Anomaly (9 Dec 2007 20:45:11 to 10 Dec 2007 09:14:30, passes 172 to 187)
- RA-2 was switched down into Standby for the System Memory Test (13 Dec 2007 06:44:00 to 13 Dec 2007 12:39:30, passes 270 to 277)

10.57. Cycle 065

- On 16th January an anomaly occurred in the HSM from 16 Jan 2008 16:11:00 to 17 Jan 2008 10:35:21, passes 253 to 276
- Envisat RA-2 (A-Side) S-band transmission power suddenly dropped on 17 January 2008, 23:23:40, UTC. Consequently, all S-band parameters as well as the dual ionospheric correction are not relevant anymore and must not be used from this date onwards.

10.58. Cycle 066

- Orbit Inclination Maneuver (2008/02/12 03:35:23 to 2008/02/12 05:49:28, 9)

10.59. Cycle 067

- None

10.60. Cycle 068

- Orbit Inclination Maneuver (2008/04/22 start : 04:37:04 TAI, end : 04:47:48 TAI).

10.61. Cycle 069

- None

10.62. Cycle 070

- Orbit Inclination Maneuver (2008/07/01 from 04:41:17 to 04:43:49 TAI).

10.63. Cycle 071

- None

10.64. Cycle 072

- Orbit Inclination Manoeuver (2008/09/09 from 04:34:21 to 2008/09/09 04:50:26 TAI).
- From 2008/09/11 18:59:00 TAI to 2008/09/12 01:13:00 TAI, ARTEMIS (ENVISAT relay satellite) was unavailable due to ATV operation. This impacted the data availability from pass 86 to 90.

10.65. Cycle 073

- During the period covered by cycle 073 one SFCM manoeuvre was executed as planned on the 7th of September at 01:36:05.

11. Appendix 2: Orbit Standards

11.1. Envisat CNES POE (after cycle 41): GDR-B

Reference systems:
- polar motion and UT1: IERS bulletin D with IERS 1996 daily and sub-daily corrections
- stations coordinates (ITRF 2000): DPOD 2000 reference for Doris Stations,
ITRF 2000 with minor corrections for a few SLR (updates GPS const JPL IGS00)
- satellite reference: Post-Launch value of Mass + variations generated by Control Center, attitude model: Nominal Yaw Steering Law

Force models:
- EIGEN-CG03C gravity field model
- IERS 2003 Solid Earth tides
- FES 2004 (all principal constituents, with admittance) ocean tides
- Ocean pole tides: None
- Atmospheric contribution to the gravity field: None
- Haurwitz and Cowley atmospheric tides
- Sun, Moon, Venus, Mars and Jupiter third bodies
- thermo-optical coefficient from pre-launch box and wing model for solar radiation with smoothed Earth shadow model
- MSIS86 model (ENVISAT), DTM 94(Jason), best available solar activity (unchanged), physical box and wing model for atmospheric drag with 1 Cd adjustment per 2Rev with a priori constraint
- Knocke-Ries albedo and IR model for Earth radiation
- 1/rev along-track and cross-track constant per 24 hours for empiricals
- Time varying gravity: Drift only on zonal harmonics up to degree 4

Tracking data:
DORIS:
- Troposphere correction: CNET1 model, vertical bias adjusted
- Solid earth tide applied to both SLR and DORIS stations
- Frequency: Bias per pass adjusted
- Weight: underweighting of the SAA stations before cycle 91
- 6.5 microseconds datation bias on ENVISAT in order to cope with a 4.5 cm along-track bias with Laser orbits (6 microseconds on Jason).

LASER
- Troposphere correction: Marini-Murray following IERS 2000
- Retroreflector correction: Constant radial correction of 5.0 cm (Jason) and cm (ENVISAT) for all stations
- Ocean loading and pole tides only applied to SLR stations
- Bias/Pass: Solved-for for a few stations
- Weight: Globally 10 cm
- Ocean loading correction (FES99)

GPS (for Jason only)
- Constellation ephemeris and clocks (5 min): precise JPL solution - Measurements sampling in orbit determination: 5 min - JPL Antenna diagram phase correction (Jason receiver) - phase windup correction - Receiver clock adjusted at every epoch - phase ambiguity per pass - Weight: 10 cm on phase, 1 m on code - GPS overweights DORIS/Laser

11.2. Envisat CNES POE (after cycle 69): GDR-C

Reference systems:
- polar motion and UT1: IERS bulletin D with IERS 1996 daily and sub-daily corrections
- stations coordinates (ITRF 2005): DPOD 2005 reference for Doris Stations,
ILRS 2005 with updates GPS const JPL IGS05
- satellite reference: Post-Launch value of Mass + variations generated by Control Center, attitude model: Nominal Yaw Steering Law

Force models:
- **EIGEN-GL04S (GRGS) ANNUAL gravity field including seasonal variations up to degree/order 50 (Time varying gravity: Drift + Annual + Semi annual 50x50 from EIGEN-GL04S-ANNUAL (GRGS)**)
- IERS 2003 Solid Earth tides
- FES 2004 (all principal constituents, with admittance) ocean tides
- Ocean pole tides: Desai model from IERS 2003 standards
- Atmospheric contribution to the gravity field: NCEP derived 20x20 field provided by AGRA service (GSFC)
- Haurwitz and Cowley atmospheric tides
- Sun, Moon, Venus, Mars and Jupiter third bodies
- thermo-optical coefficient from pre-launch box and wing model for solar radiation with smoothed Earth shadow model
- MSIS86 model (ENVISAT), DTM 94(Jason), best available solar activity (unchanged), physical box and wing model for atmospheric drag with 1 Cd adjustment per 2Rev with a priori constraint
- Knocke-Ries albedo and IR model for Earth radiation
- 1/rev along-track and cross-track constant per 24 hours for empiricals
- Surface forces updates

Tracking data:
DORIS:
- Troposphere correction: CNET1 model, vertical bias adjusted
- Solid earth tide applied to both SLR and DORIS stations
- Ocean loading and pole tides applied to both SLR and DORIS stations
- Frequency: Bias per pass adjusted
- Weight: underweighting of the SAA stations before and after cycle 91 + review of AT bias
- 6.5 microseconds datation bias on ENVISAT in order to cope with a 4.5 cm along-track bias with Laser orbits (6 microseconds on Jason).

LASER
- Troposphere correction: **Mendes-Pavlis**
- Retroreflector correction: **Elevation dependent** radial correction of 5.0 cm (Jason) and ? cm (ENVISAT) for all stations
- Ocean loading and pole tides applied to both SLR and DORIS stations
- Bias/Pass: Solved-for for a few stations
- Weight: Globally 10 cm
- Ocean loading correction (FES99)

GPS (for Jason only)
- Constellation ephemeris and clocks (5 min): precise JPL solution
- Measurements sampling in orbit determination: 5 min
- JPL Antenna diagram phase correction (**receiver updated + emitter**)
- phase windup correction
- Receiver clock adjusted at every epoch
- phase ambiguity per pass
- Weight: 10 cm on phase, 1 m on code

- increase of the weight of DORIS/Laser relative to GPS (at least after cycle 91 TBC)

11.3. Envisat CNES POE (after cycle 71): GDR-C'

In order to avoid the long term drift introduced by the new time varying gravity field (see [7] or [10]), a new GDR C' version was computed. The only change with the GDR-C version is the following :
- Time varying gravity: Drift on zonal harmonics up to degree 4 + Annual + Semiannual 50x50

11.4. Envisat ESOC POE - Version V2

Solution generated mid **November 2007** for CLS (files: yymmdd.env.v2.sp1) period form 4-October-2002 until 5-October-2007
REFERENCE SYSTEM:
- **polar motion and UT1: IERS bulletin A with IERS 2003 daily and sub-daily corrections**
- **stations coordinates: ITRF-2005 reference for Doris Stations, ITRF 2005 rescaled append with ITRF-2000 for station not in ITRF-2005**
- satellite reference: Post-Launch value of Mass + variations generated by Control Center, attitude model: Nominal Yaw Steering Law

FORCE MODELS:
- **EIGEN-GL04C gravity field model**
- IERS 2003 Solid Earth tides
- FES-2004, 99 major constituents to order and degree 30
- Sun, Moon, and all Planets
- ANGARA model for drag, solar, infrared and albedo radiation
- MSIS-90 model for atmospheric density

PARAMETERS:
- 7-Day arcs, estimated Satellite State Vector, Solar radiation pressure per arc (constrained)
- ten drag coefficient and two 1/rev along-track and cross-track constant per 24 hours.

TRACKING DATA: (from CDDIS)
- All station displaced corrections according to IERS 2003
- DORIS:
- Frequency: Bias per pass adjusted
- Weight: 0.5 mm/s
- Laser
- Troposphere correction: Mendes-Pavlis following IERS 2003 update
- Retroreflector correction: Constant radial correction of 5.12 cm for all stations
- Weight: Globally 4 cm

11.5. Envisat ESOC POE - Version V3 (and V3_CR)

REFERENCE SYSTEM:
- **polar motion and UT1: IERS bulletin 05 C04 (IAU2000A) with IERS 2003 daily**

and sub-daily corrections
- station coordinates: **(version v3) ITRF-2005 reference for Doris Stations, ITRF 2005 rescaled for SLR. Appended with ITRF-2000 for station not in ITRF-2005 (both DORIS and SLR)**
- station coordinates: **(version v3_00) ITRF-2000 for DORIS and SLR**
- satellite reference: Post-Launch value of Mass + variations generated by Control Center, attitude model: Nominal Yaw Steering Law

FORCE MODELS:
- **EIGEN-GL04S-ANNUAL gravity field including seasonal variations up to degree/order 50**
- **Atmospheric contribution to the gravity field up to degree/order 20 (AGRA service at GSFC)**
- IERS 2003 Solid Earth tides
- FES 2004 ocean tides (all principal constituents, with admittance) up to degree/order 50
- Sun, Moon, and all Planets (DE-405)
- ANGARA model for drag, solar, infrared and albedo radiation
- MSIS-90 model for atmospheric density

PARAMETERS:
- 7-Day arcs, estimated Satellite State Vector, Solar radiation pressure per arc (constrained)
- ten drag coefficient and two 1/rev along-track and cross-track constant per 24 hours

TRACKING DATA: (from CDDIS)
- All station displaced corrections according to IERS 2003
- DORIS:
- Frequency: Bias per pass adjusted
- Weight: 0.5 mm/s
- 6.5 microsecond datation bias before October 2005
- Laser
- Troposphere correction: Mendes-Pavlis following IERS 2003 update
- Retroreflector correction: Constant radial correction of 5.12 cm for all stations
- Weight: Globally 4 cm

11.6. Envisat ESOC POE - Version V4

Configuration used for the solution generated end **October 2008** for CLS on the period form 4-October-2002 until 21-September-2008

Reference systems:
- polar motion and UT1: IERS bulletin 05 C04 with IERS 2003 daily and sub-daily corrections
- stations coordinates: **DPOD-2005 reference for Doris Stations,**
LPOD-2005 reference for SLR stations
- satellite reference: Post-Launch value of Mass + variations generated by Control Center, attitude model: Nominal Yaw Steering Law

Force models:
- EIGEN-GL04S-ANNUAL gravity field including seasonal variations up to degree/order 50
- Atmospheric contribution to the gravity field up to degree/order 20 (AGRA service at GSFC)
- IERS 2003 Solid Earth tides

- FES 2004 ocean tides (all principal constituents, with admittance) up to degree/order 50
- Sun, Moon, and all Planets (DE-405)
- ANGARA model for drag, solar, infrared and albedo radiation
- MSIS-90 model for atmospheric density

Parameters

- 7-Day arcs, estimated Satellite State Vector, Solar radiation pressure per arc (constrained)
- ten drag coefficient and two 1/rev along-track and cross-track constant per 24 hours.

Tracking data:(from CDDIS)

- All station displaced corrections according to IERS 2003
- DORIS:
- **Troposphere: Saastamoinen with GPT, GMF with estimated zenith delay (wet)** - Frequency: Bias per pass adjusted
- Weight: 0.5 mm/s
- Laser
- Troposphere correction: Mendes-Pavlis following IERS 2003 update
- Retroreflector correction: Constant radial correction of 5.12 cm for all stations
- Weight: Globally 4 cm